Title
Elucidation of a proteolytic mechanism required for Kaposi's sarcoma-associated herpesvirus replication

Author
Marnett, Alan Brown

Publication Date
2005

Peer reviewed|Thesis/dissertation

Elucidation of a Proteolytic Mechanism Required for Kaposi's Sarcoma-associated Herpesvirus Replication

by

Alan Brown Marnett

DISSERTATION

Submitted in partial satisfaction of the requirements for the degree of

DOCTOR OF PHILOSOPHY

in

Chemistry and Chemical Biology

in the

GRADUATE DIVISION

of the

UNIVERSITY OF CALIFORNIA, SAN FRANCISCO

To my family: Lawrence, Nancy, Leslie and Kirem for their unconditional love and support over the years.

Preface

Whether my scientific career officially began in 1980 in the kitchen of 20 Hanover Street where I mixed every powder and liquid I could find in an attempt to create an explosion or at least some fizz; or at the science fair at Bloomfield Hills Middle School, where I mixed together chemicals my father had brought home to demonstrate chemiluminescence; or in college at Trinity University when I mixed Jack Daniels, Mountain Dew and an Andes mint to inadvertently prove that the sum of the parts is not always greater than the individual parts themselves, is really just semantics. However, it is clear that along the way there were many people that were critical in my development both scientifically and personally who each deserve a tremendous amount of credit.

I have often been described by friends and family as someone who appreciates "the rules", so when it came time to declare a major in college all I knew was that philosophy, religion, and politics certainly weren't defined enough for me to ever feel comfortable. Although I wasn't sold on chemistry yet, given that both my grandfather and father were chemists, I figured there was no way genetics would let me down. That epiphany was followed by a C in general chemistry. So much for genetics. Interestingly, that marked the beginning, and not the end, of my research career. I will forever be indebted to Dr. Michael Doyle, who overlooked a few bad grades and gave me the opportunity to learn synthetic organic chemistry in his laboratory. At the time, a new postdoctoral fellow, Dr. Chad Peterson, arrived in the lab and took on the responsibility of developing my scientific "hands". Drs. Doyle and Peterson instilled in me the work ethic, critical thought process and skill sets necessary to be a successful organic chemist.

Their tutelage gave me the confidence as a scientist to apply my training in organic chemistry to other scientific disciplines.

To me, the most interesting part of making a molecule was discovering if it had a biological function. Of course, I had no training or education in biology or biochemistry, so after college graduation I sought to learn how to apply my chemistry skills to biological problems. My first exposure to the power of chemistry in biology came during work performed in my father's laboratory at Vanderbilt University in the months following graduation. Working with Dr. Amit Kalgutkar, I helped synthesize compounds that selectively targeted cyclooxygenase-2, one of the two isoforms of the enzyme targeted by aspirin. The fact that single atom changes on a molecule could vastly affect biological function amazed me and guided my scientific pursuits to biologically relevant problems.

If ignorance is bliss, then I was ecstatic. Although I wanted to work at the interface of chemistry and biology, I knew absolutely nothing about one of the disciplines. In the summer of 1998, Dr. Palmer Taylor generously offered me a position as a research assistant in the Department of Pharmacology at the University of California San Diego. It was through the patience and generosity of Dr. Taylor and Dr. Aileen Boyd, then a graduate student, that I was able to learn the basics of biochemistry and how to work with protein and DNA. It was also at this time that I mastered the art of looking like I knew what someone was talking about and then running to look up all of the terms as soon as they left.

A year later, I started graduate school in Chemistry and Chemical Biology at UCSF where I would meet and work for Drs. Paul Ortiz de Montellano and Charles

Craik, both of whom profoundly impacted my scientific career. Their willingness to work together and create an environment in which I felt truly welcome in each lab is something for which I am very appreciative. Throughout his career, Paul has worked on a number of enzymes, none of which even closely resembled a "herpesvirus protease". Even in the absence of an obvious benefit to his field of expertise, Paul was willing to take me into his lab to allow me to pursue my interest in synthesizing small molecule inhibitors, and I will always be grateful to him for this. To me, Paul represents the model of efficiency — whether it's conducting research, writing grants or running group meetings — and this is something I've strived to emulate. His selfless nature and unbelievable breadth of chemistry knowledge never ceased to amaze me.

Over the years, the project evolved in such a way that most of my time was spent in the Craik lab. Charly's characteristic enthusiasm, optimism and sense of humor permeate the lab. In a profession with a 95% daily failure rate, Charly focuses on the 5% and moves forward, a skill I am desperately working to obtain. The environment in the lab fosters independent thought and creativity, which allows the ultimate freedom in pursuing scientific interests. In fact, to this day, Charly has no idea I spent the better part of two years trying to put a pig's head on a dog's body. Yet, despite the hands-off approach to running a lab, Charly was always there with his door open when I needed advice or guidance. He was instrumental in teaching me not only the art of writing, but also the finer points of being a scientist that are only obtained from experience. A master in personal relationships, Charly taught me the importance of always trying to find something positive in interactions with everyone.

Within both the Craik and Ortiz de Montellano labs, there were many fellow graduate students and postdocs that were also important in helping me over the years. Drs. Alex Aronov, Todd Pray and Kinkead Reiling were essential in establishing the project. Dr. Sami Mahrus was critical in initiating the phosphonate project as well as acting as a general sounding board. He was also a workout partner who helped relieve the stress from the 95% that didn't work that day. Although an inorganic chemist at heart, Dr. Tommaso Vannelli provided a tremendous amount of insight, not only to the protease project, but also to scientific discussions in general. He was also instrumental in developing my scotch palette, which has made both Glenlivet and Bayer a lot of money. Within the daily workings of the KSHV project, Drs. Anson Nomura and Nobuhisa Shimba were essential. Anson always provided insightful feedback that helped move the project forward and his sense of humor made the daily grind much more fun. It was a privilege to collaborate and publish with him over the years. I owe a tremendous amount of credit to Nobu, who single-handedly pushed the project in the right direction with one experiment. It was truly an honor to be able to interact with him on a daily basis and learn from his thorough and fearless experimental design. As the project moved towards virology, I was extremely fortunate to collaborate with Dr. Jill Bechtel in Dr. Don Ganem's laboratory. A brilliant virologist, Jill's patience and generosity not only made performing the virus replication experiments possible, but also a pleasure.

Of course, no experiments would be performed without the help of Christine Olson and Marissa Lee-Baird, who keep the graduate program and Craik lab, respectively, running like well-oiled machines.

To me, graduate school requires much more than memorization of facts and techniques to be successful. Personal strength and character are essential, as is a solid support system to pick you up when you stumble along the way. I am extremely fortunate to have an amazing family that has not only influenced who I am today, but also supported me throughout the process.

My parents provided a household where love, adventure, courtesy and humor reigned supreme. Whether trying new food, making new friends, playing a new sport or moving to a new city, the supportive environment at home nurtured my general curiosity. My father, a professor of Biochemistry and founder of the Institute for Chemistry and Chemical Biology at Vanderbilt University, remains my role model not only as a scientist, but also as a man. It seems he always knew the right time to give me a push or let me go and his ability to juggle a family and academic career only becomes more amazing to me as I embark along a similar path. Of course, the success of that balance would not have been possible without my mom. She has always made sure that I had all of the tools necessary for success, and spent most of her life working to ensure this. She taught me that hard work is essential in life and although the rewards may not be immediately evident, they will come. Her guidance and support helped steer my moral development and is a big part of who I am today. Without their help and influence, I would have never made it this far.

Just as with my parents, my sister deserves a huge piece of this degree. If anyone took the brunt of my "rules", it was Les. She endured years of imaginary lines dividing the back seat of the car into "my 60%" and "her 40%", of lies about the things that came out of her closet when she went to sleep at night, and of reasons she actually lost the

game because I had changed a rule without her knowing. But somehow she managed and is a hilarious, independent and successful adult. Her fearlessness and sense of adventure is something I've always admired and strived to incorporate into my own life, if only a fraction of the amount that she has. Hopefully, we will live in the same city one day and I'll let her son draw the line at 60% in the back seat to clear my conscience.

Science can be a difficult profession, oftentimes resembling a foreign language to those who are not scientists themselves. It takes a truly amazing person to understand when I am thirty minutes late to dinner because I could not get a solid compound to dissolve in a liquid, or because the bacteria were growing slower than usual. I am unbelievably fortunate to have shared the last few years of graduate school and my life with Kirem. She has worn many hats- therapist, comedian, artist, chef, bartender, consultant, travel agent, librarian and most importantly, my best friend. An invaluable resource for dealing with personal interactions, she has taught me how to navigate even the most complicated situations. While wise beyond her years, she has a childlike enthusiasm for life that is infectious. Kirem has made getting through the 95% possible and made celebrating the 5% unforgettable. Although I shudder to think where I would be if she were not in my life, I'm almost certain it involves a white jacket and padded room.

I am honored to have shared my graduate career with so many talented people and I will forever be indebted to everyone for their support and guidance.

Alan Marnett

August 19, 2005

Elucidation of a Proteolytic Mechanism Required for Kaposi's Sarcoma-associated Herpesvirus Replication

Alan Brown Marnett

Herpesviruses represent one of the most prevalent human pathogens worldwide. Infection results in a number of diseases ranging from cold sores to cancer. Yet despite the large clinical variation in disease states, the proteins expressed during the lytic cycle of all herpesviruses are highly conserved. A maturational serine protease is expressed late in viral replication and is required for production of properly assembled infectious progeny. *In vitro* structural and functional analysis has revealed the enzyme possesses a novel protein fold and is activated by dimerization. However, the mechanism of regulation of the enzyme both at a molecular level and in the context of viral replication is unknown.

Positional scanning synthetic combinatorial libraries were used to define the substrate specificity of the protease encoded by Kaposi's Sarcoma-associated herpesvirus (KSHV). The strict specificity observed was used to guide the design and synthesis of a peptidyl-diphenylphosphonate inhibitor targeting the active site of the enzyme. Covalent modification of the active site serine of the enzyme by the transition-state analog inhibitor dramatically shifted the equilibrium toward dimeric enzyme illustrating the intimate communication between the spatially separate active sites and dimer interface of the protease.

To elucidate the mechanism of stabilization and activation during catalysis, structural analysis was performed on purely monomeric (M197D), purely dimeric

(inhibited) and an equilibrium mixture (uninhibited wild-type) by circular dichroism and nuclear magnetic resonance. A massive conformational change was observed upon loss of dimerization in which helices 5 and 6, at the interface and active site, respectively, become disordered, which destabilizes essential catalytic components. A disulfide bond was engineered into the protease at helix 6 that prevented the conformational change and subsequent inactivation of the enzyme. Addition of oxidant or reductant reversibly recovered or abolished enzymatic activity, respectively, even in a monomeric variant of the protease.

A reduction in viral replication similar to currently available therapies targeting the viral polymerase was observed upon treatment of reactivated KSHV with the protease inhibitor. The work not only validated the virally-encoded protease as a potential therapeutic target, but also presented a mechanism by which protease inhibition may occur *in vivo*.

TABLE OF CONTENTS

LIST OF TABLES

LIST OF FIGURES

Chapter 1 | **Introduction**

Originally described over a century ago, Kaposi's Sarcoma (KS) is a life threatening disease characterized by painful lesions on the surface of the skin that may rapidly disseminate to vital organs and become life threatening. Although classic KS, as first reported by Hungarian dermatologist Moritz Kaposi, presents as a slow growing tumor on elderly Mediterranean men, three other forms of KS have emerged during the 20th century that vary biologically and epidemiologically. In fact, it is the more recently described forms of the disease that have made KS a serious public health concern. The variability in both epidemiology and virulence of KS demonstrates the complexity of the disease and the numerous factors that affect disease progression.

Unlike classic KS, in which tumors are slow growing and rarely the actual cause of death, transplant-associated KS is a more aggressive form of the disease. Presumably contracted through transplantation with an infected organ, this form of KS is generally controlled upon removal of immunosuppressive therapy. So despite the increased virulence, full remission of the disease is achieved upon reestablishment of a functional immune system and is rarely a serious problem. Endemic KS, on the other hand, affects women and children in equatorial African countries and is a significant health risk. In fact, KS infection of children under 12 is usually fatal. However, it was not until the early 1980's, with the onset of HIV infection, that KS emerged as a worldwide health concern.

A hallmark of HIV infection, AIDS-KS presents as purple lesions covering much of the body of infected individuals and remains the most common neoplasm afflicting AIDS patients today (Figure 1)[1-5]. In fact, an estimated 30% of HIV infected individuals

will develop KS at some point during their disease progression. Although the incidence of KS has declined in the United States with the development of AIDS specific therapies, such as highly active antiretroviral therapy (HAART), the prevalence of KSHV infection in Africa has increased severely in recent years. Since 1985, KS has emerged as the most common cancer in men and the second most common cancer in women in Uganda and Zimbabwe, reflecting nearly a 20-fold increase in incidence in these countries[6-9]. Recent studies have detected the causative agent of KS in greater than 80% of the population of African countries that prior to the HIV epidemic reported only a few cases of the disease.

Despite the persistence of clinical reports documenting KS for over 120 years, it was not until 1994 that the causative agent of the disease was identified as a novel human herpesvirus, referred to as human herpesvirus 8 (HHV-8), or Kaposi's Sarcoma-associated herpesvirus (KSHV)[10]. Only two years after discovery of the virus in an AIDS-KS lesion, sequencing of the entire coding genome of KSHV was completed[11, 12]. KSHV is a double-stranded DNA virus belonging to the Rhadinovirus (γ-2 herpesvirus) genus with the subfamily Gammaherpesvirinae and is currently the only known human rhadinovirus. All human herpesviruses are grouped into one of three subfamilies based on similar biological properties, the neurotropic α-(HHV1-3), the lymphotropic β-(HHV5, 6A, 6B, 7) and the γ-(HHV4 and HHV8) herpesviruses (Figure 2). In addition to KS, herpesviruses are responsible for a number of human diseases, including herpes simplex viruses-1 and -2 (HHV1and HHV2), Varicella Zoster virus (HHV3), cytomegalovirus (HHV5) and Epstein Barr virus (HHV4). Both *in vitro* and *in vivo* model systems have been established for several members (HHV2, 4, 5) of this important class of human pathogens, however significant differences at both the genetic and the

biological level have prevented application of these systems to KSHV. Recent advances in laboratory culture and infection of the virus have led to important advances in understanding the biology of KS infection, the maintenance of viral latency and the mechanism of tumor formation[13-16].

KSHV establishes latent infection primarily in B cells and endothelium, although infection of macrophages, prostate epithelia and dorsal root sensory ganglion cells has been reported. Following initial infection, KSHV expresses a small number of gene products critical for maintaining latency, including the latency-associated nuclear antigen (LANA), which maintains a stable viral episome and ensures segregation of episomes to daughter cells upon cell division. A unique facet of KSHV biology in comparison to other human tumor viruses is the number of pirated cellular regulatory genes. Among these cellular homologs are immune regulatory proteins, G-protein coupled receptors, viral chemokines, cell cycle regulatory proteins and anti-apoptotic proteins. Together, these gene products provide protection from host immune surveillance and produce chemical signals for growth and differentiation. Upon stimulation of lytic replication, immediate early genes are expressed, followed by early and late lytic gene products. Mature infectious particles are produced by lytically replicating cells and are released into the extracellular space, where they proceed to infect new cells.

Although cell-to-cell infection is relatively well understood, much less is known about person-to-person transmission of KSHV. Viral particles have been detected in blood, saliva and semen leading to the belief that KS is predominantly a sexually transmitted disease[17]. However, classic KS essentially infects only elderly Mediterranean men, indicating a strong genetic, geographic, and gender-specific component. Endemic

KS, on the other hand, infects women and children in equatorial Africa. Interestingly, current hypotheses focus on transmission from mother to child upon kissing open wounds or insect bites (saliva to blood) rather than vertical transmission during childbirth[18]. However, the correlation between sexual activity and KS is much stronger among AIDS-KS patients. KSHV has been detected in over 50% of the saliva of homosexual men and increased numbers of sexual partners and "risky" sexual behavior (unprotected anal and oral-anal sex) strongly correlate with incidence of KS[17, 19-21]. One study revealed 38% of homosexual men in San Francisco were KSHV positive in the 1980's. The high infectivity observed in homosexual males may be a reflection of synergism between HIV infection and KSHV, both of which homosexual men are at an increased risk of contracting due to sexual practices.

Despite the wealth of knowledge compiled regarding latent and lytic characteristics of KSHV, there remain no KS-specific therapies. Although patients may undergo local or systemic treatments similar to most cancer patients (surgery, radiation, paclitaxel), success rates are average at best. Standard herpesvirus drugs targeting the viral DNA polymerase also show promise, yet high variability between clinical studies and emerging resistance to these drugs make these therapies less than exciting. Interestingly, the most effective treatment for AIDS-KS has not been targeting KS, but rather targeting HIV. Highly active antiretroviral therapy (HAART) has resulted in regression of AIDS-KS in patients receiving at least one HIV protease inhibitor[22, 23]. A combination of multiple effects, it appears that HAART therapy boosts the host immune system, reduces the level of HIV Tat (which enhances KS growth) and reduces angiogenesis by reduction of growth factors[23-25].

All herpesviruses encode a homologous protease that is expressed during lytic replication. Functional analysis of herpes simplex virus-1 demonstrated that virus containing a temperature sensitive mutant of the viral protease was incapable of forming infectious particles at the non-permissive temperature[26]. A null protease HSV-1 was produced and also failed to produce mature viral particles[27]. In fact, mice injected with null protease HSV-1 were protected from subsequent lethal HSV-1 exposure, demonstrating the inability of the null virus to produce infectious progeny while stimulating the immune system to illicit a response against active virus[28]. Proteolytic activity of the enzyme was shown to be essential by site-specific mutation of the catalytic residues in which viral replication was significantly attenuated[29, 30]. However, it is important to note that in cell-free capsid assemblies lacking the protease, a reduction in only 80% of capsid population was observed relative to a sample containing protease[31]. That any capsids were produced raises the possibility of alternate maturation mechanisms in the absence of protease, of a minimal rate of maturation required to support replication *in vivo* or of an artificial mechanism of capsid maturation *in vitro*.

Extensive virological and genetic analysis has resulted in a proposed mechanism of the role of the protease in viral replication[32-34]. The virally encoded protease is expressed as an N-terminal fusion protein to roughly 10% of viral assembly protein, as a result of an internal promoter that results in expression of assembly protein alone. Upon oligomerization of assembly proteins and binding of the major capsid protein, a nuclear localization signal is exposed resulting in translocation of the complex to the nucleus where it catalyzes formation of immature capsids (Figure 3)[35, 36]. As the nascent capsid forms, the viral protease is activated and cleaves at its two natural subsites: the release

site (R-site), which releases protease from the assembly protein, and the maturation site (M-site), which frees the scaffolding from the capsid shell[37-42]. The cleavage events result in a metastable capsid that undergoes a major conformational change as the linear viral genome is packaged inside of the capsid[34, 43-45]. Capsid egress from the nucleus involves an envelopment/de-envelopment process as it passes through the nuclear membrane. Production of the mature capsid is completed upon tegumentation in the cytosol and envelopment by budding into secretory vesicles that ultimately release the infectious particle from the cell (Figure 4) [46].

Although the mechanism of protease activation during replication was originally unclear, *in vitro* analysis of recombinantly produced enzyme demonstrated that the enzyme was regulated by dimerization[47-51]. Thus, at high local concentrations inside of the forming capsid, protease dimerization results in cleavage and subsequent capsid maturation. Herpesvirus proteases show no homology to known protein folds, yet inhibition of enzymatic activity by diisopropylfluorophosphate demonstrated they were serine proteases[52]. Due to poor solubility of the protease-assembly protein construct, most characterization of the enzyme has been with the purified protease domain. Analytical size exclusion and analytical ultracentrifugation demonstrated the protease dimerizes with a low micromolar dissociation constant and activity assays confirmed the dimer is the active species[47, 52-54].

Currently, crystal structures for five of the human herpesvirus proteases have been solved (Figure 5)[55-62]. All structures reveal the active homodimer, which consists of two 25-kD monomers, each a seven-stranded β-barrel surrounded by 6 α-helices. The structures also provided a framework for designing point mutations of each enzyme to

elucidate the molecular mechanism of activation in this class of proteases. A single point mutation at the dimerization interface of KSHV protease (M197D) rendered the enzyme monomeric and inactive even at millimolar concentrations of protease[54]. Circular dichroism and fluorescence analysis suggested a large conformational change upon protease activation[63]. Though the details of the relationship between dimerization and activity were unclear, it was reported that protein-protein interactions involving >2000 $Å^2$ (2500 $Å^2$ in herpesvirus proteases) often involve large conformational rearrangements[64, 65].

Compared to digestive serine proteases herpesvirus proteases display a severely reduced catalytic efficiency. Even with increased rates of substrate hydrolysis in the presence of anti-chaotropic salts and glycerol, the protease exhibits k_{cat}/K_m values nearly four orders of magnitude lower than trypsin[30, 49-51]. However, the molecular basis for this reduction was not evident until the crystal structures of two family members were solved, revealing a non-canonical catalytic triad of Ser-His-His (Figure 6). Mutational analysis confirmed the role of each residue in substrate hydrolysis[30, 66].

At the beginning of my graduate studies, several major questions regarding herpesvirus proteases remained unanswered. On a molecular level, the structural transition between inactive monomers and active dimers upon dimerization was unknown and represented a potentially new mechanism of regulation of proteolytic activity. Furthermore, the possibility of communication between the spatially separate active sites during catalysis exposed herpesvirus proteases as possible model systems for long-range through-protein allostery and suggested several mechanisms of substrate processing in the maturing viral capsid. On a macroscopic level, although the importance of the

protease in the viral life cycle had been established, it was not clear if small molecule inhibitors of the protease would arrest viral replication. Since the protease is active only at high concentration in the nascent capsid located in the nucleus of the virally infected cell, issues of inhibitor concentration and accessibility were serious concerns. My work focused on addressing each of these issues and will be described in detail in the chapters that follow.

One of the greatest challenges facing protease biochemists is the identification of protease substrates. With advances in technology, new methodologies continue to emerge, yet it is becoming increasingly clear that there will not be a "magic bullet", or a single technique that is applicable to all systems. Therefore, identification of potential protease substrates will undoubtedly involve some combination of existing techniques, and in Chapter 2, Charly and I review a few recent advances in the field that will expand the toolbox of the protease biochemist. Importantly, these methods may ultimately be applicable to novel substrate discovery for KSHV Pr as discussed in Chapter 6.

In Chapter 3, work addressing mechanistic details of KSHV protease is presented. The substrate specificity of KSHV protease was determined and used to design and synthesize a transition-state analog inhibitor targeting the active site of the enzyme. The inhibitor, which arrests catalysis at the transition-state, trapped the structural link between the dimer interface and the active site that we knew existed. In fact, upon inhibition, the equilibrium was shifted completely to the dimeric form of the enzyme, as inhibited monomer was never detected. Remarkably, inhibition with another derivative of the transition-state inhibitor, diisopropylfluorophosphate, illustrated an equivalent effect on the equilibrium, indicating the minimum requirement of dimer stabilization to be

formation of the oxyanion during inhibition. Structural analysis of the enzyme in combination with the inhibitor results yielded a mechanism of dimer stabilization proposed to occur during protease activation. Furthermore, inhibitor titration experiments demonstrated that the spatially separate active sites do not display cooperativity during substrate processing and are, in fact, independent.

Chapter 4 presents our work addressing the mechanism of activation of KSHV protease. In a collaboration with Anson Nomura, we used the active site inhibitor described above to produce a purely dimeric protease sample. Comparisons of secondary structure of the inactive monomeric variant (M197D) with the dimeric sample revealed an increase of 31% α-helical content upon dimerization. The differences in helical content were localized using secondary structural analysis obtained from backbone NMR chemical shift data of the monomer. The results supported our previously proposed model of activation. To test our hypothesis, a disulfide bond was introduced into wild-type protease that prevented the conformational change on loss of dimerization. As a result, a redox-sensitive protease was produced in which addition of oxidant or reductant activated or inactivated the enzyme, respectively. In support of our proposed mechanism, incorporation of the disulfide bond into a monomeric variant of the protease recovered activity resulting in the first report of a rationally designed active monomer.

To address the validity of herpesvirus proteases as potential therapeutic targets, inhibitors targeting the active site of KSHV protease were used in a cell-based model system of KSHV infection and replication. Chapter 5 describes our work demonstrating the effect of protease inhibitors on viral replication as compared to the current therapy for herpesvirus infection, DNA polymerase inhibitors. Nuclear localization of the inhibitor

was observed upon viral reactivation and a possible mechanism for this phenomenon was presented based on protease labeling and fluorescence polarization experimental results.

Chapter 6 summarizes our findings and discusses some of the remaining questions in the field. Experiments using reagents currently available in the lab and those requiring development of new materials are presented. Additionally, both *in vitro* and cell-based experiments are proposed to address further potential regulatory roles of the viral protease.

Herpesviruses represent one of the most prevalent viral families worldwide, infecting nearly all animal species worldwide. Despite the large range of viruses, all herpesviruses express a homologous protease during replication. As a result of the high homology among herpesviruses of both the protease and the lytic cycle in which it is expressed, we anticipate that our findings will be applicable not only to KSHV, but also to the entire family of herpesviruses in general.

REFERENCES

1. Goedert, J. J. The epidemiology of acquired immunodeficiency syndrome malignancies. *Semin Oncol* 27, 390-401 (2000).
2. Gottlieb, G. J. et al. A preliminary communication on extensively disseminated Kaposi's sarcoma in young homosexual men. *Am J Dermatopathol* 3, 111-4 (1981).
3. Hymes, K. B. et al. Kaposi's sarcoma in homosexual men-a report of eight cases. *Lancet* 2, 598-600 (1981).
4. Hengge, U. R. et al. Update on Kaposi's sarcoma and other HHV8 associated diseases. Part 2: pathogenesis, Castleman's disease, and pleural effusion lymphoma. *Lancet Infect Dis* 2, 344-52 (2002).
5. Schwartz, R. A. Kaposi's sarcoma: advances and perspectives. *J Am Acad Dermatol* 34, 804-14 (1996).
6. Dedicoat, M. & Newton, R. Review of the distribution of Kaposi's sarcoma-associated herpesvirus (KSHV) in Africa in relation to the incidence of Kaposi's sarcoma. *Br J Cancer* 88, 1-3 (2003).
7. Wabinga, H. R., Parkin, D. M., Wabwire-Mangen, F. & Mugerwa, J. W. Cancer in Kampala, Uganda, in 1989-91: changes in incidence in the era of AIDS. *Int J Cancer* 54, 26-36 (1993).
8. Ziegler, J. L. & Katongole-Mbidde, E. Kaposi's sarcoma in childhood: an analysis of 100 cases from Uganda and relationship to HIV infection. *Int J Cancer* 65, 200-3 (1996).

9. Ziegler, J. L., Templeton, A. C. & Vogel, C. L. Kaposi's sarcoma: a comparison of classical, endemic, and epidemic forms. *Semin Oncol* 11, 47-52 (1984).

10. Chang, Y. et al. Identification of herpesvirus-like DNA sequences in AIDS-associated Kaposi's sarcoma [see comments]. *Science* 266, 1865-9 (1994).

11. Neipel, F., Albrecht, J. C. & Fleckenstein, B. Cell-homologous genes in the Kaposi's sarcoma-associated rhadinovirus human herpesvirus 8: determinants of its pathogenicity? *J Virol* 71, 4187-92 (1997).

12. Russo, J. J. et al. Nucleotide sequence of the Kaposi sarcoma-associated herpesvirus (HHV8). *Proc Natl Acad Sci U S A* 93, 14862-7 (1996).

13. Renne, R. et al. Lytic growth of Kaposi's sarcoma-associated herpesvirus (human herpesvirus 8) in culture. *Nat Med* 2, 342-6 (1996).

14. Lagunoff, M. et al. De novo and serial transmission of Kaposi's sarcoma-associated herpesvirus (KSHV) in cultured endothelial cells. *J Virol* 76(5), 2440-8 (2002).

15. Lukac, D. M., Renne, R., Kirshner, J. R. & Ganem, D. Reactivation of Kaposi's sarcoma-associated herpesvirus infection from latency by expression of the ORF 50 transactivator, a homolog of the EBV R protein. *Virology* 252, 304-12 (1998).

16. Lagunoff, M. et al. De novo infection and serial transmission of Kaposi's sarcoma-associated herpesvirus in cultured endothelial cells. *J Virol* 76, 2440-8 (2002).

17. Martin, J. N. et al. Sexual transmission and the natural history of human herpesvirus 8 infection. *N Engl J Med* 338, 948-54 (1998).

18. Schwartz, R. A. Kaposi's sarcoma: an update. J Surg Oncol 87, 146-51 (2004).

19. Kedes, D. H. et al. The seroepidemiology of human herpesvirus 8 (Kaposi's sarcoma-associated herpesvirus): distribution of infection in KS risk groups and evidence for sexual transmission. *Nat Med* 2, 918-24 (1996).

20. Osmond, D. H. et al. Prevalence of Kaposi sarcoma-associated herpesvirus infection in homosexual men at beginning of and during the HIV epidemic. *JAMA* 287, 221-5 (2002).

21. Pauk, J. et al. Mucosal shedding of human herpesvirus 8 in men. *N Engl J Med* 343, 1369-77 (2000).

22. Parisi, S. G. et al. Human herpesvirus 8 cytoviraemia rebound in a patient with Kaposi's sarcoma after a short interruption of efficient antiretroviral therapy. *AIDS* 16, 1089-91 (2002).

23. Tam, H. K. et al. Effect of highly active antiretroviral therapy on survival among HIV-infected men with Kaposi sarcoma or non-Hodgkin lymphoma. *Int J Cancer* 98, 916-22 (2002).

24. Mosam, A. et al. Generic antiretroviral efficacy in AIDS-associated Kaposi's sarcoma in sub-Saharan Africa. *AIDS* 19, 441-3 (2005).

25. Gill, J. et al. Prospective study of the effects of antiretroviral therapy on Kaposi sarcoma--associated herpesvirus infection in patients with and without Kaposi sarcoma. *J Acquir Immune Defic Syndr* 31, 384-90 (2002).

26. Preston, V. G., Coates, J. A. & Rixon, F. J. Identification and characterization of a herpes simplex virus gene product required for encapsidation of virus DNA. *J Virol* 45, 1056-64 (1983).

27. Gao, M. et al. The protease of herpes simplex virus type 1 is essential for functional capsid formation and viral growth. *J Virol* 68, 3702-12 (1994).

28. Hippenmeyer, P. J., Rankin, A. M., Luckow, V. A. & Neises, G. R. Protease-deficient herpes simplex virus protects mice from lethal herpesvirus infection. *J Virol* 71, 988-95 (1997).

29. Register, R. B. & Shafer, J. A. A facile system for construction of HSV-1 variants: site directed mutation of the UL26 protease gene in HSV-1. *J Virol* Methods 57, 181-93 (1996).

30. Register, R. B. & Shafer, J. A. Alterations in catalytic activity and virus maturation produced by mutation of the conserved histidine residues of herpes simplex virus type 1 protease. *J Virol* 71, 8572-81 (1997).

31. Newcomb, W. W., Homa, F. L., Thomsen, D. R., Ye, Z. & Brown, J. C. Cell-free assembly of the herpes simplex virus capsid. *J Virol* 68, 6059-63 (1994).

32. Dunn, W. et al. Functional profiling of a human cytomegalovirus genome. *Proc Natl Acad Sci U S A* 100, 14223-8 (2003).

33. Song, M. J. et al. Identification of viral genes essential for replication of murine gamma-herpesvirus 68 using signature-tagged mutagenesis. *Proc Natl Acad Sci U S A* 102, 3805-10 (2005).

34. Yu, X. et al. Dissecting human cytomegalovirus gene function and capsid maturation by ribozyme targeting and electron cryomicroscopy. *Proc Natl Acad Sci U S A* 102, 7103-8 (2005).

35. Pelletier, A., Do, F., Brisebois, J. J., Lagace, L. & Cordingley, M. G. Self-association of herpes simplex virus type 1 ICP35 is via coiled-coil interactions

and promotes stable interaction with the major capsid protein. *J Virol* 71, 5197-208 (1997).

36. Preston, V. G. & McDougall, I. M. Regions of the herpes simplex virus scaffolding protein that are important for intermolecular self-interaction. *J Virol* 76, 673-87 (2002).

37. Desai, P., Watkins, S. C. & Person, S. The size and symmetry of B capsids of herpes simplex virus type 1 are determined by the gene products of the UL26 open reading frame. *J Virol* 68, 5365-74 (1994).

38. Heymann, J. B. et al. Dynamics of herpes simplex virus capsid maturation visualized by time-lapse cryo-electron microscopy. *Nat Struct Biol* 10, 334-41 (2003).

39. Matusick-Kumar, L. et al. Release of the catalytic domain N(o) from the herpes simplex virus type 1 protease is required for viral growth. *J Virol* 69, 7113-21 (1995).

40. Robertson, B. J. et al. Separate functional domains of the herpes simplex virus type 1 protease: evidence for cleavage inside capsids. *J Virol* 70, 4317-28 (1996).

41. Sheaffer, A. K. et al. Evidence for controlled incorporation of herpes simplex virus type 1 UL26 protease into capsids. *J Virol* 74, 6838-48 (2000).

42. Trus, B. L. et al. The herpes simplex virus procapsid: structure, conformational changes upon maturation, and roles of the triplex proteins VP19c and VP23 in assembly. *J Mol Biol* 263, 447-62 (1996).

43. Booy, F. P. et al. Liquid-crystalline, phage-like packing of encapsidated DNA in herpes simplex virus. *Cell* 64, 1007-15 (1991).

44. Renne, R., Lagunoff, M., Zhong, W. & Ganem, D. The size and conformation of Kaposi's sarcoma-associated herpesvirus (human herpesvirus 8) DNA in infected cells and virions. *J Virol* 70, 8151-4 (1996).

45. Schynts, F. et al. The structures of bovine herpesvirus 1 virion and concatemeric DNA: implications for cleavage and packaging of herpesvirus genomes. *Virology* 314, 326-35 (2003).

46. Mettenleiter, T. C. Herpesvirus assembly and egress. *J Virol* 76, 1537-47 (2002).

47. Cole, J. L. Characterization of human cytomegalovirus protease dimerization by analytical centrifugation. *Biochemistry* 35, 15601-10 (1996).

48. Darke, P. L. et al. Active human cytomegalovirus protease is a dimer. *J Biol Chem* 271, 7445-9 (1996).

49. Hall, D. L. & Darke, P. L. Activation of the herpes simplex virus type 1 protease. *J Biol Chem* 270, 22697-700 (1995).

50. Margosiak, S. A., Vanderpool, D. L., Sisson, W., Pinko, C. & Kan, C. C. Dimerization of the human cytomegalovirus protease: kinetic and biochemical characterization of the catalytic homodimer. *Biochemistry* 35, 5300-7 (1996).

51. Yamanaka, G. et al. Stimulation of the herpes simplex virus type I protease by antichaeotrophic salts. *J Biol Chem* 270, 30168-72 (1995).

52. DiIanni, C. L. et al. Identification of the serine residue at the active site of the herpes simplex virus type 1 protease. *J Biol Chem* 269, 12672-6 (1994).

53. Buisson, M. et al. Functional determinants of the Epstein-Barr virus protease. *J Mol Biol* 311, 217-28 (2001).

54. Pray, T. R., Nomura, A. M., Pennington, M. W. & Craik, C. S. Auto-inactivation by cleavage within the dimer interface of Kaposi's sarcoma-associated herpesvirus protease. *J Mol Biol* 289, 197-203 (1999).

55. Buisson, M. et al. The crystal structure of the Epstein-Barr virus protease shows rearrangement of the processed C terminus. *J Mol Biol* 324, 89-103 (2002).

56. Chen, P. et al. Structure of the human cytomegalovirus protease catalytic domain reveals a novel serine protease fold and catalytic triad. *Cell* 86, 835-43 (1996).

57. Hoog, S. S. et al. Active site cavity of herpesvirus proteases revealed by the crystal structure of herpes simplex virus protease/inhibitor complex. *Biochemistry* 36, 14023-9 (1997).

58. Qiu, X. et al. Unique fold and active site in cytomegalovirus protease. *Nature* 383, 275-9 (1996).

59. Qiu, X. et al. Crystal structure of varicella-zoster virus protease. *Proc Natl Acad Sci U S A* 94, 2874-9 (1997).

60. Reiling, K. K., Pray, T. R., Craik, C. S. & Stroud, R. M. Functional consequences of the Kaposi's sarcoma-associated herpesvirus protease structure: regulation of activity and dimerization by conserved structural elements. *Biochemistry* 39, 12796-803 (2000).

61. Shieh, H. S. et al. Three-dimensional structure of human cytomegalovirus protease [published erratum appears in *Nature* 1996 Nov 21;384(6606):288]. *Nature* 383, 279-82 (1996).

62. Tong, L. et al. A new serine-protease fold revealed by the crystal structure of human cytomegalovirus protease. *Nature* 383, 272-5 (1996).

63. Pray, T. R., Reiling, K.K., Demirjian, B.G., Craik, C.S. Conformational Change Coupling the Dimerization and Activation of KSHV Protease. *Biochemistry* 41, 1474-1482 (2002).

64. Janin, J. Principles of protein-protein recognition from structure to thermodynamics. *Biochimie* 77, 497-505 (1995).

65. Jones, S. & Thornton, J. M. Protein-protein interactions: a review of protein dimer structures. *Prog Biophys Mol Biol* 63, 31-65 (1995).

66. Khayat, R., Batra, R., Massariol, M. J., Lagacé, L. & Tong, L. Investigating the role of histidine 157 in the catalytic activity of human cytomegalovirus protease. *Biochemistry* 40, 6344-51 (2001).

Figure 1-1.

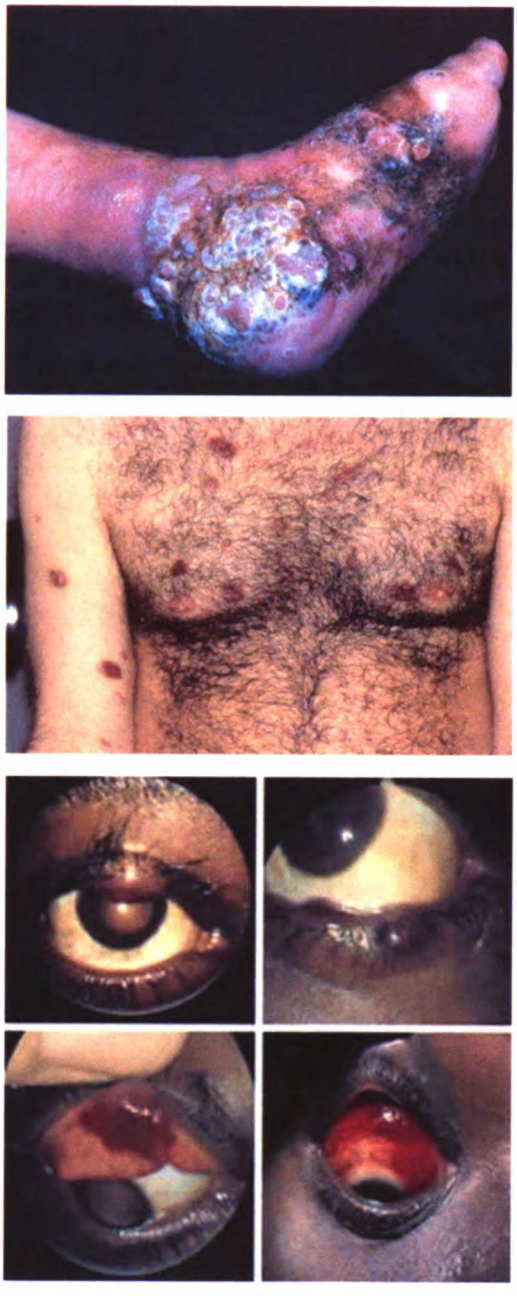

Figure 1-2.

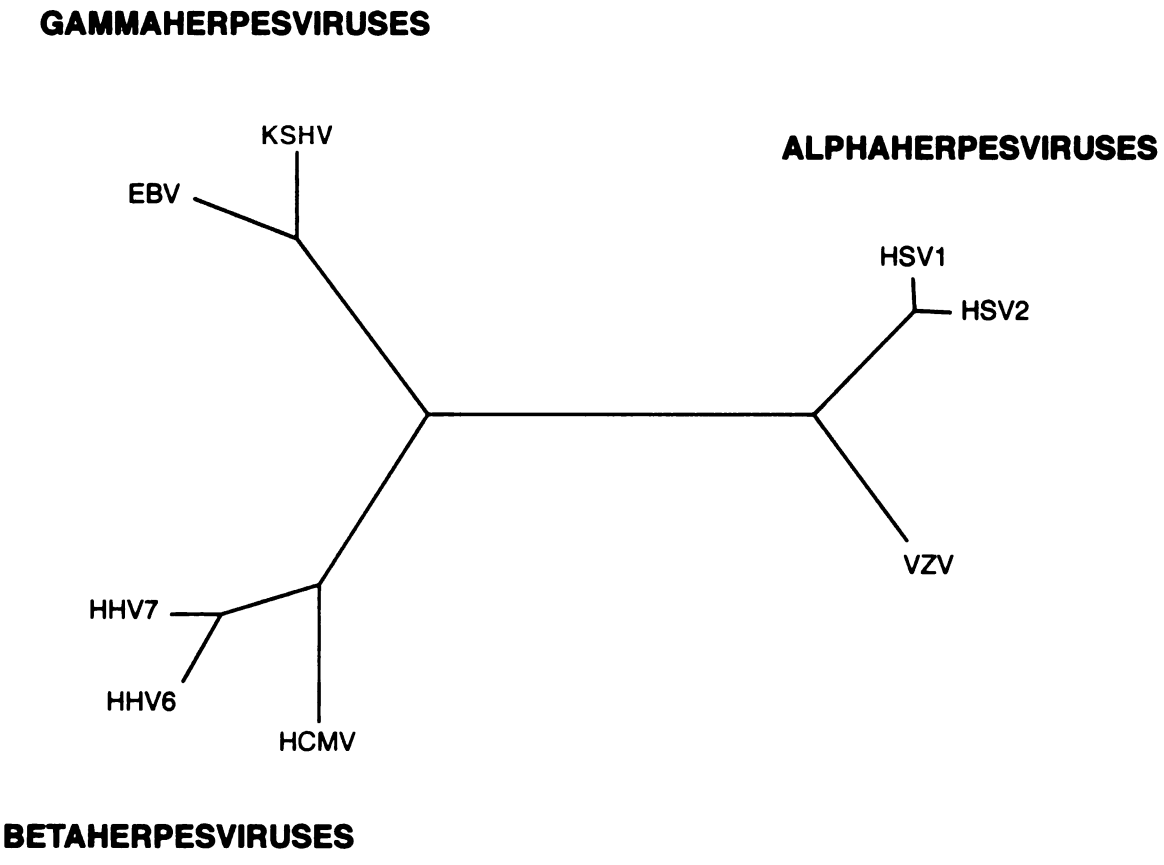
GAMMAHERPESVIRUSES
KSHV
EBV
ALPHAHERPESVIRUSES
HSV1
HSV2
VZV
HHV7
HHV6
HCMV
BETAHERPESVIRUSES

Figure 1-3. Schematic of Native Protease Construct. KSHV Protease is expressed as an N-terminal fusion protein to viral assembly protein. Assembly protein is also translated independently as a result of an internal promoter in the protease domain. The cleavage sequence for the release site (R-site), maturation site (M-site) and dimer disruptor site (D-site) are highlighted.

Figure 1-3.

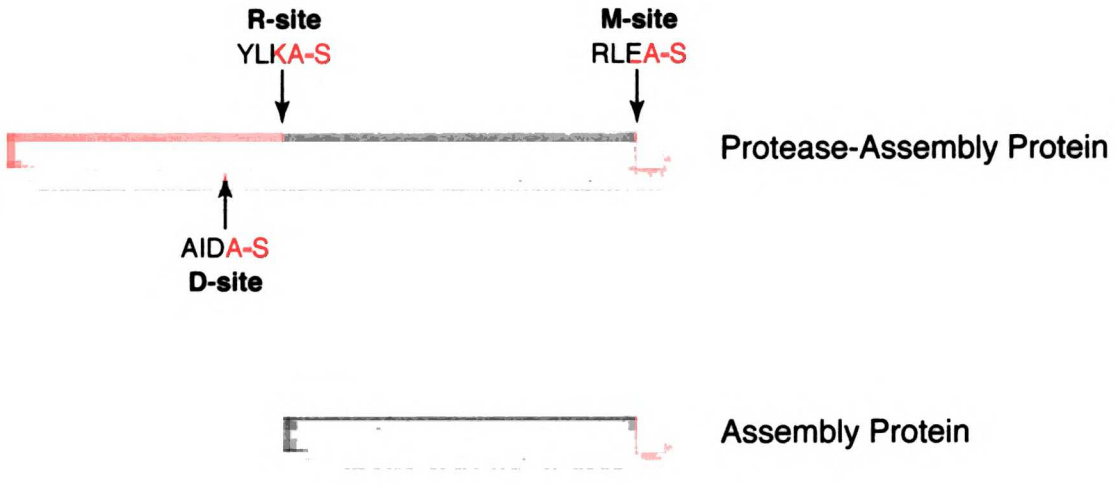
R-site
YLKA-S
M-site
RLEA-S
Protease-Assembly Protein
AIDA-S
D-site
Assembly Protein

Figure 1-4. Role of Protease in KSHV Lytic Replication. The protease is expressed as an inactive monomer fused to viral assembly protein. Assembly protein oligomerizes, binds major capsid protein and is translocated to the nucleus. The high local concentration of protease in the nascent capsid drives dimerization, resulting in protease activation and cleavage at the natural subsites. Cleavage events result in angularization of the capsid, scaffold release and DNA packaging. Following egress from the cell, the enveloped virion proceeds to infect other cells or hosts.

Figure 1-4.

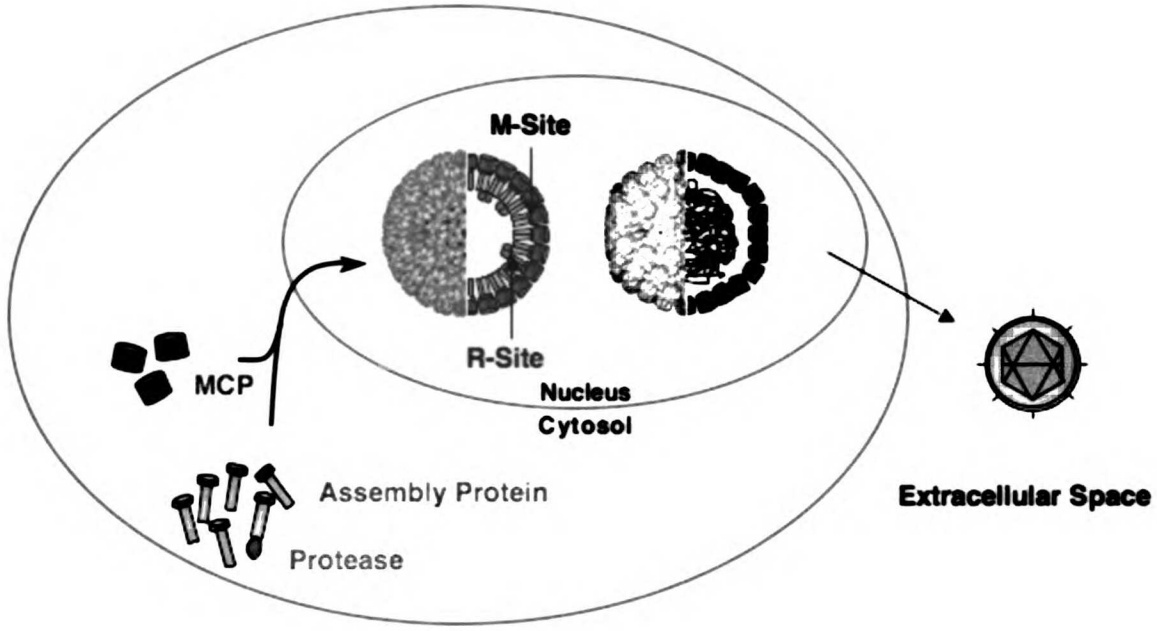
M-Site
R-Site
MCP
Nucleus
Cytosol
Assembly Protein
Protease
Extracellular Space

Figure 1-5. Crystal Structures of Human Herpesvirus Proteases. The catalytically active dimeric structures reveal each monomer to be a seven stranded β-barrel surrounded by six α-helices.

Figure 1-5.

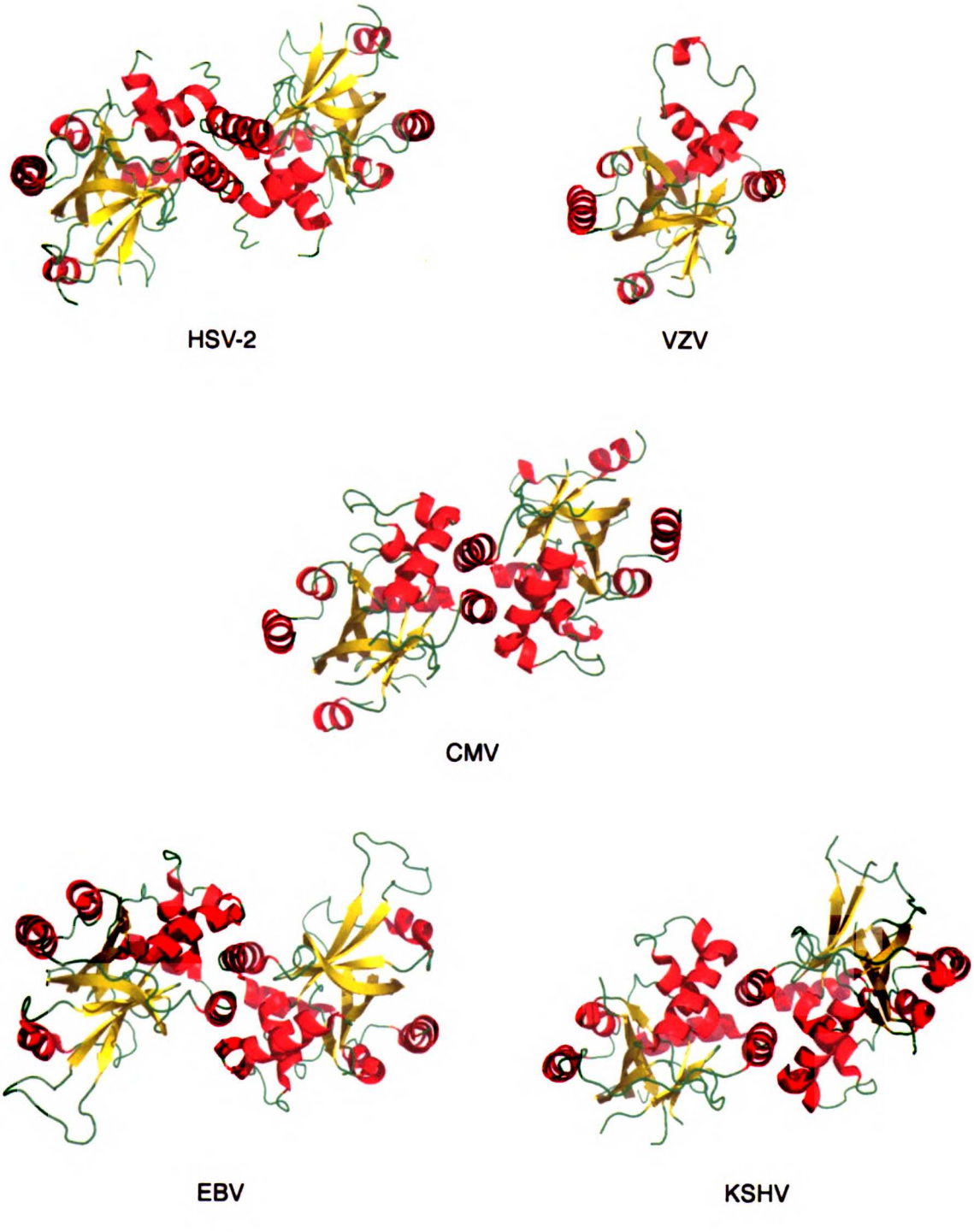

Figure 1-6. The Unique Catalytic Triad of KSHV Protease. Compared to the canonical serine protease triad (Ser-His-Asp), herpesvirus proteases utilize and alternate set of catalytic residues (Ser^{114}-His^{46}-His^{134}), which results in a significant reduction in catalytic turnover by the enzyme.

Figure 1-6.

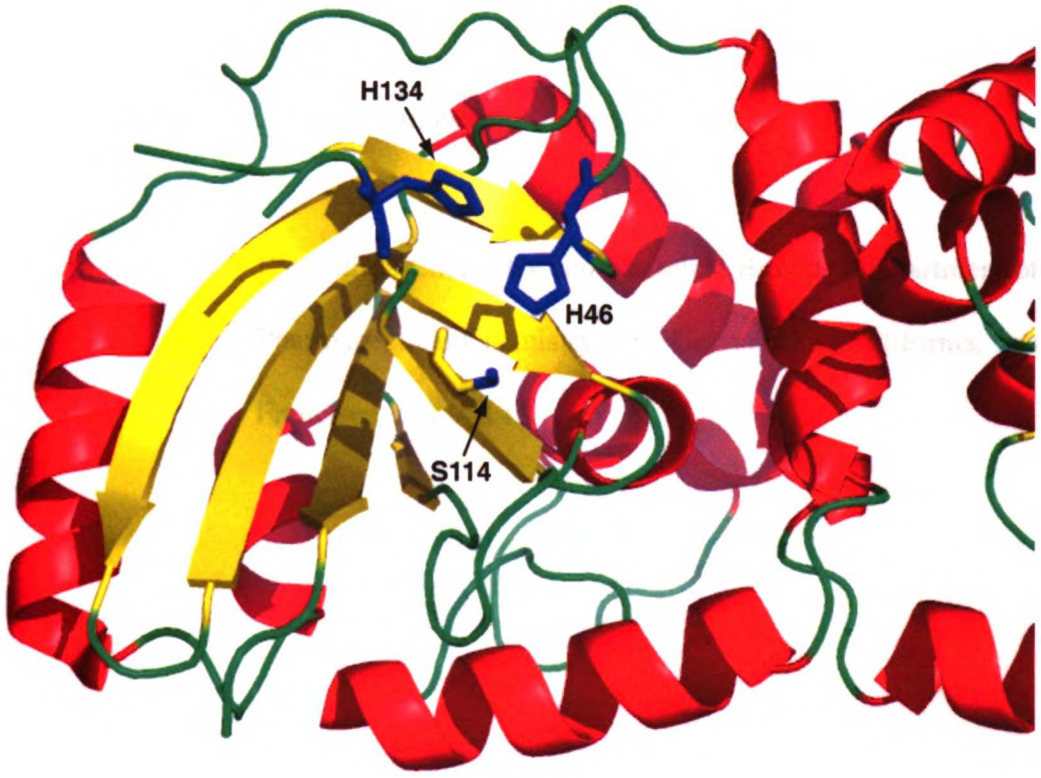

Chapter 2 | **Papa's Got a Brand New Tag: Advances in Identification of Proteases and their Substrates**

Alan B. Marnett and Charles S. Craik

Program in Chemistry and Chemical Biology, Department of Pharmaceutical Chemistry, The University of California, San Francisco, CA 94143

Reprinted from *Trends in Biotechnology*, 23(2), 59-64, copyright 2005 with permission from Elsevier.

Characterization of proteolytic enzymes and their substrates presents a formidable challenge in the context of biological systems. Despite the fact that an estimated 2% of the human genome encodes for proteases, only a small fraction of these enzymes have well-characterized functions. Much of the difficulty in understanding protease biology is a direct result of the complexity of regulation, localization and activation exhibited by this class of enzymes. Here, we focus on several recently developed techniques representing crucial advances toward identification of proteases and their natural substrates.

The Protease Problem

Currently, a total of 686 proteases and their homologues are defined in the human genome, most of which belong to one of five groups: the metallo, serine, cysteine, threonine or aspartyl proteases [1]. These enzymes are categorized by their mechanism of peptide bond hydrolysis in which either an amino acid residue in the serine, cysteine or threonine proteases or an activated water molecule in the metallo or aspartyl proteases, acts as the catalytic nucleophile. Although originally regarded as tenacious digestive enzymes, proteases have crucial roles in several exquisitely regulated physiological processes, including development, innate and adaptive immunity, cell cycle regulation and apoptosis. Clearly proteolysis is a finely choreographed event *in vivo* ensuring cleavage of the appropriate substrate at a precise time, location and cellular context. Aberrant regulation of endogenous protease activity results in a variety of life-threatening illnesses, such as hemophilia, cancer and heart disease. As a result, there is significant

interest in proteases as therapeutic targets. However, a lack of knowledge of the explicit roles of proteases has hindered these efforts, often resulting in unforeseen physiological effects following enzyme inhibition. Even well studied enzymes with known functions can have major roles in unexpected processes.

The possibility of multiple functions in proteases can complicate the situation further, as seen in the case of thrombin. The proteolytic activity of thrombin had been studied for decades in the selective processing of blood coagulation factors. It was then shown that thrombin could activate platelets and regulate the behavior of other cells by means of G protein-coupled protease activated receptors (PARs) [2]. PARs provide a mechanism by which a protease such as thrombin can act as a hormone and communicate directly with cells in addition to its role in the blood coagulation cascade.

Hence we are presented with the daunting challenge of understanding the physiological roles of all proteases, and the substrates they process, in their entirety (Figure 1). Recent advances in activity-based protease labeling reagents, substrate profiling and differential protein labeling methods provide promising methodologies for identification of active proteases and their natural substrates, and increase the number of tools available to the protease biologist, biochemist and cell biologist.

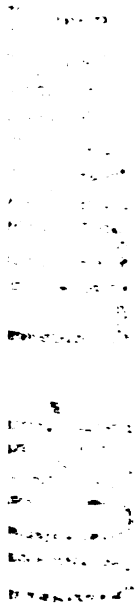

Identifying Proteases in a Cellular Context

A major challenge in elucidating the mechanism of protease involvement in a physiological process is the determination of all enzymes present. However, because of the tightly regulated controls over protease activity, mRNA levels frequently show little correlation to active protein. Even quantification of proteases at the protein level can be

misleading because enzymatic activity can vary as a result of differential levels of endogenous protease inhibitors. Therefore, the problem evolves from identification of proteases to identification of active proteases.

To determine the presence of active proteases within a lysate, cell, or tissue homogenate, mechanism-based inhibitors targeting the active site of the protease have been modified to incorporate a detection moiety such as biotin, a fluorophore, or a radioactive probe [3,4]. Referred to as activity based probes, these inhibitors predominantly label the active form of the enzyme through covalent bond formation with the catalytic center of the protease. They label a particular class of enzyme based on the reactivity of the electrophilic moiety but will not distinguish among different members of the class because specificity determinants are not present. Treatment of a given biological sample with an inhibitor, followed by SDS-PAGE analysis, detection and mass spectrometry, rapidly identifies the active enzymes (Figure 2a). The activity-based protein profiling approach has been applied to serine and cysteine proteases as a result of the formation of a covalent enzyme-inhibitor adduct during inactivation. However, analogous mechanism-based inhibitors are ineffective against the large class of metalloproteases and the important aspartyl proteases because water is the active nucleophile and no covalent intermediate is formed with the enzyme.

Recent work by Saghatelian et al circumvented the requirement for covalent bond formation during mechanism-based inhibition of metalloproteases [5]. A broad-spectrum zinc chelating hydroxamate was modified to include a benzophenone photocrosslinker in the S_2' position of the inhibitor, transforming the compound from a reversible to irreversible inhibitor upon irradiation at 365 nm. Incorporation of the crosslinker only

minimally affected the IC_{50} values against MMP-2, -7, and –9 and resulted in an inhibitor capable of discriminating between the active or zymogen form of the enzyme. Profiling both invasive and non-invasive melanoma cell lines for active metalloproteases, the authors discovered the dramatic upregulation of neprilysin activity, a peptide hormone processing enzyme, in invasive melanomas. Interestingly, the enzyme shares no sequence homology with known MMPs, and reflects the versatility of the probe in labeling many subgroups within the metalloprotease superfamily.

With the expansion of activity-based protein profiling technology to include metalloproteases, in theory greater than 90% of proteolytic enzymes might now be monitored in many complex cellular contexts. However, since currently available chemistries do not label all members of a given class, further development of the electrophilic moieties will be necessary to profile all proteases.

From Protease to Substrates

Another challenge is the identification of the natural substrates of a protease among the thousands of cellular proteins, which is critical for defining the role of "orphan" proteases with unknown function. Perhaps the most widely applied methodology in the search for protease substrates is the candidate approach, in which the substrate recognition sequence of the protease is determined and used to search the proteome for potential matches. Originally, determining substrate specificity was an arduous process that involved monitoring cleavage of commercially available individual peptides by HPLC. The emergence of substrate phage display in the early 1990's provided an unbiased method for selecting optimized protease cleavage sequences,

spanning both the prime and non-prime sides, from millions of potential substrates [6]. Although significantly more exhaustive in searching sequence space than screening individual substrates, the entire process can be technically challenging and time consuming even for a single enzyme.

A major advance toward increasing the throughput of substrate specificity determination was the development of positional scanning synthetic combinatorial libraries (Figure 2b) [7-15]. These libraries systematically profile each subsite of an enzyme, resulting in either non-prime or prime side preferred substrate sequences (see Table 1 for substrate nomenclature [16]). The tandem use of these libraries provides amino acid sequence data spanning P4-P4'. To date, substrate libraries are the fastest method for determining the specificity of an enzyme and have proven effective in identifying substrates of highly selective proteases. Although pooled libraries do not address cooperativity, arrays of single substrates and inhibitors printed on glass chips provide insight into cooperativity and might prove useful in understanding substrate specificity. With the development of positional scanning libraries, the time required to obtain protease specificity information has been reduced from days to minutes.

Substrate specificity information is proving crucial not only for identifying potential substrates, but also for incorporation of specificity determinants into inhibitors, providing highly selective activity based probes. These are useful in examining the role of an enzyme in a complex biological solution as well as dissecting structure/function relationships in a given protease. For example, Marnett et al used specific activity-based probes to determine the intramolecular communication between two independent active

sites of a herpesvirus protease, thereby identifying a novel site for therapeutic intervention [17].

Natural Substrate Discovery by Protein Labeling

Ultimately, defining the preferred substrate specificity to scan the proteome for potential substrates is an indirect method. Many factors, such as exosites and extended substrate interactions are not accounted for and may therefore render the libraries less applicable in certain cases. Accordingly, a methodology for monitoring substrates directly is desirable. Proteomic approaches to substrate identification have been reviewed and critically evaluated by Lopez-Otin and Overall [18].

Recently, two reports described differential protein labeling techniques for rapid identification of variations in protein levels as a result of protease cleavage that were used to identify both intra- and extracellular substrates. Tam et al employed an isotope coded affinity tag (ICAT) labeling strategy to monitor the relative abundance of proteins present in conditioned medium resulting from a human breast carcinoma cell line transfected with a matrixmetalloprotease (MT1-MMP) or vector control [19]. Decreased protein levels in the presence of MT1-MMP were attributed to direct substrate cleavage by the enzyme, whereas increased levels were attributed to sheddase activity of the enzyme, releasing membrane-bound substrate molecules from the cell into the medium (Figure 3a).

To examine the consequences of proteolysis on intracellular substrates, Bredemeyer et al subjected mouse lymphoma cell lysates to serine proteases Granzyme A or B [20]. Lysine residues of control or enzyme treated lysates were subsequently

modified by 1-(5-carboxypentyl)-1'-propylindocarbocyanide halide *N*-hydrosuccinimidyl ester (Cy3), or 1-(5-carboxypentyl)-1'-methylindodicarbocyanide halide *N*-hydrosuccinimidyl ester (Cy5), respectively, and combined for global protein analysis (Figure 3b). Fluorescence two-dimensional differential gel electrophoresis (FL-2D-DIGE) clearly identified several proteins with altered abundance as a result of protease cleavage. The procedure was used to identify novel substrates of Granzyme B, and the physiological consequence of cleaving these putative substrates is currently being pursued.

Prospects for the Future of Protease Biology

Over the past 20 years it has become clear that proteases range from non-specific digestive enzymes to specific processing enzymes, and are involved in many diverse and elegant physiological processes. It is anticipated that ultimately proteases will be implicated in virtually every biological process and understanding their role will become crucial in taking advantage of their tremendous therapeutic potential. Unfortunately, it is the breadth and variety of roles that make proteases extremely difficult to study because each protease varies in expression, activation and localization. Therefore, it is increasingly unlikely that a single methodology will be developed to identify every active protease, or every natural substrate. Substrate profiling of a protease is a rapid and powerful initial step towards deorphaning a protease. Protein labeling has recently been shown to be a promising technique with diverse applications. Specifically, activity-based probes, ICAT and 2D-FL-DIGE have been successfully employed for identification of active proteases and for the implication of presumed substrates in a biological context.

Coupled with substrate profiling, we expect that continued advances in mass spectrometry and proteomic analysis will result in new methods for use in combination on a protease specific basis.

However, the exciting recent advances in substrate identification highlight candidate substrates that must ultimately be validated in an actual biological setting. Frequently, the process of substrate validation is limited to traditional biochemical techniques and represents the rate-limiting step, requiring a specific inhibitor, antibody or knockout to address the issue. Although outside the scope of this article, the development of a methodology such as RNAi has decreased the time necessary for substrate validation relative to traditional techniques. It has been successfully used to reveal Taspase-1 cleavage of the mixed-lineage leukemia gene product [21]. Similar developments in the biological validation of substrates will complement the recent advances in identification of proteases and their natural substrates and help define the roles of proteases in all physiological processes.

Acknowledgements

We are grateful to Carly R.K. Loeb for critical review of the manuscript. This work was supported by a University of California President's Dissertation Year Fellowship (A.B.M) and NIH Grants GM56531 and CA72006 (C.S.C.).

REFERENCES

1. Rawlings, N.D. et al. (2004) MEROPS: the peptidase database. *Nucleic Acids Res* 32 Database issue, D160-164
2. Vu, T.K. et al. (1991) Molecular cloning of a functional thrombin receptor reveals a novel proteolytic mechanism of receptor activation. *Cell* 64 (6), 1057-1068
3. Greenbaum, D. et al. (2000) Epoxide electrophiles as activity-dependent cysteine protease profiling and discovery tools. *Chem Biol* 7 (8), 569-581
4. Liu, Y. et al. (1999) Activity-based protein profiling: the serine hydrolases. *Proc Natl Acad Sci U S A* 96 (26), 14694-14699
5. Saghatelian, A. et al. (2004) Activity-based probes for the proteomic profiling of metalloproteases. *Proc Natl Acad Sci U S A* 101 (27), 10000-10005
6. Matthews, D.J. and Wells, J.A. (1993) Substrate phage: selection of protease substrates by monovalent phage display. *Science* 260 (5111), 1113-1117
7. Greenbaum, D.C. et al. (2002) Small molecule affinity fingerprinting. A tool for enzyme family subclassification, target identification, and inhibitor design. *Chem Biol* 9 (10), 1085-1094
8. Harris, J.L. et al. (2000) Rapid and general profiling of protease specificity by using combinatorial fluorogenic substrate libraries. *Proc Natl Acad Sci U S A* 97 (14), 7754-7759
9. Barrios, A.M. and Craik, C.S. (2002) Scanning the prime-site substrate specificity of proteolytic enzymes: a novel assay based on ligand-enhanced lanthanide ion fluorescence. *Bioorg Med Chem Lett* 12 (24), 3619-3623

10. Salisbury, C.M. et al. (2002) Peptide microarrays for the determination of protease substrate specificity. *J Am Chem Soc* 124 (50), 14868-14870

11. Winssinger, N. et al. (2002) Profiling protein function with small molecule microarrays. *Proc Natl Acad Sci U S A* 99 (17), 11139-11144

12. Turk, B.E. et al. (2001) Determination of protease cleavage site motifs using mixture-based oriented peptide libraries. *Nat Biotechnol* 19 (7), 661-667

13. Thornberry, N.A. et al. (1997) A combinatorial approach defines specificities of members of the caspase family and granzyme B. Functional relationships established for key mediators of apoptosis. *J Biol Chem* 272 (29), 17907-17911

14. Zhu, L. et al. (2003) The role of dipeptidyl peptidase IV in the cleavage of glucagon family peptides: in vivo metabolism of pituitary adenylate cyclase activating polypeptide-(1-38). *J Biol Chem* 278 (25), 22418-22423

15. Winssinger, N. et al. (2004) PNA-encoded protease substrate microarrays. *Chem Biol* 11 (10), 1351-1360

16. Schechter, I. and Berger, A. (1967) On the size of the active site in proteases. I. Papain. *Biochem Biophys Res Commun* 27 (2), 157-162

17. Marnett, A.B. et al. (2004) Communication between the active sites and dimer interface of a herpesvirus protease revealed by a transition-state inhibitor. *Proc Natl Acad Sci U S A* 101 (18), 6870-6875

18. Lopez-Otin, C. and Overall, C.M. (2002) Protease degradomics: a new challenge for proteomics. *Nat Rev Mol Cell Biol* 3 (7), 509-519

19. Tam, E.M. et al. (2004) Membrane protease proteomics: Isotope-coded affinity tag MS identification of undescribed MT1-matrix metalloproteinase substrates. *Proc Natl Acad Sci U S A* 101 (18), 6917-6922

20. Bredemeyer, A.J. et al. (2004) A proteomic approach for the discovery of protease substrates. *Proc Natl Acad Sci U S A* 101 (32), 11785-11790

21. Hsieh, J.J. et al. (2003) Taspase1: a threonine aspartase required for cleavage of MLL and proper HOX gene expression. *Cell* 115 (3), 293-303

Figure 2-1. The protease problem: A) The human genome encodes an estimated 25,000 proteins, 686 of which are proteases and their homologues. Thrombin, a serine protease, cleaves fibrinogen and protease acitivated receptors-1 and -3 (PAR-1 and PAR-3). B) Identification of natural substrates may implicate an orphan protease in a physiological process.

Figure 2-1.

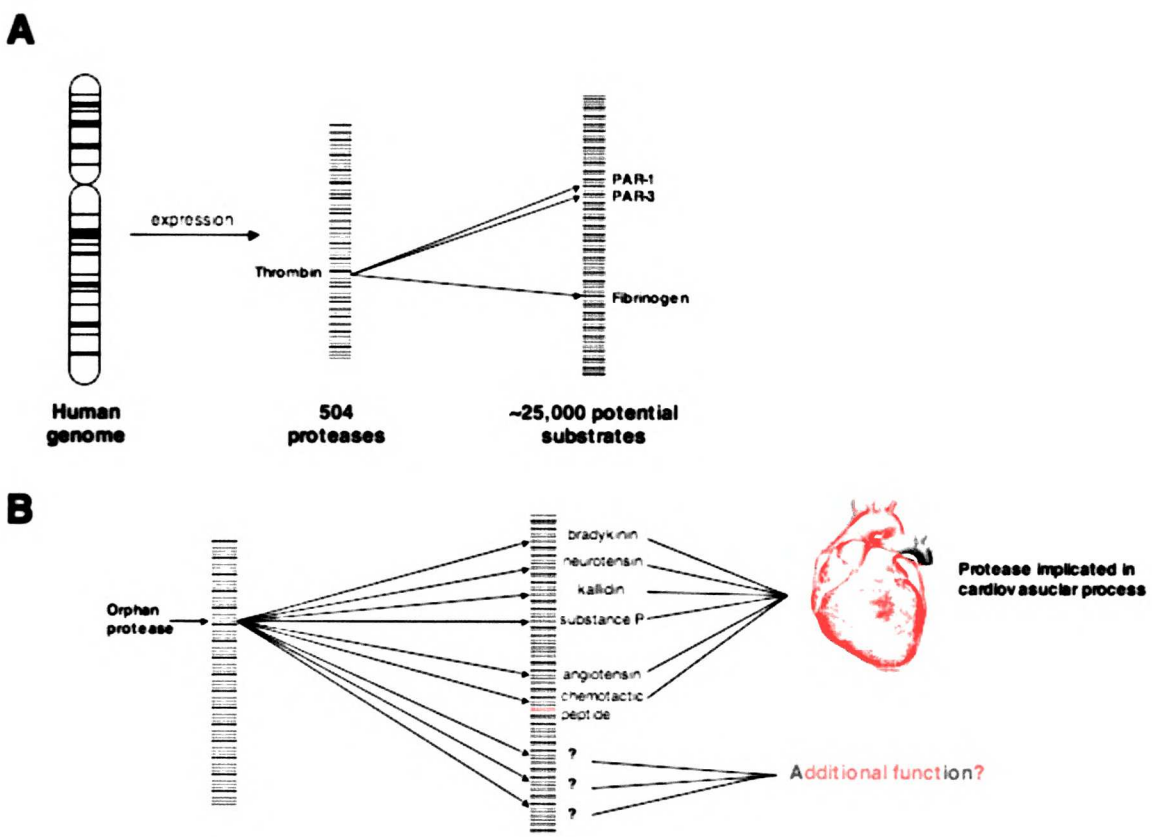
A
expression
Thrombin
PAR-1
PAR-3
Fibrinogen
Human genome
504 proteases
~25,000 potential substrates
B
Orphan protease
bradykinin
neurotensin
kallidin
substance P
angiotensin
chemotactic peptide
?
?
?
Additional function?
Protease implicated in cardiovascular process

Figure 2-2. Recently developed techniques for protease and substrate identification. A) Activity based profiling identifies active proteases (gray) using fluorescently labeled (red) inhibitors. Lysates from non-invasive (NI) and invasive (I) cells are analyzed by gel electrophoresis. B) Positional scanning libraries are used to determine substrate specificity of proteases from many organisms. Substrate information may be used to discover candidate protease substrates or to develop specific enzyme inhibitors.

Figure 2-2.

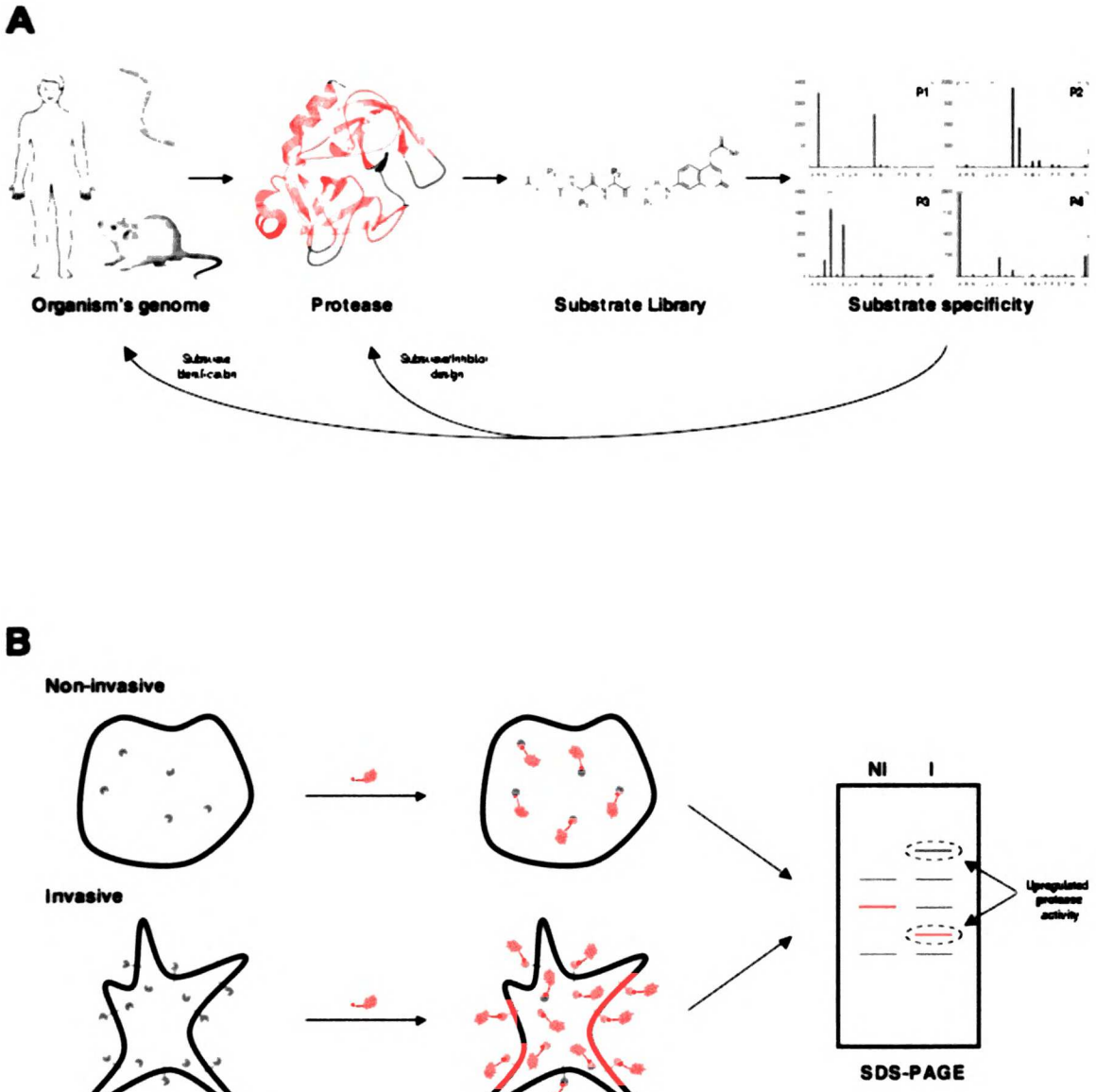
A
P1
P2
P3
P4
Organism's genome
Protease
Substrate Library
Substrate specificity
B
Non-invasive
Invasive
NI
I
SDS-PAGE

Figure 2-3. Mass spectrometry based approaches to substrate discovery. A) Isotope coded affinity tags containing $^{13}C_0$ (0) or $^{13}C_9$ (9) label thiols in differentially treated protein mixtures and are analyzed by mass spectrometry; m/z, mass to charge ratio. B) Differential gel electrophoresis is used to analyze differences in protein content following treatment with Cy3 (green) or Cy5 (red); MW, molecular weight; pI, isoelectric point.

Figure 2-3.

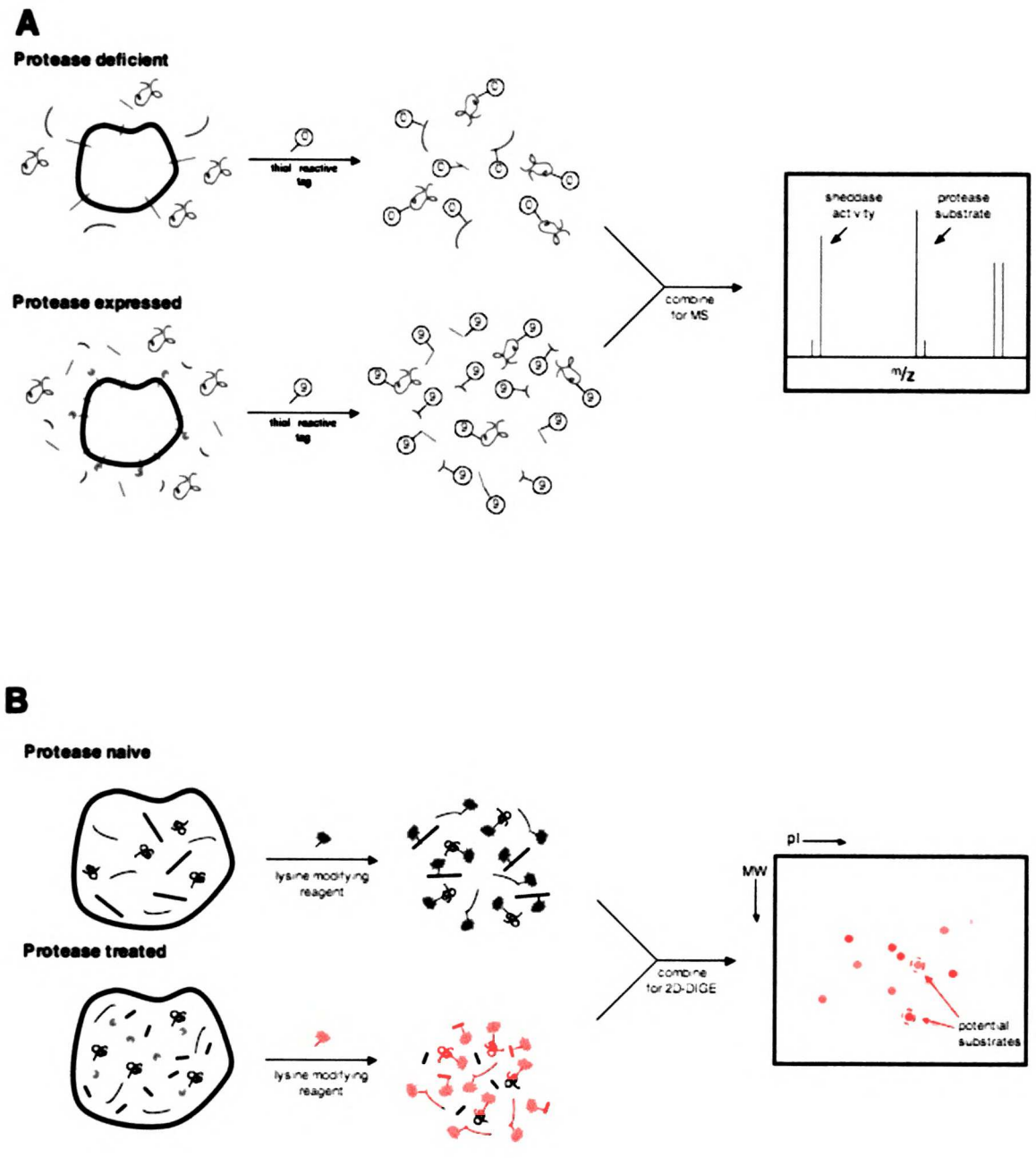
A
Protease deficient
thiol reactive tag
Protease expressed
thiol reactive tag
combine for MS
sheddase activity
protease substrate
m/z
B
Protease naive
lysine modifying reagent
Protease treated
lysine modifying reagent
combine for 2D-DIGE
pI
MW
potential substrates

Table 2-1. Currently available chemical-based substrate profiling methods. Libraries are categorized according to the substrate information obtained from each method. P4-P4' represent amino acids of the substrate, where cleavage occurs at the scissile bond, between P1 and P1'.

Table 2-1.

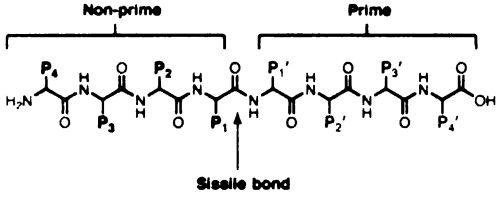

Specificity	Mechanism	Method	Detection	Refs
Non-prime side	Coumarin-based peptide substrates	Solution, 96-well plate	Fluorescence	[8,13]
	Peptide-based epoxide inhibitors	Solution inhibition, SDS–PAGE	Radioactivity	[7]
	Coumarin-based peptide substrates	Solid phase, glass slide	Fluorescence	[10]
	PNA-tagged peptidyl inhibitors	Solution inhibition, array hybridization	Fluorescence	[11,15]
Prime side	Lanthanide ion chelating substrates	Solution, 96-well plate	Fluorescence	[9]
	Biotinylated peptide substrates	Solution cleavage	Sequencing	[12]
Both	Peptide mixtures	Solution cleavage	Mass spectrometry	[14]

*Libraries are categorized according to the substrate information obtained from each method. P4-P4′ represent amino acids of the substrate where cleavage occurs at the scissile bond, between P1 and P1′.

Chapter 3 | Communication between the Spatially Separate Active Site and Dimer Interface of KSHV Protease Revealed by Small Molecule Inhibition

Alan B. Marnett, Anson M. Nomura, Nobuhisa Shimba, Paul R. Ortiz de Montellano and Charles S. Craik

Graduate Program in Chemistry and Chemical Biology, Department of Pharmaceutical Chemistry, The University of California, San Francisco, CA 94143

Reprinted from the *Proceedings of the National Academy of Sciences USA*, 101 (18), 6870-75,

Abbreviations: KSHV Pr, Kaposi's Sarcoma-associated herpesvirus protease; PS-SCL, positional scanning-synthetic combinatorial libraries; DFP, diisopropylfluorophosphate; ACC, 7-amino-4-carbamoylmethylcoumarin; H-Ala^{P}-$(OPh)_2$, diphenyl [α-aminoethyl] phosphonate; tBug, *tert*-butylglycine.

ABSTRACT

Structurally diverse organophosphonate inhibitors targeting the active site of the enzyme were used to investigate the relationship of the active site of the enzyme and the dimer interface of active, wild-type protease in solution. Positional scanning-synthetic combinatorial libraries (PS-SCL) revealed Kaposi's sarcoma-associated herpesvirus protease (KSHV Pr) to be a highly specific protease, even at sites distal to the peptide bond undergoing hydrolysis. Specificity results were used to synthesize a tetrapeptide diphenylphosphonate inhibitor of KSHV Pr. The transition state analog inhibitors covalently phosphonylate the active site serine upon inhibition, freezing the enzyme structure during catalysis. An NMR-based assay was developed to monitor the native monomer-dimer equilibrium in solution and was used to demonstrate the effect of protease inhibition on the quaternary structure of the enzyme. NMR, circular dichroism, and size exclusion chromatography analysis showed active site inhibition strongly regulates the binding affinity of the monomer-dimer equilibrium at the spatially separate dimer interface of the protease, shifting the equilibrium to the dimeric form of the enzyme. Furthermore, inhibitor studies revealed that the catalytic cycles of the spatially separate active sites are independent. These results provide direct evidence that peptide bond hydrolysis is integrally linked to the quaternary structure of the enzyme, establish a molecular mechanism of protease activation and stabilization during catalysis, and highlight potential implications of substoichiometric inhibition of the viral protease in developing herpesviral therapeutics.

INTRODUCTION

Herpesviruses represent one of the most prevalent viral families worldwide, with roughly 100 viruses identified, affecting almost every animal species. The nine known human herpesviruses are responsible for a variety of diseases ranging from relatively harmless ailments, such as cold sores (Herpes simplex virus-1, HHV-1) and chicken pox (Varicella-Zoster virus, HHV-3), to life threatening illnesses caused by cytomegalovirus (hCMV, HHV-5) and Kaposi's Sarcoma-associated herpesvirus (KSHV, HHV-8). In the United States, Kaposi's Sarcoma (KS) emerged as a serious problem in the early 1980's with the onset of AIDS and remains the most common neoplasm afflicting homosexual and bisexual men diagnosed with AIDS (1-3). Although the incidence of KS in this country has been reduced, in part, by AIDS-specific therapies such as highly active antiretroviral therapy (HAART)(4, 5), the prevalence of KSHV infection in Africa has increased severely in recent years. In fact, since 1985, KS has emerged as the most common cancer in men and the second most common cancer in women in Uganda and Zimbabwe, reflecting nearly a 20-fold increase in incidence in these countries (6).

Despite their clinical diversity, all human herpesviruses use a homologous virally encoded maturational protease for the formation of infectious virions. The 25 kDa protease is expressed as an inactive monomer fused to the viral assembly protein (AP), a capsid scaffolding protein. Upon formation of the immature viral capsid, the high local concentration of protease is thought to drive dimerization of monomers, which activates the protease and results in cleavage at the two natural proteolysis sites, the release site (R-site) and the maturation site (M-site), leading to formation of mature virions (7-9). Genetically modified herpes simplex virus (HSV) mutants indicated that these protease

cleavage events are essential for viral replication (10, 11). As a result, the protease has been implicated as a potential therapeutic target (12).

Although herpesvirus proteases are serine proteases, the crystal structures of HSV, VZV, EBV, hCMV, and KSHV proteases reveal both a novel catalytic triad and a novel protein fold (13-20). The altered Ser-His-His catalytic triad results in a severely disabled protease with a catalytic efficiency (k_{cat}/K_m) approximately four orders of magnitude reduced when compared to digestive serine proteases such as trypsin (21, 22). The proteases are active only as homodimers, yet despite burying nearly 2500 $Å^2$ of hydrophobic surface area upon dimerization, they interact with weak dissociation constants in the low micromolar range (23-25).

Several previous reports have provided circumstantial evidence supporting a link between activity and dimerization in herpesvirus proteases (18, 23, 26-29). The results in this report provide the first indisputable link between the active site serine and the dimer interface of wild-type protease in solution during catalysis and the first characterization of the individual active sites as catalytically independent. They also allow for conclusions addressing the contributions of substrate binding determinants to dimer stabilization, the molecular mechanism of activation and stabilization during the enzymatic reaction and potential impacts of targeting the active site of the protease in drug development.

MATERIALS AND METHODS

Recombinant Expression and Purification of KSHV Protease. A protease variant stable to autolysis (24), referred to in this paper as KSHV Pr, was expressed and purified from bacterial pellets following a previously described experimental protocol (30). Purified protease was stored in assay buffer (25 mM potassium phosphate, pH 8.0, 150 mM potassium chloride, 100 μM EDTA, and 1 mM β-mercaptoethanol) at 4°C.

Positional Scanning-Synthetic Combinatorial Library Analysis of KSHV Pr. KSHV Pr (200 μM) was added to 80 wells of a 96-well microtiter plate in assay buffer. A DMSO stock (1μL) of a completely diverse positional scanning synthetic combinatorial library (Choe and Craik, unpublished results; (31)) was added to each of the 80 wells resulting in 8000 compounds per well and 250 μM in total substrate per well. Substrate turnover was monitored for 1 h at 30°C as an increase in fluorescence using an excitation wavelength of 380 nm, an emission wavelength of 460 nm, and a cutoff filter at 435 nm. The reaction rates remained linear over the entire 1 h interval.

Synthesis and Kinetic Analysis of Individual ACC substrates. Single ACC substrates were synthesized and purified as described previously (31). Concentrated KSHV Pr was diluted into assay buffer and incubated at room temperature for 1 h to ensure monomer-dimer equilibrium was established. Aliquots of KSHV Pr (1 μM were placed in individual wells of a 96-well microtiter plate. Peptide substrate stocks were prepared in DMSO and added to each protease-containing well. Following initiation of substrate

hydrolysis, reaction rates were monitored by an increase in fluorescence over 60 minutes at 30°C, as described above.

Synthesis of Biotinyl-Pro-Val-Tyr-tBug-Gln-Ala^P-(OPh)$_2$. Diphenyl [α-aminoethyl] phosphonate (H-Ala^P-(OPh)$_2$) was synthesized as reported by Oleksyszyn (32). Biotinyl-Pro-Val-Tyr-tBug-Gln-OH was synthesized by standard Fmoc-chemistry using 2-chlorotrityl chloride resin. Biotin was incorporated in order to monitor protease labeling by a streptavidin-horseradish peroxidase blot (33). The peptide was purified by reversed-phase HPLC and characterized by mass spectrometry.

Free peptide (230 mg, 0.27 mmol), PyBOP (140 mg, 0.27 mmol), and diisopropylethylamine (104 mg, 0.81 mmol) were dissolved in DMF (2 mL). H-Ala^P-(OPh)$_2$ (75 mg, 0.27 mmol) was added and the reaction was stirred for 18 h at room temperature. Solvent was removed and the resulting oil was purified by reversed-phase HPLC, yielding pure product, as confirmed by mass spectrometry. Active and inactive diastereomers were separated by an additional reversed-phase HPLC purification. Stocks of Biotinyl-Pro-Val-Tyr-tBug-Gln-Ala^P-(OPh)$_2$ were prepared in DMSO and stored at -20°C.

Characterization of Protease Inhibition. Inhibition was monitored based on the method of Kitz and Wilson (34). Prior to addition of inhibitor, KSHV Pr was diluted to 10 μM in activity buffer and incubated at room temperature for 1 h to establish the monomer-dimer equilibrium. Upon addition of inhibitor (100X in DMSO), aliquots of

the reaction solution were removed at various timepoints and remaining protease activity was monitored (at 2.□ μM protease) as described above.

Inhibitor titration experiments were performed by incubation of a range of Biotinyl-Pro-Val-Tyr-tBug-Gln-Ala^{P}-$(OPh)_2$ (2.3 - 20 μM) with KSHV Pr (20 μM) for 60 hours. KSHV Pr was incubated for 3 hours at room temperature prior to addition of inhibitor. Following complete inhibition, reactions were diluted to a final protease concentration of 200 nM, incubated for 2 hours at room temperature, and characterized by monitoring remaining activity as described above. The experimental data is an average of four repetitions. Methods for determination of protease concentration and derivation of theoretical activity curve are described in supporting information.

DFP inhibition was carried out using KSHV Pr (20 μM) in assay buffer at room temperature. As a result of the high rate of hydrolysis in buffer, DFP was added in 100 μM aliquots every 16 h for 64 h. A portion of the inhibition reaction was removed, diluted to 6 μM, incubated at room temperature for 1 h, and subsequently analyzed by size exclusion chromatography. Biotinyl-Pro-Val-Tyr-tBug-Gln-Ala^{P}-$(OPh)_2$ (100 μM) was then added to the original inhibition reaction and the solution was incubated at room temperature for an additional 72 h prior to size exclusion analysis.

FPLC Analysis of Quaternary Structure of the Protease. KSHV Pr (20 μM) was incubated with inhibitor (95 μM) or DMSO at 25 °C until no residual protease activity was detectable. Aliquots of enzyme were removed from each reaction and diluted to final concentrations of 5 μM and 300 nM. Prior to size exclusion analysis, samples were incubated for 1 h at room temperature. Monomer-dimer equilibrium of the protease was

examined at both concentrations using a Superdex 75 analytical column (Pharmacia) equilibrated in assay buffer. KSHV Pr dimers and monomers eluted at approximately 10.5 mL and 12 mL, respectively, as originally reported by Pray et al (24).

Nuclear Magnetic Resonance and Circular Dichroism Spectroscopy. NMR experiments were measured on a Bruker 500 MHz Avance NMR instrument equipped with a 5 mm triple resonance cryoprobe with a z axis gradient coil. NMR spectra were recorded using 500 μL solutions in H_2O/D_2O (93%/7%), 25 mM potassium phosphate pH 8.0, 0.1 mM EDTA, 1 mM β-mercaptoethanol, at 27 °C. ^{13}C-^{1}H heteronuclear single quatum coherence (HSQC) spectra of KSHV Pr labeled with methyl ^{13}C methionine (25 μM) with and without inhibitor were recorded in 2.5 h with 64 scans, 128 and 512 complex t_1 and t_2 increments with 3000 Hz F_1 and 7002 Hz F_2 spectral widths, respectively. The ^{13}C-^{1}H HSQC spectrum of KSHV Pr Met197L labeled with methyl ^{13}C methionine was recorded with 4 scans using the same increments and spectral widths as KSHV Pr spectra.

Circular dichroism spectra were acquired on a Jasco 710 spectropolarimeter using a 0.1 cm pathlength sample cuvette. Inhibitor and DMSO-treated protease samples (30 μM) were dialyzed against assay buffer to remove DMSO and excess inhibitor. Melting curves were generated by monitoring the elipticity at 222 nm as a function of temperature. Temperature was varied from 10 to 90 °C at a rate of 0.5 °C min^{-1}.

RESULTS

Substrate Profiling of KSHV Pr using Positional Scanning Synthetic Combinatorial Libraries and Assay Development. The PS-SCL results reveal KSHV Pr to be a highly specific protease (Figure 1). As expected, based on the strongly conserved P1-alanine seen in all herpesvirus protease cleavage site sequences, alanine is the preferred amino acid at the at the P1 position. Despite lack of an obvious substrate binding pocket at the S4 position upon examination of the crystal structure of KSHV Pr, a dramatic preference for aromatic residues is demonstrated at P4.

Given the ability of the protease to cleave the tetrameric ACC substrates in the PS-SCL library, individual ACC substrates were synthesized to develop an improved enzyme activity assay. Although the optimal sequence from the library was Tyr (P4), Val (P3), Nle (P2), Ala (P1), poor solubility limited the utility of this extremely hydrophobic substrate. Accordingly, norleucine was replaced by glutamine to improve solubility. Additionally, previous results suggest a preference for tert-butylglycine at the P3 position, so this information was also incorporated into the modified substrate (35). Kinetic analysis of the tetrameric ACC substrate revealed Michaelis-Menten kinetics with a K_m of 81 ± 11 μM and a k_{cat} of 0.022 ± 0.001 s^{-1}, a dramatic improvement over the intramolecularly quenched substrate previously used in enzymatic assays (24). Furthermore, the vastly increased solubility of the tetrapeptide substrate (high micromolar) as compared to the intramolecularly quenched substrate (low micromolar) renders it far superior for use in enzymatic activity assays. In addition to assay development, substrate specificity information was used to design a potent peptide-based

organophosphonate inhibitor. Analysis of a natural protease cleavage site (release site) resulted in incorporation of proline and valine at the P6 and P5 positions, respectively, to increase binding affinity of the inhibitor (Figure 2).

Covalent Modification of the Active Site Serine by an (α-aminoalkyl)phosphonate diphenyl ester. Incubation of KSHV Pr with the diphenylphosphonate revealed time-dependent inhibition of enzymatic activity. A streptavidin blot identified the biotinylated inhibitor bound to KSHV Pr, whereas no inhibitor was detected bound to a point mutant removing the catalytic serine of the protease (S114A/S204G) (data not shown).

Because of the low activity of the protease, enzyme concentration could not be significantly decreased without approaching the limit of detection of the assay. Therefore, inhibitor concentrations were limited as well. Kinetic analysis, even at the lowest concentrations of inhibitor, indicated that the inhibitor concentration is still well above the K_i (data not shown). As a result, a $k_{obs}/[I]$ of 6 $M^{-1}s^{-1}$ was determined as a lower limit for k_{inact}/K_i.

To determine whether the enzyme reactivated due to hydrolysis of the phosphonylated protease, KSHV Pr (30 μM) was incubated with inhibitor (100 μM) in activity assay buffer until all enzyme activity was removed. Excess inhibitor was removed by size exclusion chromatography and activity assays using aliquots of the protease solution revealed no significant recovery of activity over 100 h.

Determination of Monomer-Dimer Equilibrium Upon Protease Inhibition. Other than the N-terminus of the protein, only one methionine is present in KSHV Pr. Its

location in the middle of the dimer interface made it a potentially attractive probe for monitoring the oligomerization state of the protease. As predicted, HSQC analysis of a sample of KSHV Pr labeled with methyl ^{13}C methionine revealed three peaks in the protease spectrum corresponding to the N-terminus, Met197(monomer) and Met197(dimer). These assignments were confirmed by an Met197L variant (36), eliminating two of the peaks, and by increasing protease concentration and observing a concomitant increase in the dimeric peak. As seen in Figure 3A, a comparison of inhibitor or DMSO treated protease reveals the disappearance of the M197 (monomer) peak. The NMR experiments demonstrate that upon protease inhibition, the equilibrium is shifted dramatically towards dimeric protease. Gel filtration of the inhibited sample confirmed the dramatic dimer stabilization (Figure 3B).

In order to compare relative protease stability, KSHV Pr was subjected to thermal denaturation in the presence and absence of the inhibitor (Figure 3C). Strikingly, a 13 °C increase in T_m was observed in the inhibited dimer. In native (DMSO treated) protease, a steady loss in elipticity occurred from 20 °C to 57 °C, which was followed by a rapid loss in elipticity. The gradual loss in elipticity was attributed to a dimer to monomer transition, while the sharp transition represented global folding. However, the inhibited dimer shifts the dimer-monomer transition nearly 30 °C, to 65 °C. It appears that the dimer is the predominant species, even at 50 °C, and if an inhibited monomeric species exists, it is very short lived.

KSHV Pr inhibition was also observed following incubation with the smaller organophosphate, DFP. A small population of monomeric protease remained after inhibition of the enzyme with DFP, even following multiple additions of DFP. This

population was not inhibited monomer, reflective of a higher K_d of the DFP-inhibited dimer, but rather was uninhibited protease at a concentration well below the dimerization constant. Accordingly, given the high rate of hydrolysis of DFP in water and the exceedingly low population of uninhibited dimers remaining in solution, most of the DFP added to the reaction simply hydrolyzed prior to further protease inhibition. This was confirmed by addition of the significantly more stable diphenylphosphonate to the sample, which resulted in complete inhibition of the remaining protease (Figure 4).

Protease Active Sites are Capable of Simultaneous Substrate Processing. Upon incubation of various molar equivalents of inhibitor with high concentrations of protease, three protease species were obtained: uninhibited, singly inhibited, and doubly inhibited dimers. Given the increased stability of the inhibited dimer, remaining activity of the singly inhibited dimer was examined by diluting the inhibited protease sample, thereby minimizing contributions from the uninhibited dimer. The remaining activity profile clearly demonstrates that singly inhibited protease was still active, even though one active site was locked in a transition-state conformation (Figure 5 and supporting information). In fact, singly inhibited protease showed increased activity relative to the uninhibited protease at low concentrations as a result of the augmented stability of the singly inhibited species. Titration of the remaining active site with increased molar equivalents of inhibitor resulted in a complete loss of protease activity. The experimental data fits well to a theoretical model based on two fully active, independent active sites.

DISCUSSION

As a result of their critical role in the viral life cycle, there has been significant interest in herpesvirus proteases as therapeutic targets. Indirect evidence has associated dimerization with activity in herpesvirus proteases; however a direct link between the active site and the dimer interface has not been illustrated. Furthermore, the effect of substrate binding determinants and oxyanion formation on dimerization is also unknown. In the present work, we clearly demonstrate the link between the active site and dimer interface and elucidate the importance of substrate structural features on enzymatic catalysis. We also show the independence of catalytic activity of the two active sites within an intact dimer. Taken together, the data suggests several important impacts of active site inhibition of the protease and supports the hypothesis that an alternative mechanism of protease inhibition may also be effective as a therapeutic strategy.

To address the association of the active site and dimer interface, an active site inhibitor was synthesized. Organophosphonates provide insight into the catalytic mechanism as a result of their structural similarity to the tetrahedral transition state upon covalent modification of the active site serine (37, 38). Accordingly, upon covalent inhibition of KSHV Pr, the enzyme is locked in a conformation arguably most relevant to catalysis. Development of a transition-state analog inhibitor has allowed for a glimpse into the solution properties of the enzyme during the process of peptide bond hydrolysis. In the protein-protein interaction required for activation, one monomer acts essentially as a cofactor for the other monomer, repositioning and stabilizing the opposite active site, nearly 20 Å away, for catalysis. However, this repositioning is transient, as dimers and monomers are in constant exchange. Upon covalent modification of the active site serine

by a phosphonate inhibitor, the monomer-dimer equilibrium is dramatically shifted toward dimer, demonstrating a clear structural link between the oxyanion hole and the dimer interface.

To analyze the contribution of binding determinants to enzyme stabilization, an inhibitor was synthesized containing an optimized peptide sequence for KSHV Pr. A PS-SCL was used to assess protease specificity, providing an exhaustive search of potential substrates. The PS-SCL substrates provide a completely diverse profiling of amino acid preference at each position, P4-P1, in the context of a tetrapeptide substrate. KSHV Pr proved to be a highly specific protease with distinct specificity even at the P4 position, where a strict aromatic preference was observed, despite the lack of an obvious binding pocket upon examination of the crystal structure.

In an effort to separate the importance of oxyanion formation from substrate binding, the effects of inhibition by diisopropylfluorophosphate on quaternary structure were examined. Upon inhibition with DFP, the protease exhibited the same structural stability as seen with diphenylphosphonates. Since DFP is devoid of any structural binding determinants, it appears that generation of the oxyanion alone is sufficient for stabilization. Although not directly transferable to substrate hydrolysis, this result strongly suggests that generation and stabilization of the oxyanion as opposed to substrate binding pockets are the predominant factors in protease activation and stabilization.

Similarly, it is unlikely that the inhibitors are capable of inducing dimerization by binding to and reacting with the monomer. This is reflected by the difficulty in attaining complete inhibition of the protease with DFP. This situation indicates that DFP completely hydrolyzes before reacting with the protease, presumably as a result of the

low levels of dimer present in the low concentration of uninhibited protease remaining. If the inhibitor was capable of inducing dimerization by reacting with the monomer, the difficulty in obtaining complete inhibition would not exist. This model is confirmed by the inhibition of the remaining protease upon addition of a diphenylphosphonate, which is significantly less susceptible to hydrolysis. Additionally, no dimer stabilization is observed upon incubation of the diphenylphosphonate with a catalytically inactive protease variant with the active site serine removed or upon incubation with a monomeric variant (M197D) containing a complete catalytic triad (data not shown). These findings suggest that substrate binding of monomers *in vivo* does not induce the active form of the enzyme and that catalysis only occurs upon binding to the active dimeric form of the protease.

We suggest the mechanism for stabilization involves four structural elements, the active site serine, the loop supporting the oxyanion hole, helix 6, and helix 5 (Figure 6). Phosphonylation of the active site serine by the inhibitor yields a tetrahedral phosphonate adduct, placing a strong negative charge in the oxyanion hole. Based on previous mutagenesis data and crystal structures with inhibitor bound, it is anticipated that this conformation is stabilized by the formation of hydrogen bonds to Arg143, through a water molecule, and the backbone amide of Arg142, located on the oxyanion hole loop (19, 26, 39, 40). This interaction provides additional stabilization of the oxyanion hole loop not present in the native dimer. The oxyanion hole loop, in turn, establishes hydrogen bonds and electrostatic interactions with residues in helix 6, including an interaction from Arg144 to Asp216 and two H-bonds from Arg209 to the carbonyl of Ala139 (18). Helix 6, stabilized by H-bonds to the oxyanion hole loop and by intrahelix

H-bonds, is directly connected to helix 5, the main dimer interface contact, which is stabilized by intrahelix H-bonds, as well as significant intermolecular contacts to the adjacent monomer. These results provide a potential pathway for protease activation and stabilization and are consistent with crystallographic data on CMV Pr mutants (26).

Assuming that all herpesvirus proteases undergo a similar mechanism of activation, conservation of the proposed structural connection between the active site and dimer interface was examined. Among α, β, and γ human herpesvirus proteases, the oxyanion hole loop is nearly identical, with 8 of 9 residues functionally conserved. The α herpesviruses appear to have diverged from the β and γ herpesviruses in helix 6, resulting in only 3 of 14 functionally conserved residues among the entire family. Despite the structural diversity in most of helix 6, Arg209 is strictly conserved among all herpesviruses. Perhaps the most striking difference is the absence of Asp216 in the α herpesviruses, one of the main intersubunit contacts seen in KSHV Pr. Interestingly, the α herpesvirus proteases contain an Arg at this position, and the corresponding Arg (144) in the oxyanion hole loop seen in KSHV Pr, is a Val in the α-herpesviruses, eliminating a potentially unfavorable charge-charge interaction. Examination of the crystal structure of HSV-2 confirms that the Arg establishes stabilizing intersubunit H-bonds with the oxyanion hole loop. The high conservation of the oxyanion hole loop and the rational differences seen in helix 6, support the hypothesis that the extended network of intersubunit H-bonds and electrostatic interactions established upon formation of the transition state may contribute significantly to the exceptional stabilization of the dimer upon inhibition.

Given the intimate association of the active site to the dimer interface, we sought to address the possibility of communication between active sites during catalysis. A number of dimeric proteins with spatially separate active sites have been reported in which binding of substrate induces asymmetry in the dimer, preventing substrate binding at the second active site (41, 42). Inhibitor titration results demonstrate that the active sites of KSHV Pr support catalysis independently, and do not exhibit half-of-sites reactivity. This finding has significant implications for therapeutically targeting the protease with transition-state analog inhibitors.

Although many of the details regarding the fate of the protease during capsid maturation remain unclear, a singly inhibited stabilized protease may alter many steps in the process. Substoichiometric amounts of inhibitor stabilize the dimer and result in singly inhibited active protease that could affect capsid processing, DNA encapsidation, and ultimately viral replication. The development of a selective peptide based transition state inhibitor provides the opportunity to determine the efficacy at inhibiting viral replication.

Considering the reduced catalytic activity and the shallow active site of herpesvirus proteases and the difficulty in achieving high inhibitor concentrations inside the capsid, alternative mechanisms of protease inhibition may be more successful. The direct link between transition-state stabilization and dimerization has been established and highlights the possibility of inhibiting activity by preventing association of monomers. Using the assays developed in this report, it is possible that the dimer interface, with increased surface area and deep grooves, will provide a target more amenable to inhibitor development.

ACKNOWLEDGEMENTS

We thank Sami Mahrus, Dr. Jeohoong Sun and Dr. Christopher Eggers for helpful discussions and critical review of the manuscript. We also thank Prof. Jon Ellman for generously supplying ACC resin used to synthesize the protease substrate. This work was supported by a Research Training in Chemistry and Chemical Biology NIH Training Grant GM64337-01 (A.B.M) and a NIH Grant GM56531 (P.O.M. and C.S.C.).

REFERENCES

1. Goedert, J. J. (2000) *Semin Oncol* **27,** 390-401.
2. Gottlieb, G. J., Ragaz, A., Vogel, J. V., Friedman-Kien, A., Rywlin, A. M., Weiner, E. A. & Ackerman, A. B. (1981) *Am J Dermatopathol* **3,** 111-4.
3. Hymes, K. B., Cheung, T., Greene, J. B., Prose, N. S., Marcus, A., Ballard, H., William, D. C. & Laubenstein, L. J. (1981) *Lancet* **2,** 598-600.
4. Parisi, S. G., Mazzi, R., Sarmati, L., Carolo, G., Uccella, I., Rianda, A., Nicastri, E., Concia, E. & Andreoni, M. (2002) *AIDS* **16,** 1089-91.
5. Tam, H. K., Zhang, Z. F., Jacobson, L. P., Margolick, J. B., Chmiel, J. S., Rinaldo, C. & Detels, R. (2002) *Int J Cancer* **98,** 916-22.
6. Dedicoat, M. & Newton, R. (2003) *Br J Cancer* **88,** 1-3.
7. Welch, A. R., Woods, A. S., McNally, L. M., Cotter, R. J. & Gibson, W. (1991) *Proc Natl Acad Sci U S A* **88,** 10792-6.
8. Weinheimer, S. P., McCann, P. J., 3rd, O'Boyle, D. R., 2nd, Stevens, J. T., Boyd, B. A., Drier, D. A., Yamanaka, G. A., DiIanni, C. L., Deckman, I. C. & Cordingley, M. G. (1993) *J Virol* **67,** 5813-22.
9. Sheaffer, A. K., Newcomb, W. W., Brown, J. C., Gao, M., Weller, S. K. & Tenney, D. J. (2000) *J Virol* **74,** 6838-48.
10. Preston, V. G., Coates, J. A. & Rixon, F. J. (1983) *J Virol* **45,** 1056-64.
11. Gao, M., Matusick-Kumar, L., Hurlburt, W., DiTusa, S. F., Newcomb, W. W., Brown, J. C., McCann, P. J., 3rd, Deckman, I. & Colonno, R. J. (1994) *J Virol* **68,** 3702-12.
12. Waxman, L. & Darke, P. L. (2000) *Antivir Chem Chemother* **11,** 1-22.

13. Chen, P., Tsuge, H., Almassy, R. J., Gribskov, C. L., Katoh, S., Vanderpool, D. L., Margosiak, S. A., Pinko, C., Matthews, D. A. & Kan, C. C. (1996) *Cell* **86,** 835-43.

14. Tong, L., Qian, C., Massariol, M. J., Bonneau, P. R., Cordingley, M. G. & Lagacé, L. (1996) *Nature* **383,** 272-5.

15. Shieh, H. S., Kurumbail, R. G., Stevens, A. M., Stegeman, R. A., Sturman, E. J., Pak, J. Y., Wittwer, A. J., Palmier, M. O., Wiegand, R. C., Holwerda, B. C. & Stallings, W. C. (1996) *Nature* **383,** 279-82.

16. Qiu, X., Culp, J. S., DiLella, A. G., Hellmig, B., Hoog, S. S., Janson, C. A., Smith, W. W. & Abdel-Meguid, S. S. (1996) *Nature* **383,** 275-9.

17. Qiu, X., Janson, C. A., Culp, J. S., Richardson, S. B., Debouck, C., Smith, W. W. & Abdel-Meguid, S. S. (1997) *Proc Natl Acad Sci U S A* **94,** 2874-9.

18. Reiling, K. K., Pray, T. R., Craik, C. S. & Stroud, R. M. (2000) *Biochemistry* **39,** 12796-803.

19. Hoog, S. S., Smith, W. W., Qiu, X., Janson, C. A., Hellmig, B., McQueney, M. S., O'Donnell, K., O'Shannessy, D., DiLella, A. G., Debouck, C. & Abdel-Meguid, S. S. (1997) *Biochemistry* **36,** 14023-9.

20. Buisson, M., Hernandez, J. F., Lascoux, D., Schoehn, G., Forest, E., Arlaud, G., Seigneurin, J. M., Ruigrok, R. W. & Burmeister, W. P. (2002) *J Mol Biol* **324,** 89-103.

21. Register, R. B. & Shafer, J. A. (1997) *J Virol* **71,** 8572-81.

22. Khayat, R., Batra, R., Massariol, M. J., Lagacé, L. & Tong, L. (2001) *Biochemistry* **40,** 6344-51.

23. Buisson, M., Valette, E., Hernandez, J. F., Baudin, F., Ebel, C., Morand, P., Seigneurin, J. M., Arlaud, G. J. & Ruigrok, R. W. (2001) *J Mol Biol* **311,** 217-28.

24. Pray, T. R., Nomura, A. M., Pennington, M. W. & Craik, C. S. (1999) *J Mol Biol* **289,** 197-203.

25. Cole, J. L. (1996) *Biochemistry* **35,** 15601-10.

26. Batra, R. K., R; Tong, L. (2001) *Nat Struct Biol* **8,** 810-817.

27. Darke, P. L., Cole, J. L., Waxman, L., Hall, D. L., Sardana, M. K. & Kuo, L. C. (1996) *J Biol Chem* **271,** 7445-9.

28. Margosiak, S. A., Vanderpool, D. L., Sisson, W., Pinko, C. & Kan, C. C. (1996) *Biochemistry* **35,** 5300-7.

29. Schmidt, U. & Darke, P. L. (1997) *J Biol Chem* **272,** 7732-5.

30. Unal, A., Pray, T. R., Lagunoff, M., Pennington, M. W., Ganem, D. & Craik, C. S. (1997) *J Virol* **71,** 7030-8.

31. Harris, J. L., Backes, B. J., Leonetti, F., Mahrus, S., Ellman, J. A. & Craik, C. S. (2000) *Proc Natl Acad Sci U S A* **97,** 7754-9.

32. Oleksyszyn, J., Subotkowska, L., Mastalerz, P. (1979) *Synthesis*, 985-986.

33. Thornberry, N. A., Peterson, E. P., Zhao, J. J., Howard, A. D., Griffin, P. R. & Chapman, K. T. (1994) *Biochemistry* **33,** 3934-40.

34. Kitz, R. a. W., I.B. (1962) *J Biol Chem* **237,** 3245-3249.

35. Ogilvie, W., Bailey, M., Poupart, M. A., Abraham, A., Bhavsar, A., Bonneau, P., Bordeleau, J., Bousquet, Y., Chabot, C., Duceppe, J. S., Fazal, G., Goulet, S., Grand-Maître, C., Guse, I., Halmos, T., Lavallée, P., Leach, M., Malenfant, E.,

O'Meara, J., Plante, R., Plouffe, C., Poirier, M., Soucy, F., Yoakim, C. & Déziel, R. (1997) *J Med Chem* **40,** 4113-35.

36. Shimba, N., Nomura, A. M., Marnett, A. B. & Craik, C. S. (2004) *J Virol in press.*

37. Sampson, N. S. & Bartlett, P. A. (1991) *Biochemistry* **30,** 2255-63.

38. Oleksyszyn, J. & Powers, J. C. (1991) *Biochemistry* **30,** 485-93.

39. Liang, P. H., Brun, K. A., Feild, J. A., O'Donnell, K., Doyle, M. L., Green, S. M., Baker, A. E., Blackburn, M. N. & Abdel-Meguid, S. S. (1998) *Biochemistry* **37,** 5923-9.

40. Khayat, R., Batra, R., Qian, C., Halmos, T., Bailey, M. & Tong, L. (2003) *Biochemistry* **42,** 885-91.

41. Biemann, H. P. & Koshland, D. E., Jr. (1994) *Biochemistry* **33,** 629-34.

42. Xiao, B., Singh, S. P., Nanduri, B., Awasthi, Y. C., Zimniak, P. & Ji, X. (1999) *Biochemistry* **38,** 11887-94.

SUPPORTING INFORMATION

This equation is derived based on a model in which the spatially separate active sites are independent and a given subunit is fully active, even if the other subunit is inhibited. That is, inhibition at one active site does not affect the activity at the adjacent active site. The experimental values fit well to a model in which the protease K_d is 1.8 μM, very close to the value of 1.3 μM measured by activity assays (1).

In order to determine the amount of theoretical activity expected at a given inhibitor concentration, two values must be taken into consideration, 1) the amount of active dimer in the sample, and 2) the amount of singly, doubly, and un-inhibited protease in the sample.

[M] = concentration of monomers (μM), $[E_T]$ = total enzyme (μM), and [AD] = concentration of fully active dimers (μM) and is calculated from $([E_T] - [M])/2$.

According to the following equation,

$$[M] = \frac{\sqrt{1 + \frac{8(E_T)}{K_d}} - 1}{4/K_d}$$

at 20 μM total enzyme (E_T), and a K_d= 1.8 μM,

[M] = 3.82 μM

[AD] = 8.09 μM

Upon addition of a substoichiometric amount of inhibitor, three species are obtained and their relative abundance is dependent of the amount of inhibitor added and can be described by probability theory using the following equations: x^2 (doubly), $2x-2x^2$ (singly), and $(1-x)^2$ (uninhibited) as shown in Figure 7.

For example, addition of 0.5 molar equivalents of inhibitor to 10 μM fully active dimer ([AD]), would result in the following proportions:

Uninhibited: $(1-0.5)^2 * 10 = 2.5$ μM

Doubly inhibited: $(0.5)^2 * 10 = 2.5$ μM

Singly inhibited: $(2*0.5 - 2*0.5^2) * 10 = 5$ μM

At 20 μM KSHV Pr, however, only 80.9% of the protease is in the active conformation (16.18 μM / 20 μM).

Upon inhibition, only two of the three potential species are active, the singly inhibited and the uninhibited protease. Therefore, estimation of the concentrations of these two species in the assay provides an estimate of the expected protease activity upon dilution.

Total protease activity = singly inhibited + uninhibited

The singly inhibited species

The following equations were established, where x represents the molar equivalent of inhibitor added:

$(2x-2x^2)*[AD]$

gives the concentration of singly inhibited [AD]. Upon 1:100 dilution, the equation becomes:

$((2x-2x^2)*[AD])/100$

and based on the hypothesis that a singly inhibited dimer (one active site) has exactly half the activity of a fully active dimer (two active sites), the equation becomes:

$((2x-2x^2)*[AD])/200$

since the singly inhibited dimer is dramatically more stable, it will not reequilibrate upon dilution. Therefore, this equation represents the concentration of protease in fully active dimer equivalents.

The uninhibited species

The uninhibited protease contains two parts: 1) the portion of enzyme that is originally active dimer (16.18 μM) that is uninhibited following inhibitor titration, and 2) the portion of enzyme originally in monomeric form (3.82 μM).

$(1-x)^2*[AD]$

gives the concentration of uninhibited protease from the active dimeric population (in dimeric equivalents).

$(1-x)^2*[AD]*2$

gives concentration of uninhibited protease in monomer equivalents.

$(1-x)^2*[AD]*2 + 3.82$

yields the total amount of uninhibited protease in monomer equivalents.

$((1-x)^2*[AD]*2 + 3.82)/100$

gives the total concentration of protease following dilution.

Since the protease is uninhibited, it will reequilibrate upon dilution to give a fraction of active dimers and inactive monomers, and this can be calculated using the equilibrium equation described above.

$$\frac{\sqrt{1+\frac{8\frac{(1-x)^2*16.18+3.82}{100}}{1.8}}-1}{\frac{4}{1.8}}$$

which gives the amount of monomers present upon reequilibration of the enzyme. Accordingly, the amount of active dimers present can be represented as the total enzyme upon dilution minus the amount of monomers divided by two.

$$\frac{\left(\frac{16.18(1-x)^2+3.82}{100}\right)-\left(\frac{\sqrt{1+\frac{8\frac{(1-x)^2*16.18+3.82}{100}}{1.8}}-1}{\frac{4}{1.8}}\right)}{2}$$

This equation represents the total amount of active dimers present upon reequilibration of uninhibited protease. The sum of this number and the singly inhibited species gives the

total amount of active protease. This number can be compared to the amount of active dimer in the sample untreated with inhibitor to give the relative remaining activity, described by the following equation:

$$\frac{\left(\frac{8.09*(2x-2x^2)}{200}\right)+\frac{\left(\frac{16.18(1-x)^2+3.82}{100}\right)-\left(\frac{\sqrt{1+\frac{8\frac{(1-x)^2*16.18+3.82}{100}}{1.8}}-1}{2.222}\right)}{2}}{\left(\frac{E_T/100-\left(\frac{\sqrt{1+\frac{8(E_T/100)}{1.8}}-1}{2.222}\right)}{2}\right)}$$

Finally, only 16.18 μM enzyme is in the active dimeric conformation (16.18 / 20 = 0.809) in the reaction. Although the remaining 3.82 μM would reequilibrate upon dilution after comlete inactivation of the active dimeric species, the amount of active dimer in that solution would only result in 4.7% remaining activity, a very minor amount. Therefore, as an approximation of theoretical activity expected, we divided the x-value by 0.809 in

the final equation to reflect the fact that the theoretical data would titrate at 0.809, or at an amount of inhibitor capable of inhibiting the total amount of active species, giving the following final equation.

$$\frac{\left(\frac{8.09*(2x/0.809-2(x/0.809)^2)}{200}\right)+\left(\frac{16.18(1-x/0.809)^2+3.82}{100}\right)-\left(\frac{\sqrt{1+\frac{8\frac{(1-x/0.809)^2*16.18+3.82}{100}}{1.8}}-1}{2.222}\right)}{\left(E_T/100-\left(\frac{\sqrt{1+\frac{8(E_T/100)}{1.8}}-1}{2.222}\right)\right)}$$

REFERENCES (SUPPORTING INFORMATION)

1. Shimba, N., Nomura, A. M., Marnett, A. B. & Craik, C. S. (2004) *J Virol* 78(12) 6657-65

Figure 3-1. Substrate specificity profile of KSHV Pr. Complete diversity positional scanning-synthetic combinatorial library results for each subsite P4-P1. The y-axis reflects picomolar concentrations of free ACC generated per second upon enzymatic hydrolysis. The x-axis reveals the spatially addressed amino acid at each position, "n" represents norleucine, a methionine isostere. *In vivo* protease cleavage sites are: R-site (YLKA), M-site (RLEA), and D-site (AIDA).

Figure 3-1.

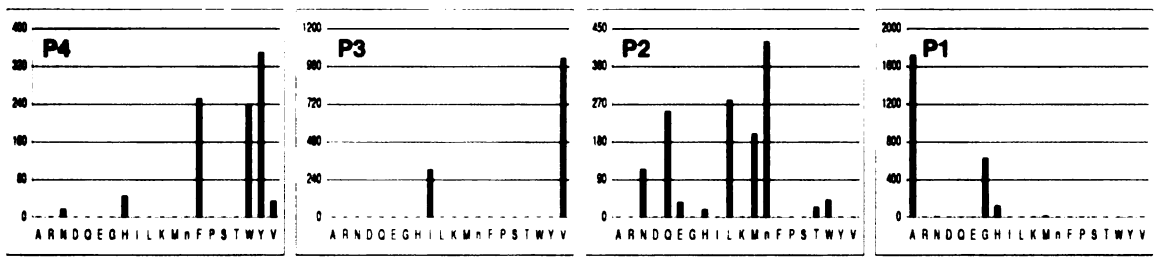

Figure 3-2.

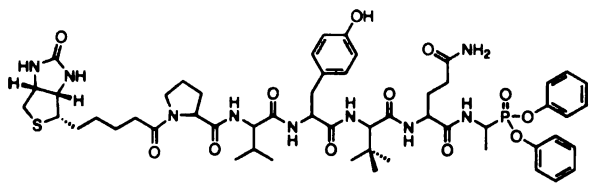

Figure 3-3. Inhibition of KSHV Pr stabilizes the dimeric conformation. (A) HSQC spectra of KSHV Pr labeled with methyl ^{13}C methionine following incubation with or without inhibitor. Signals reveal solution oligomeric state of protease: M1, N-terminus; M197(M), monomer; M197(D), dimer. (B) Size exclusion chromatography of KSHV Pr. Following treatment with inhibitor (solid) or DMSO (dashed), KSHV Pr (5 μM) was incubated for 1 h prior to analysis on Superdex 75 analytical column. (C) Circular dichroism temperature melts. Elipticity of KSHV Pr (30μM) following incubation with (solid) or without (dashed) inhibitor was monitored at 222 nm as a function of temperature.

Figure 3-3.

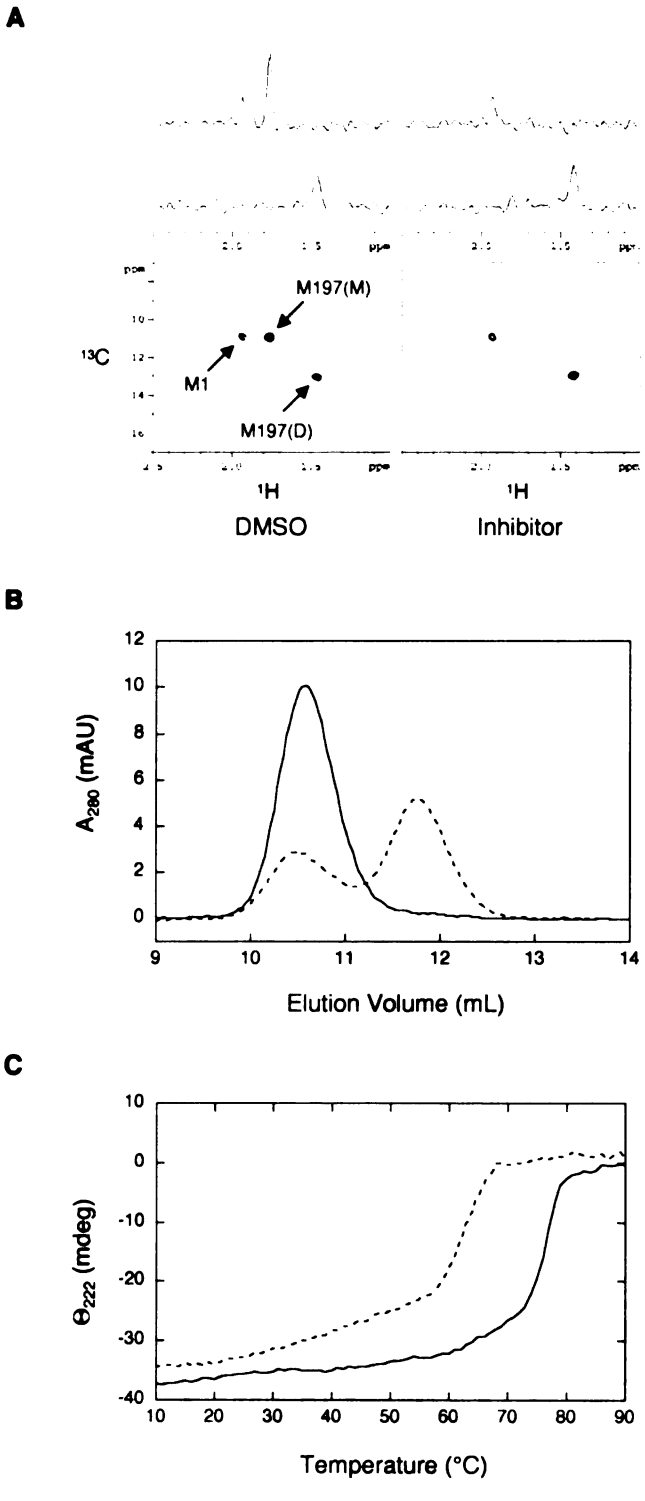
A
M197(M)
M1
M197(D)
13C
1H
DMSO
1H
Inhibitor
B
A280 (mAU)
Elution Volume (mL)
C
θ222 (mdeg)
Temperature (°C)

Figure 3-4. DFP induces stabilization of the KSHV Pr dimer. Protease (6 μM) was incubated with DMSO (long dashes), DFP (solid line), or DFP followed by diphenylphosphonate (short dashes). Samples were equilibrated at room temperature for 1 h prior to analysis.

Figure 3-4.

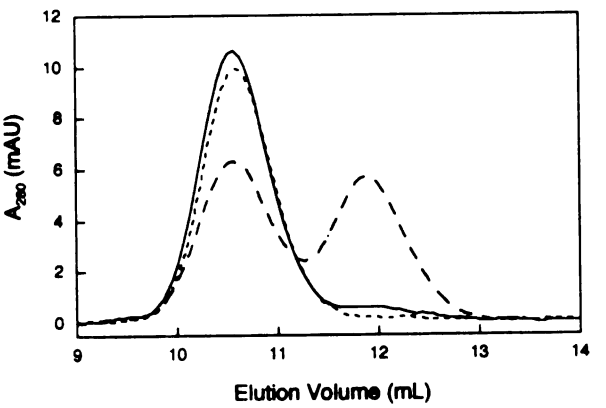

Figure 3-5. Inhibitor titration reveals independent active sites. Protease (20 μM) was incubated with various molar equivalents of inhibitor followed by dilution of the protease to 200 nM. Remaining protease activity was monitored as described. Experimental data (solid) fit well to theoretical data (dashed) generated using a K_d of 1.8 μM as described in the supporting information. Kinetic schemes show the effect of inhibitor (red circle) on KSHV Pr equilibrium (X, inactive protease; circle, active protease). Although negligible, the equilibrium between doubly inhibited protease and inhibited monomers was omitted for clarity.

Figure 3-5.

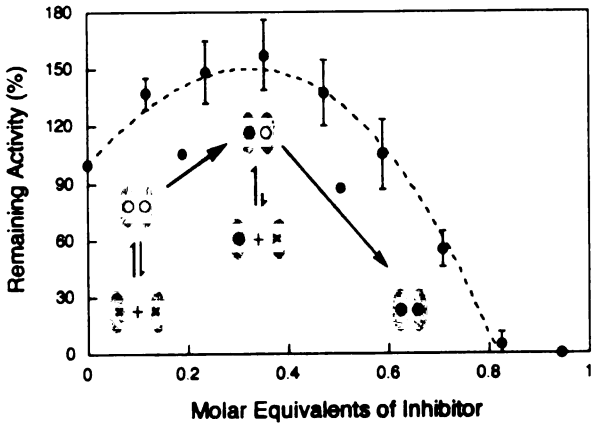
Remaining Activity (%)
180
150
120
90
60
30
0
0
0.2
0.4
0.6
0.8
1
Molar Equivalents of Inhibitor

Figure 3-6. Structural model for protease stabilization upon inhibition. Catalytic Ser114, His46, His134 (orange), Oxyanion residues Arg143 and Arg142 (yellow, density for Arg142 unsolved in crystal structure), critical sidechains colored by atom (oxygen, red; nitrogen, blue; carbon, green), all others represented only as backbone chain for clarity.

Figure 3-6.

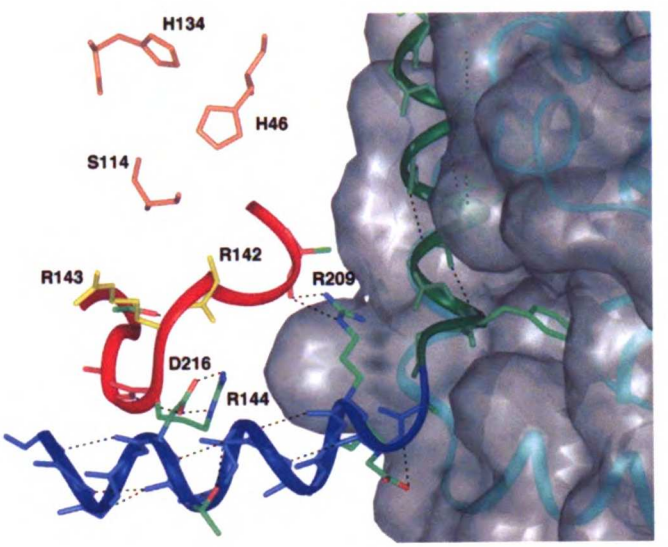

Figure 3-7. Probability distribution of inhibited KSHV Pr species. The three possible species are shown: uninhibited dimers (short dashes); doubly inhibited dimers (long dashes); and singly inhibited dimers (solid).

Figure 3-7.

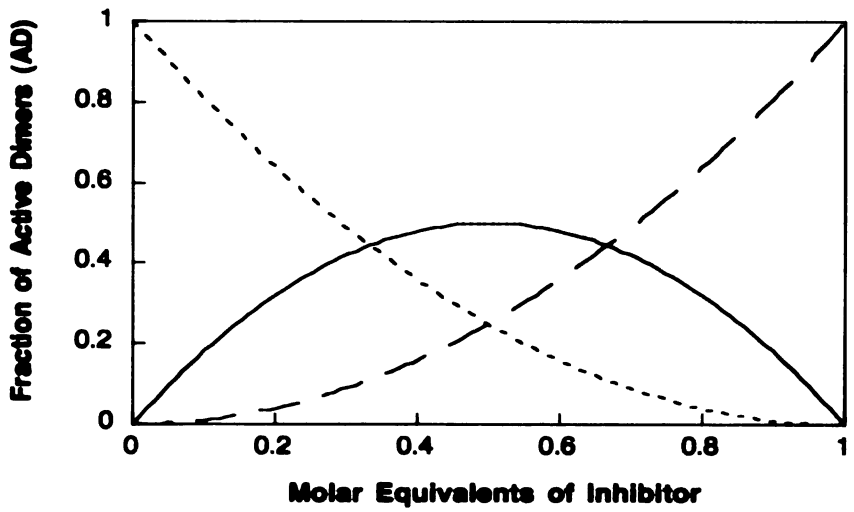
Fraction of Active Dimers (AD)
1
0.8
0.6
0.4
0.2
0
0
0.2
0.4
0.6
0.8
1
Molar Equivalents of Inhibitor

Chapter 4 | Induced Structure: A Transitional Helix Switch that Regulates Enzyme Activity

Alan B. Marnett*, Anson M. Nomura*, Nobuhisa Shimba, Volker Dotsch and Charles S. Craik

Chemistry and Chemical Biology Graduate Program, Department of Pharmaceutical Chemistry, The University of California, San Francisco, CA 94143

*These authors contributed equally to this work

Organisms have evolved diverse mechanisms for controlling the activity of enzymes, particularly proteolytic enzymes. Kaposi's Sarcoma-associated herpesvirus (Human herpesvirus 8) encodes a protease that is activated by homodimerization at high enzyme concentrations during lytic replication. Although crystal structures of the homodimer have been solved for six family members[1-7], a lack of structural information regarding the inactive monomeric enzyme has prevented characterization of the dimerization-dependent mechanism of activation. We have assigned the backbone NMR resonances of an inactive monomeric variant and used the chemical shift data, in combination with circular dichroism and an active site inhibitor, to describe an oligomerization-induced helical switch of enzyme activity, characterized by the folding and unfolding of 31% α-helical content of the protein. To demonstrate the necessity of helix formation for activity, we have engineered an intramolecular disulfide bond, which regulates protease activity by preventing or promoting unfolding of the helices in the presence of an oxidant or reductant, respectively. Here we show the molecular details of a concentration-dependent timing mechanism that regulates an essential biological function of a human pathogen through acquisition of quaternary structure.

Proteolysis has devastating consequences when unregulated but can serve as a powerful binary switch when controlled. Human herpesvirus 8 encodes a protease whose activity is required for viral lytic replication and virion formation[8-11]. To prevent premature substrate processing, the protease is expressed as an inactive monomeric precursor fused to viral scaffolding proteins. Association of scaffolding proteins during assembly of the immature capsid results in a high local concentration inside the nascent virion that drives protease dimerization, which in turn activates the enzyme[12-16]. The activated protease cleaves the scaffolding proteins from the capsid shell, resulting in angularization of the capsid, packaging of DNA and ultimately formation of a mature infectious particle.

Although crystal structures of active, recombinant dimer have been solved for nearly all family members, no structural information exists regarding the inactive monomer and therefore the detailed regulatory mechanism for this important class of potential therapeutic targets has remained unknown. The dimeric structure consists of two seven-stranded β-barrels each surrounded by six α-helices and shows that each monomer contains an active site that is distal from the dimer interface. Previous reports demonstrated a conformational change upon loss of dimerization by circular dichroism, however the results were qualitative and did not provide the molecular details of the structural transition upon activation[17, 18]. Subsequently, inactive variants of cytomegalovirus protease were produced that assume a dimeric conformation dramatically different from the native enzyme. These distorted dimers lacked electron density in an α-helix near the active site of the enzyme and although many of the conformational changes were attributed to the mutations themselves, the work suggested

a possible mechanism of activation involving folding of an α-helix near the active site[17]. Despite this progress, the molecular details of enzyme regulation upon dimerization have remained unknown. We have shown previously that inhibition of wild-type enzyme using an active site directed transition-state analog dramatically stabilized the dimeric form of the enzyme, reflecting the intimate structural association between the active site and the dimer interface[19]. These results led to a model of protein communication from the active site to the dimer interface upon small molecule inhibition.

These findings and the reagents they provided presented KSHV protease as an ideal model system in which to study the concept of enzyme regulation upon acquisition of quaternary structure. Generation of a single point mutation at the interface of KSHV protease (M197D) resulted in an inactive monomeric variant of the enzyme. Importantly, both circular dichroism and NMR analysis revealed the variant monomer to be structurally indistinguishable from the wild-type monomer produced by heat induced dissociation of the native enzyme[18] (and unpublished results). Our finding that active site inhibition of the enzyme resulted in a complete shift in the equilibrium to dimer provided us with the unique opportunity to structurally analyze both purely monomeric and dimeric enzymes reflective of the native monomer and dimer that normally exist in dynamic equilibrium. Because of the relationship between activity and dimerization, monitoring structural changes as a function of dimerization relates directly to the mechanism of activation of the enzyme. Dramatic structural changes were observed upon comparison of monomeric and dimeric enzyme.

We have used NMR and circular dichroism to characterize the solution secondary structure of an inactive monomeric variant and to identify a novel mechanism of protease

activation. Analysis of the purely monomeric and dimeric proteins by circular dichroism revealed a dramatic loss of 31% α helicity upon dissociation of the dimer (Figure 1). This loss of secondary structure was defined and localized by multi-dimensional NMR. The poor solution behavior of the protease, coupled with its size, precluded the use of most traditional NMR triple resonance experiments for backbone assignments. Despite these limitations, utilization of selected triple resonance experiments and amino acid specific labeling resulted in assignment of 94% of the backbone α carbons, including all but one of the residues in helices 5 and 6. Analysis of the Cα chemical shifts of monomeric KSHV protease provides amino acid specific secondary structural information through chemical shift measurements[20-22] and shows a strong correlation with helices observed in the dimeric crystal structure, with the exception of helices 5 and 6 (Figure 2a). Observed chemical shift index data for C', N and H^N support this finding (data not shown).

Hydrogen/deuterium NMR experiments were used to measure the rates of exchange of labile protons in the dimeric enzyme with the bulk solvent. These experiments identify stable structural elements in well-folded proteins as well as protein folding intermediates, by exploiting the differential lifetimes of backbone amides, which depend on individual solvent exposure or participation in hydrogen bonding interactions. The exchange experiments on KSHV protease further support the chemical shift secondary structural analysis by showing that the β-barrel and first four α-helices of the monomer are stable, while helices 5 and 6 unfold upon dissociation (Figure 2c). The difference between protection of the six helices is not due to different inherent exchange rates, as calculation of predicted exchange rates based on primary sequence cannot

account for the differences[23]. Therefore, the loss in protection of the two carboxyl terminal helices is due to differential stability of the helices. Based on the dimeric crystal structure, the unfolding of helices 5 and 6 accounts for 22 out of 71 (31%) residues in α helical secondary structure, corroborating the circular dichroism results.

The activity of this viral enzyme appears to be regulated by a local "helical switch" rather than global protein unfolding. To support this mechanism, we engineered a chemically-controlled structural element to stabilize the α-helical disorder to order transition. The link between the structural rearrangement and activity was controlled through a critically placed engineered disulfide bond that stabilized the interaction of helix 6 with the active site of the enzyme. Since wild-type enzyme is devoid of disulfide bonds, incorporation of a cysteine in both helix 6 and the loop supporting important catalytic residues provided the opportunity to form the only possible productive intramolecular disulfide bond in the molecule. To prevent nonproductive intermolecular disulfide bond formation, the three endogenous surface cysteines in KSHV protease were mutated to serine with no significant effect on the catalytic constants (Figure 3). This redox switch controls the conformational rearrangement with a concomitant regulation of the enzyme activity. Oxidizing conditions, favoring the formation of the disulfide bond between helix 6 and the active site loop, stabilize the engineered dimer and result in an active enzyme. Addition of reductant breaks the disulfide bond, abolishes enzyme activity and results in dissociation of the dimer as helix 6 is allowed to unfold and adopt an unpacked conformation. Figure 4a shows a complete cycle of the activity of the engineered disulfide variant in oxidizing (active), reducing (inactive), and oxidizing conditions (active) again. Concomitant with the attainment of enzyme activity is the

acquisition of quaternary structure of the dimer as shown in the panel insets in Figure 4a. HSQC experiments confirm the correlation between disulfide bond formation and oligomerization of the enzyme (Figure 4b). These results show activity is dependent on disulfide formation and stabilization of the interaction between helix 6 and the active site loop. To further illustrate this point, the intramolecular disulfide bond was engineered into the inactive monomeric variant of the protease and resulted in the first demonstration of a rationally designed active monomer (Figure 5).

Although oligomerization is known to affect protein function as first seen in hemoglobin, circular dichroism, NMR and protein engineering provide the molecular details of a unique mechanism of enzyme regulation upon oligomerization of herpesvirus proteases (Figure 6a). Association of monomers results in the folding of helix 5, which completes the protein-protein interface and comprises nearly 80% of the surface area buried upon dimerization. Helix 6 also folds upon dimerization and positions a loop that contains several key components of the catalytic machinery that are required for stabilization of the transition state during substrate hydrolysis. Arg142 and Arg143 provide hydrogen bonds shown previously to be essential for catalysis[24]. The engineered disulfide in its oxidized state at positions 145 and 219 stabilizes these components and is depicted in Figure 6b.

Does this concentration dependent acquisition of protein function described above have a biological role? The concentration of the protease in an infected cell is 5 nM based on the empirically determined number of mature capsids produced per cell[25] and the number of protease molecules per capsid. Upon formation of the mature capsid the local concentration of protease increases to almost 100 μM, based on the capsid size[26, 27].

This increase in protease concentration is greater than four orders of magnitude and represents an increase from 1% active enzyme to 93% active enzyme upon capsid formation, given the measured enzyme dissociation constant (K_d) of 1 μM[28]. It is important to note that although the protease is expressed as a fusion protein, significant enhancement of the measured protease dimerization constant in the cytosol would only result in premature activation of the protease yielding no mature capsids. It appears that herpesvirus proteases have evolved a weak dimerization constant to reduce the amount of active protease in the cytosol, which would disrupt formation of mature infectious particles. The negative entropy of helix folding represents a mechanism through which, despite burying more than 2000 $Å^2$ of hydrophobic surface area upon dimerization, herpesvirus proteases display only micromolar dissociation constants.

Multi-component cellular processes must integrate many disparate enzymatic activities to ensure survival of the organism. Oligomeric complexes of proteins are ubiquitous and their assembly offers a mechanism for controlling protein function. We have used the activity of a herpesvirus protease to monitor concentration dependent acquisition of quaternary structure. The large conformational changes in secondary structure that occur in herpesvirus proteases upon dimerization regulate the enzymatic function. These multi-layered allosteric controls allow the integration of proteolytic activity into the lytic cycle in a controlled manner and illustrate the large differences that exist between the isolated and oligomeric forms of a protein. We anticipate that this transitional helical switch is not unique to the regulation of enzymatic activity but may be applicable to other diverse protein functions as well. This induced structure phenomenon

need not be restricted to oligomerization events but rather to any chemical transition and provides control of biological processes via acquisition of quaternary structure.

METHODS

Recombinant Expression, Purification, and Quantification of KSHV Protease. A protease variant stable to autolysis, referred to as wild-type protease, and a monomeric variant containing both the M197D and S204G mutations, were expressed and purified as previously described[29]. Protease samples incorporating isotopically labeled Asp, Phe, Ile, Leu, Val, or Tyr were recombinantly expressed in *E. coli* DL39 using M9 media supplemented with the appropriate amino acids. Samples incorporating isotopically labeled Ala, Cys, His, Pro, Arg were recombinantly expressed in *E. coli* strain BL21-DE3 in M9 media supplemented with all amino acids, nucleosides, and vitamins. Samples incorporating full ^{13}C and ^{15}N isotopic labeling or ^{2}H, ^{13}C, ^{15}N labeling were recombinantly expressed in *E. coli* BL21-DE3 in either M9 medium supplemented with 2g/L ^{13}C-labeled glucose, 1g/L ^{15}N-labeled ammonium chloride, in H_2O or D_2O or in Silantes *E. coli* OD2 CDN media containing ^{2}H, ^{13}C, ^{15}N.

Disulfide-linked Protease Purification and Characterization. Kinetic analysis of KSHV protease with surface cysteines removed showed no significant reduction in k_{cat} or K_m as compared to wild-type enzyme. A redox-switch was incorporated by mutations G145C and V219C. Expression and purification were performed as described[29]. Purified protein was treated with oxidized glutathione (10 mM) and isolated by size exclusion chromatography. Activity and gel filtration assays were performed as described previously[19].

Secondary Structure Measured by Circular Dichroism (CD). CD measurements were performed on a Jasco J-715 spectropolarimeter in 0.1 cm temperature-controlled quartz cuvettes at 27° C. Protease samples were diluted into CD buffer (25 mM potassium phosphate, pH 8.0/1 mM 2-mercaptoethanol) to ~0.1 mg/mL and allowed to equilibrate for one hour before measurements. Mean molar residue ellipticities were obtained after solvent spectrum subtraction and 10-fold signal averaging. Secondary structure content was estimated using the self-consistent method contained in the Dicroprot software.

NMR Backbone Resonance Assignments. NMR samples were prepared in NMR buffer (25 mM potassium phosphate, pH 7.0/0.1 mM EDTA/1 mM 2-mercaptoethanol) with D_2O added to 10% final concentration for deuterium lock. Uniformly labeled protease samples were roughly 0.5-0.7 mM, while selectively labeled samples were between 0.25 and 0.7 mM. All NMR experiments were conducted at 27° C on either a Bruker Avance 500 MHz, DRX 600 MHz, or Avance 800 MHz NMR instrument equipped with a triple resonance cryoprobe with Z-axis gradients. All Proton chemical shifts were referenced to an internal DSS standard at 0 ppm. Carbon and Nitrogen chemical shifts were indirectly referenced to the internal DSS standard using the ratios 0.251449537 and 0.101329118 respectively. 2D ^{1}H, ^{15}N heteronuclear single-quantum coherence (HSQC) spectra of M197D were collected with Ala, Arg, Asp, Cys, His, Ile, Leu, Lys, Phe, Tyr, Val, and uniformly 15N labeled samples. 2D ^{1}H, ^{15}N HNCO spectra were collected with uniformly 15N labeled samples with one of the amino acids; Ile, Leu, Phe, Pro, Tyr, Val, ^{13}C labeled on the carbonyl carbon. 3D experiments for sequential backbone assignments were comprised of an HNCA, HN(CO)CA, HNCO, ^{1}H, ^{15}N NOESY HSQC with a

mixing time of 100 msec, TROSY HNCA, TROSY HN(CO)CA, and TROSY HNCAC. All spectra were transformed using the XWINNMR software and data visualization and spectra assignments utilized the XEASY and Sparky software packages.

Hydrogen/Deuterium Exchange Experiments. Hydrogen/Deuterium (H/D) exchange samples were prepared in NMR buffer in H_2O, lyophilized, and resuspended in an equal volume of D_2O. NMR samples used for measurement of slowly exchanging backbone amides were at roughly 0.4 mM and measurement of intermediate exchange rate backbone amides were conducted with a 0.7 mM sample. All H/D exchange measurements were conducted at 27° C utilizing a Bruker Avance 500 MHz NMR instrument equipped with a triple resonance cryoprobe with Z-axis gradients. 2D ^{1}H, ^{15}N HSQC experiments were conducted for 24 hours, with individual experimental times of 11 minutes. 2D ^{1}H, ^{15}N HSQC experiments measuring slowly exchanging backbone amides were conducted for two weeks, with experimental times of 3 hours. Spectra were transformed and integrated in XWINNMR, visualized with XEASY, and exchange rates were calculated using the Kaleidagraph software.

REFERENCES

1. Buisson, M. et al. The crystal structure of the Epstein-Barr virus protease shows rearrangement of the processed C terminus. J Mol Biol 324, 89-103 (2002).
2. Chen, P. et al. Structure of the human cytomegalovirus protease catalytic domain reveals a novel serine protease fold and catalytic triad. Cell 86, 835-43 (1996).
3. Hoog, S. S. et al. Active site cavity of herpesvirus proteases revealed by the crystal structure of herpes simplex virus protease/inhibitor complex. Biochemistry 36, 14023-9 (1997).
4. Qiu, X. et al. Unique fold and active site in cytomegalovirus protease. Nature 383, 275-9 (1996).
5. Qiu, X. et al. Crystal structure of varicella-zoster virus protease. Proc Natl Acad Sci U S A 94, 2874-9 (1997).
6. Reiling, K. K., Pray, T. R., Craik, C. S. & Stroud, R. M. Functional consequences of the Kaposi's sarcoma-associated herpesvirus protease structure: regulation of activity and dimerization by conserved structural elements. Biochemistry 39, 12796-803 (2000).
7. Tong, L. et al. A new serine-protease fold revealed by the crystal structure of human cytomegalovirus protease. Nature 383, 272-5 (1996).
8. Gao, M. et al. The protease of herpes simplex virus type 1 is essential for functional capsid formation and viral growth. J Virol 68, 3702-12 (1994).
9. Unal, A. et al. The protease and the assembly protein of Kaposi's sarcoma-associated herpesvirus (human herpesvirus 8). J Virol 71, 7030-8 (1997).

10. Matusick-Kumar, L. et al. Release of the catalytic domain N(o) from the herpes simplex virus type 1 protease is required for viral growth. J Virol 69, 7113-21 (1995).

11. Person, S. & Desai, P. Capsids are formed in a mutant virus blocked at the maturation site of the UL26 and UL26.5 open reading frames of herpes simplex virus type 1 but are not formed in a null mutant of UL38 (VP19C). Virology 242, 193-203 (1998).

12. Darke, P. L. et al. Active human cytomegalovirus protease is a dimer. J Biol Chem 271, 7445-9 (1996).

13. Margosiak, S. A., Vanderpool, D. L., Sisson, W., Pinko, C. & Kan, C. C. Dimerization of the human cytomegalovirus protease: kinetic and biochemical characterization of the catalytic homodimer. Biochemistry 35, 5300-7 (1996).

14. Schmidt, U. & Darke, P. L. Dimerization and activation of the herpes simplex virus type 1 protease. J Biol Chem 272, 7732-5 (1997).

15. Robertson, B. J. et al. Separate functional domains of the herpes simplex virus type 1 protease: evidence for cleavage inside capsids. J Virol 70, 4317-28 (1996).

16. Sheaffer, A. K. et al. Evidence for controlled incorporation of herpes simplex virus type 1 UL26 protease into capsids. J Virol 74, 6838-48 (2000).

17. Batra, R. K., R; Tong, L. Molecular mechanism for dimerization to regulate the catalytic activity of human cytomegalovirus protease. Nat Struct Biol 8, 810-817 (2001).

18. Pray, T. R., Reiling, K.K., Demirjian, B.G., Craik, C.S. Conformational Change Coupling the Dimerization and Activation of KSHV Protease. Biochemistry 41, 1474-1482 (2002).

19. Marnett, A. B., Nomura, A. M., Shimba, N., Ortiz de Montellano, P. R. & Craik, C. S. Communication between the active sites and dimer interface of a herpesvirus protease revealed by a transition-state inhibitor. Proc Natl Acad Sci U S A 101, 6870-5 (2004).

20. Schwarzinger, S. et al. Sequence-dependent correction of random coil NMR chemical shifts. J Am Chem Soc 123, 2970-8 (2001).

21. Schwarzinger, S., Kroon, G. J., Foss, T. R., Wright, P. E. & Dyson, H. J. Random coil chemical shifts in acidic 8 M urea: implementation of random coil shift data in NMRView. J Biomol NMR 18, 43-8 (2000).

22. Wishart, D. S. & Sykes, B. D. The 13C chemical-shift index: a simple method for the identification of protein secondary structure using 13C chemical-shift data. J Biomol NMR 4, 171-80 (1994).

23. Bai, Y., Milne, J. S., Mayne, L. & Englander, S. W. Primary structure effects on peptide group hydrogen exchange. Proteins 17, 75-86 (1993).

24. Liang, P. H. et al. Site-directed mutagenesis probing the catalytic role of arginines 165 and 166 of human cytomegalovirus protease. Biochemistry 37, 5923-9 (1998).

25. Visalli, R. J. & Brandt, C. R. The HSV-1 UL45 gene product is not required for growth in Vero cells. Virology 185, 419-23 (1991).

26. Newcomb, W. W. et al. Isolation of herpes simplex virus procapsids from cells infected with a protease-deficient mutant virus. J Virol 74, 1663-73 (2000).

27. Yu, X. K. et al. Three-dimensional structures of the A, B, and C capsids of rhesus monkey rhadinovirus: insights into gammaherpesvirus capsid assembly, maturation, and DNA packaging. J Virol 77, 13182-93 (2003).

28. Shimba, N., Nomura, A. M., Marnett, A. B. & Craik, C. S. Herpesviral Protease Inhibition by Dimer Disruption. J Virol in press (2004).

29. Pray, T. R., Nomura, A. M., Pennington, M. W. & Craik, C. S. Auto-inactivation by cleavage within the dimer interface of Kaposi's sarcoma-associated herpesvirus protease. J Mol Biol 289, 197-203 (1999).

ACKNOWLEDGEMENTS

We thank Professor Paul Ortiz de Montellano for helpful discussions throughout the course of this work. This research was funded by a UC President's dissertation year award (A.B.M.) and the NIH.

Figure 4-1. Loss of helicity upon KSHV protease dimer dissociation. Circular dichroism of pure dimer (inhibited), blue; equilibrium mixture of monomer and dimer (uninhibited), green; and pure monomer (M197D), red.

Figure 4-1.

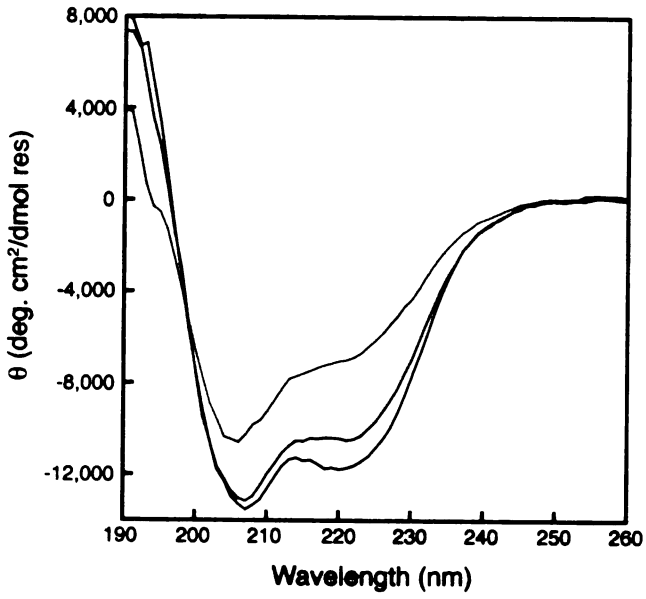
8,000
4,000
0
-4,000
-8,000
-12,000
θ (deg. cm²/dmol res)
190
200
210
220
230
240
250
260
Wavelength (nm)

Figure 4-2. Localization of the structural rearrangement upon activation. **a,** NMR chemical shift index data reveal that helices 5 and 6, that are formed in the dimeric form are not present in the monomeric form of the enzyme **b,** The NMR data pertaining to the monomeric form in solution are plotted on the dimeric form in the crystal, with colors based on solution secondary structure, sheet (yellow), helix (red) and disordered loops (green). **c,** Hydrogen/deuterium exchange rates corroborate instability of helices 5 and 6. **d,** Mapping H/D exchange rate data onto the crystal structure, slow (red), medium (orange), and fast (grey), entire secondary structural elements lost (blue). All structures visualized and rendered using PyMol (DeLano Scientific).

Figure 4-2.

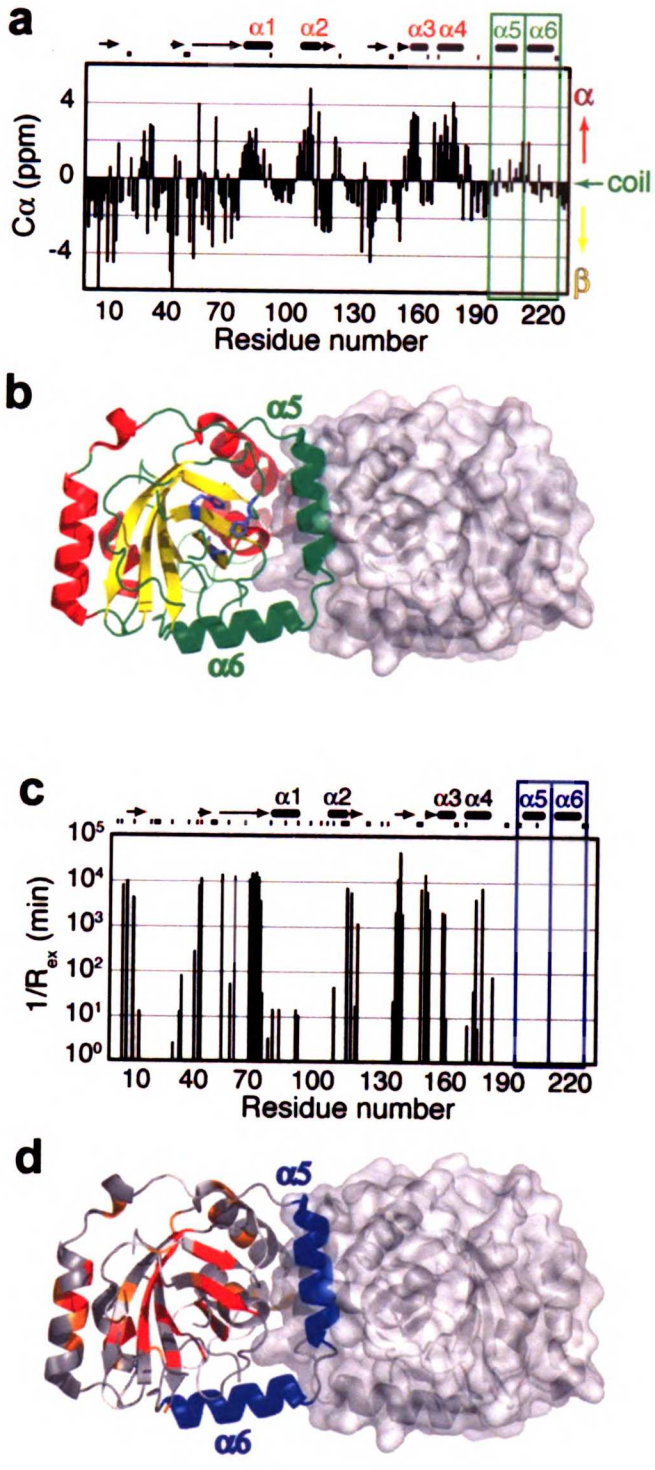
a
α1
α2
α3 α4
α5 α6
4
0
-4
Cα (ppm)
α
coil
β
10 40 70 100 130 160 190 220
Residue number
b
α5
α6
c
α1
α2
α3 α4
α5 α6
10⁵
10⁴
10³
10²
10¹
10⁰
1/R_ex (min)
10 40 70 100 130 160 190 220
Residue number
d
α5
α6

Figure 4-3.

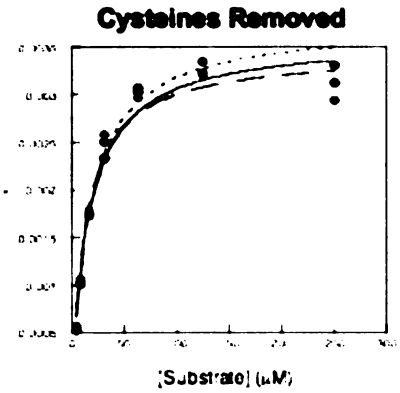

K_{cat}	K_m	k_{cat}/K_m
0.00072 ± 3 x 10^{-5} s^{-1}	16 ± 2.0 μM	44 $M^{-1}s^{-1}$

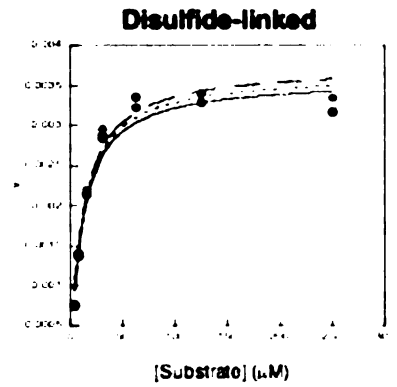

0.00122 ± 2 x 10^{-5} s^{-1}	11.2 ± 0.3 μM	109 $M^{-1}s^{-1}$
Wild-type		
0.0092 ± 0.0004 s^{-1}	7.2 ± 0.7 μM	1300 $M^{-1}s^{-1}$

Figure 4-4. Proteolytic activity controlled by a redox switch. **a,** KSHV protease (3mM) with surface cysteines removed (blue) and disulfide bond engineered (red); activity monitored by an increase in fluorescence upon cleavage of a fluorogenic coumarin-based substrate. After 60 min, DTT (1 mM) was added to the sample and activity was monitored for an additional hour before addition of oxidized glutathione, GSSG (10 mM). Quaternary structures of oxidized (untreated), reduced (1 mM DTT, 8 h at 25C) and reoxidized (reduced followed by 10 mM oxidized glutathione, 30 min at 25C) protease were analyzed by analytical size exclusion chromatography at 280 nm, shown as insets, dimer (D), monomer (M). **b** and **c**, HSQC of doubly labeled 3-^{13}C-cysteine and methyl-^{13}C-methionine protease; disulfide engineered enzyme in the absence, $\mathbf{b_i}$, or presence, $\mathbf{b_{ii}}$, of deuterated DTT (1 mM). Wild-type enzyme in the absence, $\mathbf{c_i}$, or presence, $\mathbf{c_{ii}}$, of DTT. As described previously[19], the solution quaternary structure is assessed by the chemical shifts of the interfacial methionine in the monomer ($M197^{MON}$) or dimer ($M197^{DIMER}$) versus the N-terminus (M1) of the enzyme. Isotope labeled protease reveals the shift in oligomeric structure and appearance of reduced cysteines upon reduction of the disulfide-linked protease variant. Unassigned background peaks exist in all spectra with intensities relative to number of transients (disulfide engineered, ns= 288; wild-type, ns=64).

Figure 4-4.

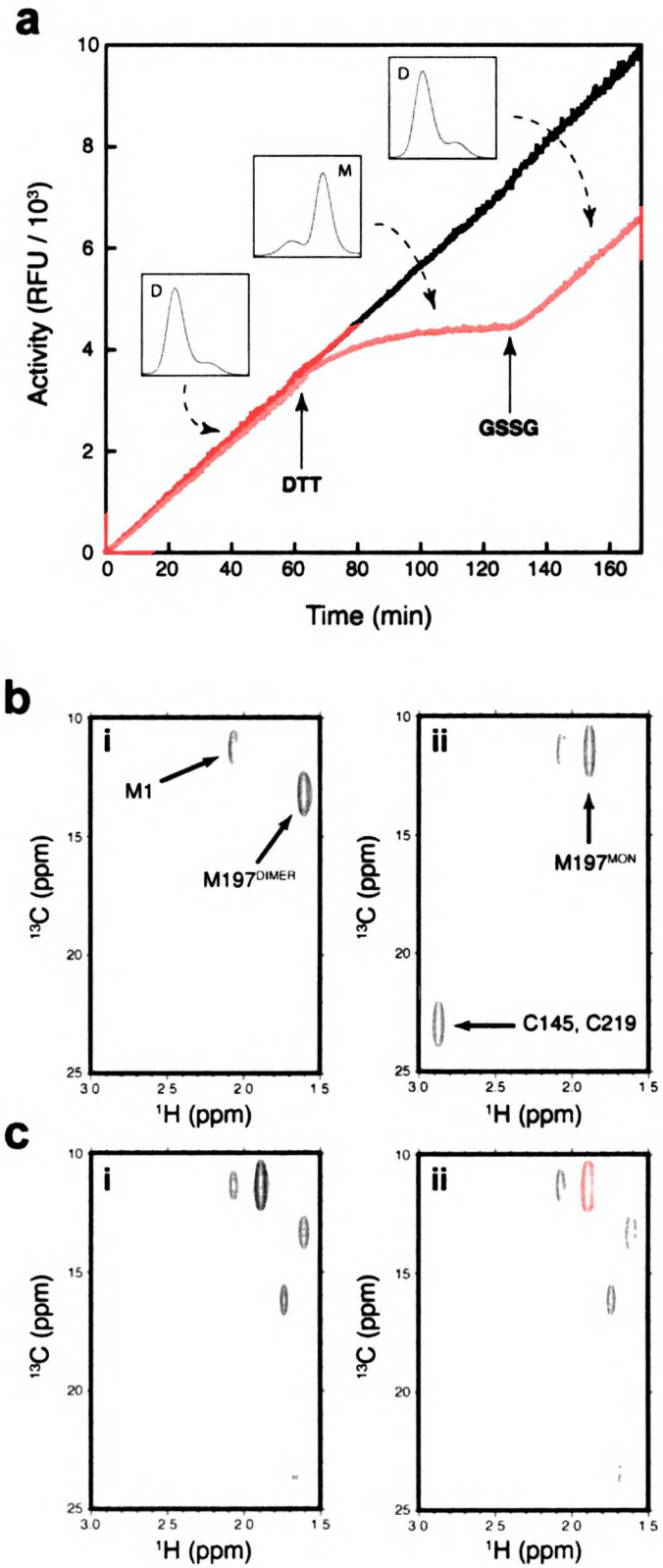
a
Activity (RFU / 10³)
Time (min)
D
M
D
DTT
GSSG
b
i
M1
M197DIMER
ii
M197MON
C145, C219
¹³C (ppm)
¹H (ppm)
c
i
ii
¹³C (ppm)
¹H (ppm)

Figure 4-5.

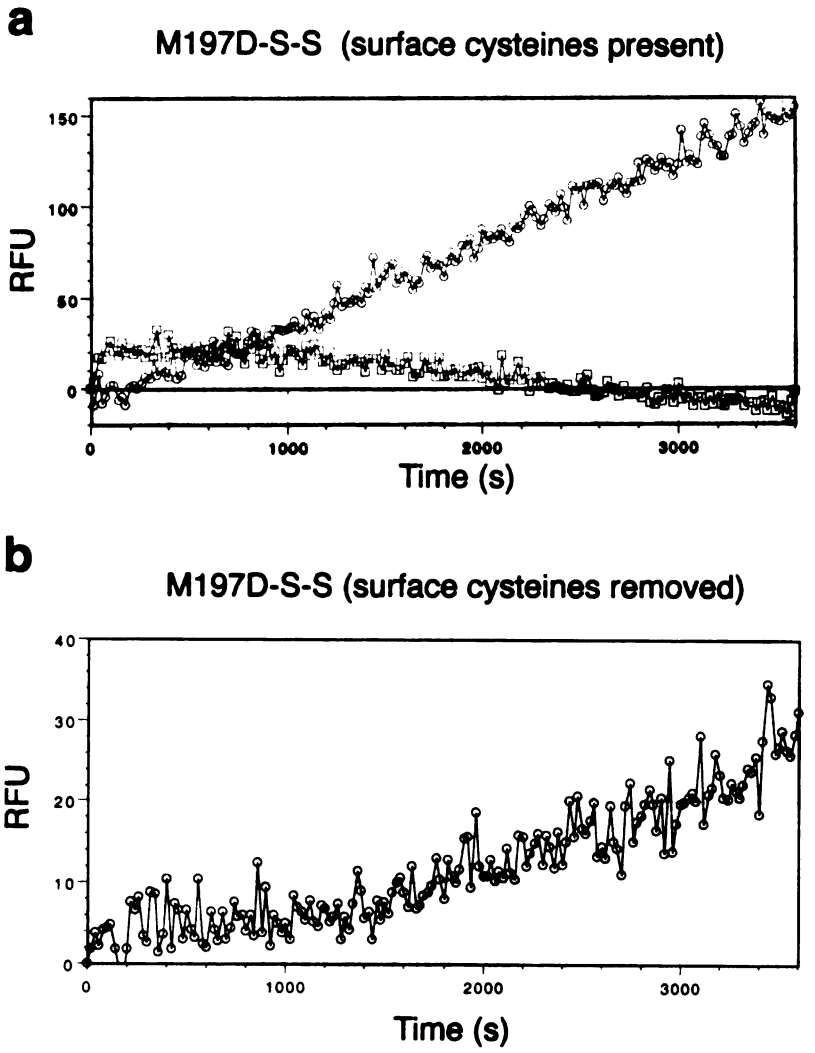
a
M197D-S-S (surface cysteines present)
RFU
150
100
50
0
0
1000
2000
3000
Time (s)
b
M197D-S-S (surface cysteines removed)
RFU
40
30
20
10
0
0
1000
2000
3000
Time (s)

Figure 4-6. Mechanism of herpesvirus protease activation. **a,** Wild-type protease exists in a monomer-dimer equilibrium governed by protease concentration. Dimerization results in folding of helices 5 and 6 and concomitant assembly of a functional active site (star) while dissociation results in loss of helices 5 and 6 and subsequent loss of a functional active site (null sign). In protease containing the redox switch, folding of helices 5 and 6 are regulated by addition of DTT or oxidized glutathione. **b,** (inset area from **a**) The modeled engineered disulfide bond (red) stabilizes the interaction between helix 6 (blue) and the loop containing critical components for catalysis (green). Hydrogen bonds provided by Arg 142 (amide proton, gray) and Arg143 (guanidinium group; green) stabilize the transition state formed upon nucleophilic attack of the active site serine (purple) on peptide substrates.

Figure 4-6.

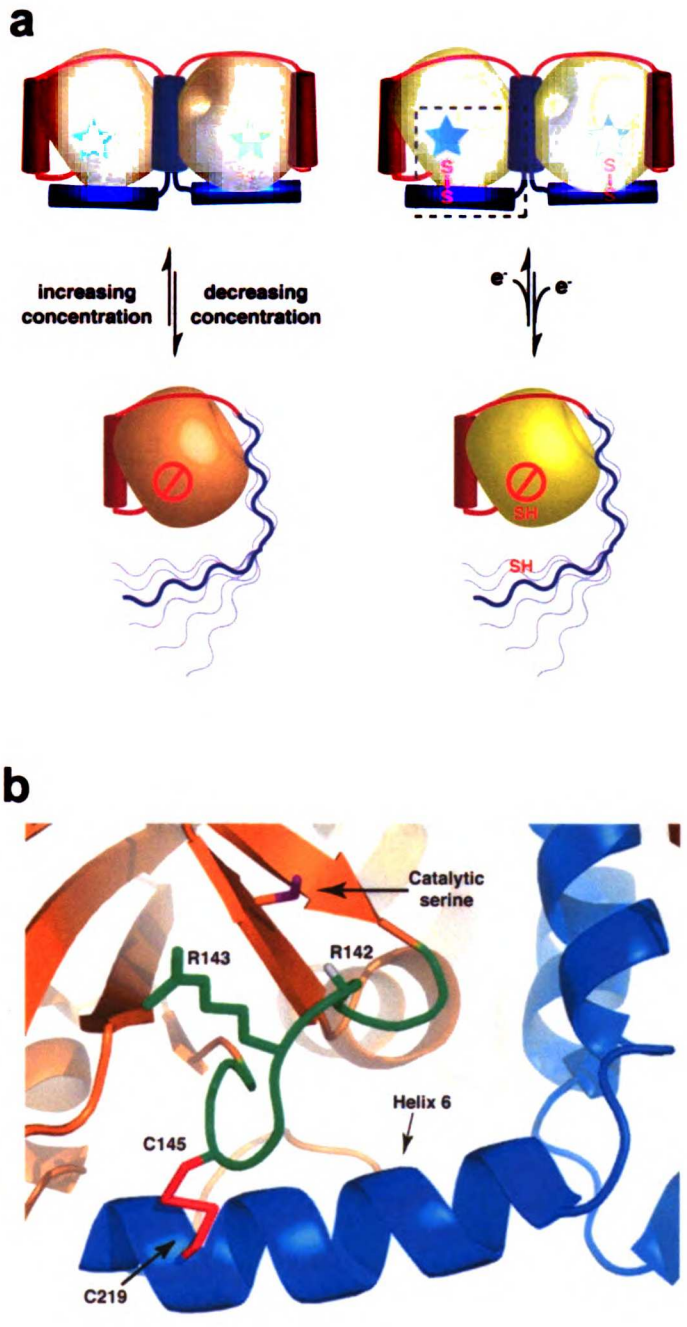
a
increasing concentration
decreasing concentration
e-
e-
SH
SH
b
Catalytic serine
R143
R142
Helix 6
C145
C219

Chapter 5 | Inhibition of Herpesvirus Replication by Inactivation of the Viral Protease

Alan B. Marnett[1], Jill T. Bechtel[2], Don Ganem[2] and Charles S. Craik[1]

Chemistry and Chemical Biology Graduate Program, Departments of Pharmaceutical Chemistry[1] and Microbiology, G.W. Hooper Foundation, Howard Hughes Medical Institute[2], University of California, San Francisco, California

Currently, nine of the more than 100 known herpesviruses infect humans and cause a range of ailments from painful cold sores (Herpes simplex virus) to life-threatening cancerous tumors (Kaposi's Sarcoma-associated herpesvirus). Immediately following infection of a host cell, herpeseviruses establish a persistent latent infection that remains for the duration of the lifetime of the host. At any point during latent infection, external stimuli may trigger the initiation of the lytic cycle, which results in expression of gene products necessary for viral replication and the production of infectious progeny. Lytic replication ultimately leads to clinical manifestations of the disease, such as formation of a sore, lesion or tumor. Although there is no cure for herpesvirus infections, traditional therapies target the viral DNA polymerase for inhibition of lytic replication[1, 2]. However, because these compounds require activation by the viral thymidine kinase prior to polymerase inhibition, these frontline therapies are susceptible to resistance at many levels. In fact, drug-resistant viruses have been isolated which contain either no thymidine kinase, mutated thymidine kinase or mutated DNA polymerase. As a result, a need for alternative mechanisms of inhibition of viral replication has arisen[3].

All herpesviruses express a virally encoded protease that shares no structural homology to human proteins and whose activity appears necessary for viral replication. During lytic replication, the 25-KD protease is expressed as an inactive monomer fused to a capsid scaffolding protein (assembly protein) in the cytosol. Ultimately, the scaffolding protein is translocated to the nucleus for the formation of an immature capsid. It is believed that the high local concentration of protease in the nascent capsid drives dimerization and activates the enzyme for proteolysis. Cleavage at the release site and

again at the maturation site releases the protease from the scaffolding and the scaffolding from the capsid shell, respectively. These proteolytic events are essential to capsid maturation and formation of infectious particles[4-15]. Furthermore, we have recently demonstrated that disrupting dimerization as well as binding at the active site of the enzyme prevents catalytic activity *in vitro*, suggesting a diverse range of therapeutic possibilities in targeting the protease for inhibition[16]. As a result, the viral protease has emerged as a potential therapeutic target for treating herpesvirus infections[17].

Although genetic evidence revealed the importance of protease activity in viral replication, it has yet to be demonstrated that specific chemical inhibition of the protease will arrest the viral lytic cycle[15, 18-20]. In fact, a number of inhibitors targeting the cytomegalovirus protease *in vitro* have been described, yet the *in vivo* mechanism of action has yet to be demonstrated[21, 22]. While inhibition of human cytomegalovirus was observed using a protease inhibitor in a viral plaque assay, a 1000-fold difference in the *in vitro* IC_{50} (nM) and the *in vivo* IC_{50} (μM) made it difficult to attribute the reduction in plaque growth to specific protease inhibition versus general toxicity[23].

Kaposi's Sarcoma-associated herpesvirus (KSHV, HHV-8) is an oncogenic herpesvirus for which no specific therapy currently exists. Following establishment of latent infection in human endothelial cells, KSHV is efficiently reactivated by infection with adenovirus expressing the lytic switch protein, RTA[24-26]. Infectious particles formed during replication may be harvested from the cellular medium for quantification. Therefore, KSHV represents an ideal model system for examining the molecular effects of specific protease inhibitors on the replication of the virus *in vivo*. The results in this report describe the first demonstration that inhibition of the viral protease arrests lytic

replication of KSHV at a comparable level to current clinically available therapeutics. Using a monomeric protease variant (M197D) we also provide evidence that protease inhibitors bind the inactive monomeric form of the enzyme in the cytosol and are translocated to the nucleus with the enzyme-assembly protein complex.

MATERIALS AND METHODS

KSHV protease inhibitor. BODIPY-P-V-Y-tBug-Q-A^P-$(OPh)_2$ was synthesized as described previously[27]. Integrity of the inhibitor in growth medium (EGM-2MV, BioWhittaker) at 37°C was monitored by mass spectrometry (MALDI). Within 25 h, nearly 80% of the inhibitor hydrolyzed to the monophenylphosphonate.

Viral replication. Telomerase-immortalized microvascular endothelial (TIME) cells were grown and infected with KSHV as described previously. KSHV replication was induced by addition of adenovirus expressing ORF50. After 2 h at 37C, cells were washed and EGM-2MV medium was replaced containing DMSO, PFA, or a diphenylphosphonate. Due to the half-life of diphenylphosphonates in the media, the media was replaced every 12 h and old media was stored at 4C for later use. Virions were harvested from the combined supernatants 72 h postinduction by centrifugation (15,000 rpm). The resulting virions were resuspended in media containing polybrene and used to perform a secondary infection of new TIME cells. Twenty four hours after infection, cells were washed with PBS and fixed in the presence of 4% paraformaldehyde. Rates of infection were monitored by immunofluorescence to detect the latency associated nuclear antigen (LANA) as described previously[28]. Quantification of infected cells is represented as the percentage of cells infected in a microscope field averaged over 15 fields. Cells were counted as either infected or non-infected and the multiplicity of LANA spots observed was not taken into account.

Inhibitor detection by confocal microscopy. BODIPY-P-V-Y-tBug-Q-A^P-$(OPh)_2$ (10 μM) was added to infected TIME cells 15 h after reactivation of the lytic cycle. Fifteen hours later, the cells were washed (3X) with PBS and fixed in 4% paraformaldehyde for 30 min at room temperature. The cells were then rinsed with PBS and mounted on a glass slide for microscopy using mounting media containing DAPI (Vector Labs). Samples were imaged using a laser scanning microscope 410 (Carl Zeiss, Inc., Thornwood, NY) equipped with an Axiovert 100 microscope (Ziess), a 63-, 1.4 NA plan-APOCHROMAT objective lens (Zeiss), and an argon/krypton laser. BODIPY was imaged by excitation at 488 nm. For all samples, slice intensity was the average of three successive scans. Images were analyzed on a UNIX workstation.

Detection of protease inhibition by streptavidin blot. Wild-type or monomeric (M197D) protease (37 μM) was incubated with the biotinylated phosphonate (200 μM) for 72 h at RT prior to SDS-PAGE separation. Protein was transferred to nitrocellulose for detection of the biotin moiety by streptavidin-HRP (Vectastain, Vector Labs).

Fluorescence polarization. KSHV Pr M197D was serially diluted from 10-0.02 μM in assay buffer (25 mM potassium phosphate, 150 mM NaCl, 1 mM dithiothreitol, 1 mM EDTA, pH 8.0) followed by addition of BODIPY-labeled inhibitor (20 nM) and placed in a 384-well plate yielding final protein concentrations of 5-0.01 μM and 10 nM fluorescent inhibitor concentration. The samples were allowed to equilibrate for 30 min at room temperature. Binding was then measured using fluorescence polarization (excitation 485 nm, emission 530 nm) on an Analyst AD (Molecular Devices). Polarization

experiments were performed in triplicate. Data were analyzed using SigmaPlot 8.0 (SPSS, Chicago, Il), and the K_d values were obtained by fitting data to the following equation (y = min + (max - min)/1 + (x/K_d) Hill slope).

RESULTS

Toxicity and cell permeability of the phosphonate inhibitor. Prior to extensive analysis of the effects of the protease inhibitor on viral replication, the toxicity of the compound was monitored by both inverted and confocal fluorescence microscopy using uninfected TIME cells. At concentrations greater than 100 μM, significant toxicity was induced as cellular debris from dead cells was observed only a few hours after incubation with inhibitor. However, at lower concentrations, cells tolerated the presence of inhibitor with no obvious defects in morphology or growth rate suggesting a lack of non-specific binding of the inhibitor to unintentional cellular targets. Confocal microscopy confirmed the presence of inhibitor in the cytosol of uninfected TIME cells, but revealed a distinct lack of fluorescence in the nuclei of all cells.

Viral replication is reduced in the presence of protease inhibitor. Treatment of lytically replicating TIME cells with the protease inhibitor results in a significant decrease in the production of infectious virions. Although not accounted for in the replication data, it should be noted that by immunofluorescence, cells infected with virions from untreated cells showed a high degree of multiplicity of LANA staining (>5). This is in direct contrast with TIME cells infected with virions harvested from protease treated samples, which rarely showed more than one punctate LANA stain in an infected cell. When compared to a clinically available polymerase-targeted treatment, foscarnet, the protease inhibitor showed a comparable decrease in virion production. Furthermore, pretreatment of TIME cells with protease inhibitor prior to KSHV infection resulted in a

slightly larger decrease in virion production as compared to TIME cells treated with inhibitor two hours post-infection.

Inhibitor localizes to the nucleus upon reactivation of lytic replication. As demonstrated by confocal microscopy, in the absence of viral infection, the inhibitor localizes exclusively to the cytosol. In fact, although the cytosolic fluorescence is at an extremely low level as a result of extensive washing, latently infected cells also exhibit nuclei devoid of a detectable fluorescence signal. However, upon viral reactivation, which results in expression of a number of viral genes including the protease, the inhibitor is observed only in the nuclei of cells. The nuclei visualized appear extremely large presumably due to the rapid capsid assembly process occurring during viral replication.

Protease inhibitor binds reversibly to the inactive monomeric protease. Incorporation of a single point mutation in the dimer interface of wild-type protease yields a completely monomeric, inactive protease (M197D). Extended incubations with high concentrations of both protease and biotinylated inhibitor revealed no detectable covalent labeling of the inactive monomer even when dramatically overloaded samples were analyzed. However, fluorescence polarization demonstrated reversible binding of the inhibitor with a dissociation constant of 220 nM. An increase in 80 millipolarization units accompanied inhibitor binding.

DISCUSSION

Herpesviruses represent one of the most prevalent human pathogens resulting in a range of disease states from cold sores to cancer. Although traditional therapies targeting the viral DNA polymerase have been successful in the past at reducing the level of replicating virus, emerging resistance mechanisms to these compounds has highlighted a demand for alternative approaches to preventing viral replication. All herpesviruses encode a maturational protease that appears required for production of infectious progeny. Here, we present the first evidence that chemical inhibition by the protease results in a reduction in viral replication, thus validating the protease as an alternative therapeutic target. Furthermore, we present evidence suggesting the inactive monomer may be important for localization of the inhibitor to the nucleus.

Previous work with human cytomegalovirus revealed a three order of magnitude increase in the IC_{50} as measured by plaque assay as compared to *in vitro* binding constants. However, in the absence of more detailed mechanistic work, it is unclear whether the effect was due to toxicity of the compound. In fact, we observe toxicity in endothelial cells at 100 μM concentrations of inhibitor, which is very similar to the IC_{50} value reported in the CMV report.

In developing a protease inhibitor targeting the viral enzyme, diphenylphosphonates were chosen as the scaffold for several reasons. First, the synthetic route was easily amenable to modification, particularly to addition of peptidyl moieties for specificity in the context of the whole cell. Second, diphenylphosphonates have been shown empirically to selectively inhibit serine proteases[29]. Therefore, cross-

reactivity between the inhibitor and other cellular proteases (cysteine-, metallo-, threonine-) was avoided.

The reduction in viral replication demonstrated upon treatment with the protease inhibitor was not statistically different than the currently available polymerase inhibitor. Although the phosphonate itself is not a therapeutic lead compound, this result highlights the validity of the protease as a potential target. As a result of the method of quantification of infected cells, the reduction in viral load is underestimated. Not only were the number of infected cells reduced, but so too was the multiplicity of infection of individual cells. The greater number of punctate LANA stains per nucleus is proportional to the level of virus used to infect the cells.

In support of a mechanism in which viral replication is reduced as a result of protease inhibition, confocal microscopy demonstrates localization of the inhibitor to the nucleus only upon reactivation of virally infected cells. The low level of non-specific reactivity of the inhibitor is reflected by the almost undetectable level of fluorescence in the non-reactivated infected cells following rinsing with PBS. The absence of inhibitor in the nuclei of non-reactivated cells followed by the dramatic localization solely to the nucleus upon reactivation suggests that the inhibitor may bind the inactive monomeric variant in the cytosol and then covalently react in the nascent capsids upon protease activation. Alternatively, it is possible that the nuclear membrane is significantly compromised upon lytic replication, although there is no evidence to support this conclusion.

A monomeric protease variant incorporating a single point mutation at the dimer interface (M197D) was utilized to address the possibility of inhibitor binding to the

inactive enzyme in the cytosol[30]. Extended incubations with the monomeric enzyme and high concentrations of the protease inhibitor yielded no covalent modification of the protease as demonstrated by a streptavidin blot. However, the same inhibitor was shown to bind reversibly to the protease variant with a nanomolar dissociation constant. While it must be noted that the actual structure of the inactive monomer in the context of the assembly protein *in vivo* is unknown, the *in vitro* model supports a mechanism in which protease inhibitors may bind the enzyme reversibly in the cytosol, be shuttled into the nucleus with the Pr-AP complex, and react upon protease activation.

The traditional role of the protease in viral replication has been as a maturational enzyme that processes capsid scaffolding proteins during lytic replication. Recent data suggests that the protease may play an additional role early in viral infection. While this proposed role is speculative, high levels of specifically packaged protease mRNA have been detected in mature virions[31, 32]. It is therefore possible that protease expression and activation plays a role in the hours immediately after infection. Accordingly, cells treated with inhibitor during viral infection show a slightly lower level of viral replication than cells treated with inhibitor two hours after infection. Although this is far from proof of an alternative role of the protease, it suggests that the inhibitor may be a useful chemical tool for addressing the question.

REFERENCES

1. Lebbé, C. et al. Clinical and biological impact of antiretroviral therapy with protease inhibitors on HIV-related Kaposi's sarcoma. *AIDS* 12, F45-9 (1998).
2. Gill, J. et al. Prospective study of the effects of antiretroviral therapy on Kaposi sarcoma--associated herpesvirus infection in patients with and without Kaposi sarcoma. *J Acquir Immune Defic Syndr* 31, 384-90 (2002).
3. Klass, C. M. & Offermann, M. K. Targeting human herpesvirus-8 for treatment of Kaposi's sarcoma and primary effusion lymphoma. *Curr Opin Oncol* 17, 447-55 (2005).
4. Booy, F. P. et al. Liquid-crystalline, phage-like packing of encapsidated DNA in herpes simplex virus. *Cell* 64, 1007-15 (1991).
5. Desai, P., Watkins, S. C. & Person, S. The size and symmetry of B capsids of herpes simplex virus type 1 are determined by the gene products of the UL26 open reading frame. *J Virol* 68, 5365-74 (1994).
6. Heymann, J. B. et al. Dynamics of herpes simplex virus capsid maturation visualized by time-lapse cryo-electron microscopy. *Nat Struct Biol* 10, 334-41 (2003).
7. Matusick-Kumar, L. et al. Release of the catalytic domain N(o) from the herpes simplex virus type 1 protease is required for viral growth. *J Virol* 69, 7113-21 (1995).
8. Pelletier, A., Do, F., Brisebois, J. J., Lagace, L. & Cordingley, M. G. Self-association of herpes simplex virus type 1 ICP35 is via coiled-coil interactions

and promotes stable interaction with the major capsid protein. *J Virol* 71, 5197-208 (1997).

9. Preston, V. G. & McDougall, I. M. Regions of the herpes simplex virus scaffolding protein that are important for intermolecular self-interaction. *J Virol* 76, 673-87 (2002).

10. Renne, R., Lagunoff, M., Zhong, W. & Ganem, D. The size and conformation of Kaposi's sarcoma-associated herpesvirus (human herpesvirus 8) DNA in infected cells and virions. *J Virol* 70, 8151-4 (1996).

11. Robertson, B. J. et al. Separate functional domains of the herpes simplex virus type 1 protease: evidence for cleavage inside capsids. *J Virol* 70, 4317-28 (1996).

12. Schynts, F. et al. The structures of bovine herpesvirus 1 virion and concatemeric DNA: implications for cleavage and packaging of herpesvirus genomes. *Virology* 314, 326-35 (2003).

13. Sheaffer, A. K. et al. Evidence for controlled incorporation of herpes simplex virus type 1 UL26 protease into capsids. *J Virol* 74, 6838-48 (2000).

14. Trus, B. L. et al. The herpes simplex virus procapsid: structure, conformational changes upon maturation, and roles of the triplex proteins VP19c and VP23 in assembly. *J Mol Biol* 263, 447-62 (1996).

15. Yu, X. et al. Dissecting human cytomegalovirus gene function and capsid maturation by ribozyme targeting and electron cryomicroscopy. *Proc Natl Acad Sci U S A* 102, 7103-8 (2005).

16. Shimba, N., Nomura, A. M., Marnett, A. B. & Craik, C. S. Herpesvirus protease inhibition by dimer disruption. *J Virol* 78, 6657-65 (2004).

17. Waxman, L. & Darke, P. L. The herpesvirus proteases as targets for antiviral chemotherapy. *Antivir Chem Chemother* 11, 1-22 (2000).

18. Dunn, W. et al. Functional profiling of a human cytomegalovirus genome. *Proc Natl Acad Sci U S A* 100, 14223-8 (2003).

19. Gao, M. et al. The protease of herpes simplex virus type 1 is essential for functional capsid formation and viral growth. *J Virol* 68, 3702-12 (1994).

20. Song, M. J. et al. Identification of viral genes essential for replication of murine gamma-herpesvirus 68 using signature-tagged mutagenesis. *Proc Natl Acad Sci U S A* 102, 3805-10 (2005).

21. Flynn, D. L., Abood, N. A. & Holwerda, B. C. Recent advances in antiviral research: identification of inhibitors of the herpesvirus proteases. *Curr Opin Chem Biol* 1, 190-6 (1997).

22. Flynn, D. L. et al. The herpesvirus protease: mechanistic studies and discovery of inhibitors of the human cytomegalovirus protease. *Drug Des Discov* 15, 3-15 (1997).

23. Ogilvie, W. et al. Peptidomimetic inhibitors of the human cytomegalovirus protease. *J Med Chem* 40, 4113-35 (1997).

24. Liang, Y., Chang, J., Lynch, S. J., Lukac, D. M. & Ganem, D. The lytic switch protein of KSHV activates gene expression via functional interaction with RBP-Jkappa (CSL), the target of the Notch signaling pathway. *Genes Dev* 16, 1977-89 (2002).

25. Lukac, D. M., Garibyan, L., Kirshner, J. R., Palmeri, D. & Ganem, D. DNA binding by Kaposi's sarcoma-associated herpesvirus lytic switch protein is

necessary for transcriptional activation of two viral delayed early promoters. *J Virol* 75, 6786-99 (2001).

26. Lukac, D. M., Kirshner, J. R. & Ganem, D. Transcriptional activation by the product of open reading frame 50 of Kaposi's sarcoma-associated herpesvirus is required for lytic viral reactivation in B cells. *J Virol* 73, 9348-61 (1999).

27. Marnett, A. B., Nomura, A. M., Shimba, N., Ortiz de Montellano, P. R. & Craik, C. S. Communication between the active sites and dimer interface of a herpesvirus protease revealed by a transition-state inhibitor. *Proc Natl Acad Sci U S A* 101, 6870-5 (2004).

28. Moore, P. S. et al. Primary characterization of a herpesvirus agent associated with Kaposi's sarcomae [published erratum appears in *J Virol* 1996 Dec;70(12):9083]. *J Virol* 70, 549-58 (1996).

29. Oleksyszyn, J. & Powers, J. C. Amino acid and peptide phosphonate derivatives as specific inhibitors of serine peptidases. *Methods Enzymol* 244, 423-41 (1994).

30. Pray, T. R., Reiling, K.K., Demirjian, B.G., Craik, C.S. Conformational Change Coupling the Dimerization and Activation of KSHV Protease. *Biochemistry* 41, 1474-1482 (2002).

31. Bechtel, J., Grundhoff, A. & Ganem, D. RNAs in the virion of Kaposi's sarcoma-associated herpesvirus. *J Virol* 79, 10138-46 (2005).

32. Bechtel, J. T., Winant, R. C. & Ganem, D. Host and viral proteins in the virion of Kaposi's sarcoma-associated herpesvirus. *J Virol* 79, 4952-64 (2005).

Figure 5-1. Cell Permeability of BODIPY-P-V-Y-tBug-Q-A^P-$(OPh)_2$. TIME cells treated with inhibitor were analyzed by fluorescence microscopy. Comparison of BODIPY fluorescence (A), DAPI nuclear staining (B), overlay (C) reveals the presence of inhibitor in all cells visualized.

Figure 5-1.

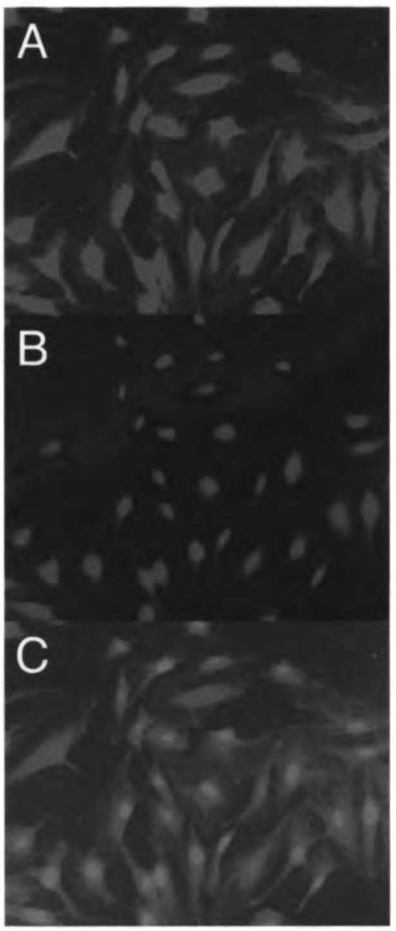

Figure 5-2. Protease Inhibitor Reduces Viral Replication. Relative to the reactivated standard (AD50), virus reactivated in the presence of protease inhibitors (Inhib+AD50 and Inhib+AD50(Pre)) show a distinct decrease in viral replication as measured by LANA immunofluorescence. Background levels of LANA staining are defined by the unreactivated samples (DMSO-AD50 and Inhib-AD50).

Figure 5-2.

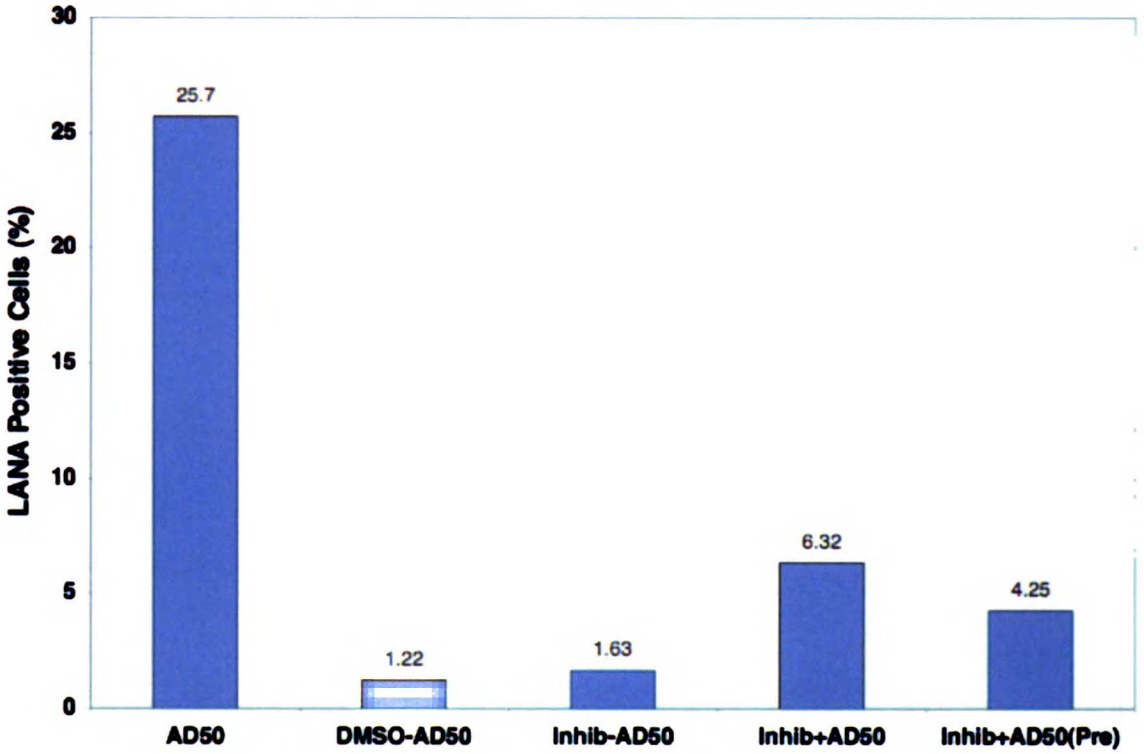
LANA Positive Cells (%)
30
25
20
15
10
5
0
25.7
1.22
1.63
6.32
4.25
AD50
DMSO-AD50
Inhib-AD50
Inhib+AD50
Inhib+AD50(Pre)

Figure 5-3. Comparison of DNA Polymerase and Protease Inhibitors. Foscarnet, a clinically used viral DNA polymerase inhibitor and the phosphonate KSHV protease inhibitor supress viral replication to a similar level.

Figure 5-3.

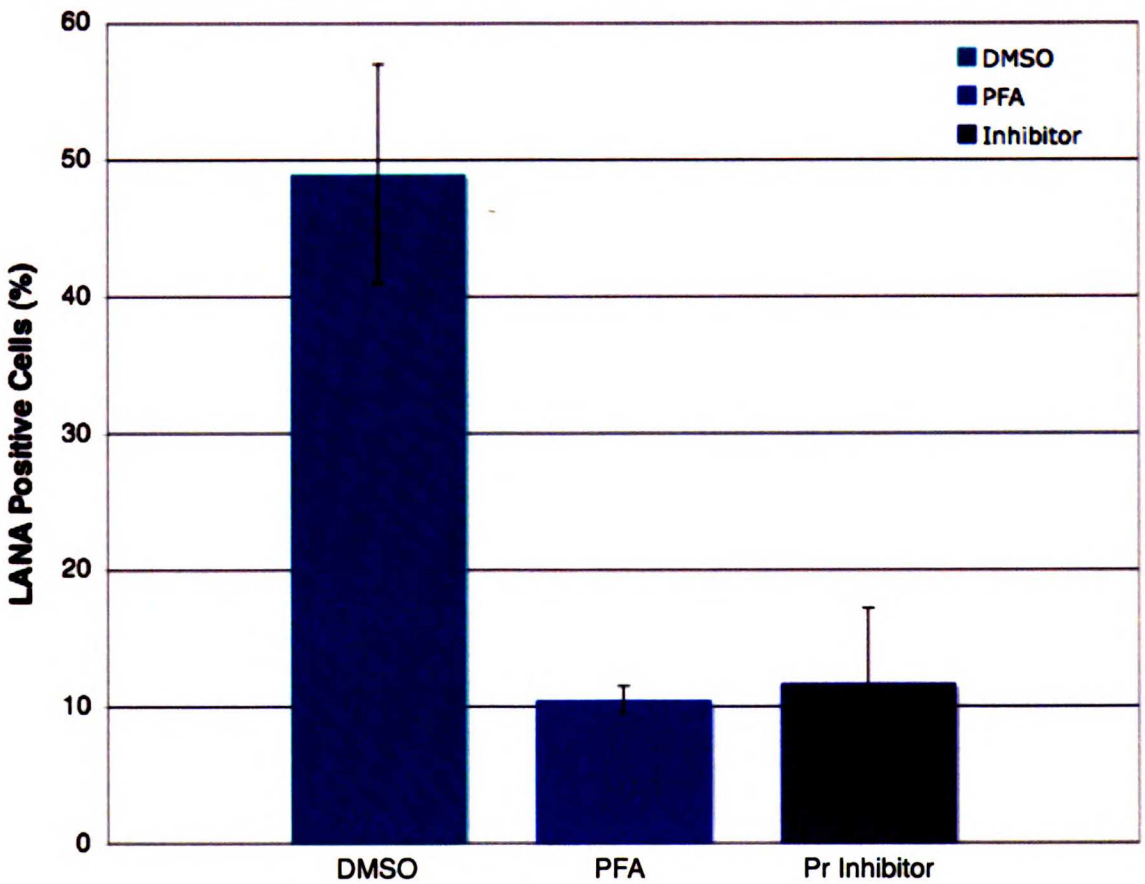
60
50
40
30
20
10
0
LANA Positive Cells (%)
DMSO
PFA
Inhibitor
DMSO
PFA
Pr Inhibitor

Figure 5-4. Inhibitor Localizes to Nucleus Upon Viral Reactivation. Virally infected TIME cells were untreated (A) or treated (B) with AD50 to induce lytic replication. Only in the presence of lytic replication is the inhibitor observed in the nucleus. Lower panels are phase contrast to reveal the presence of cells in the field.

Figure 5-4.

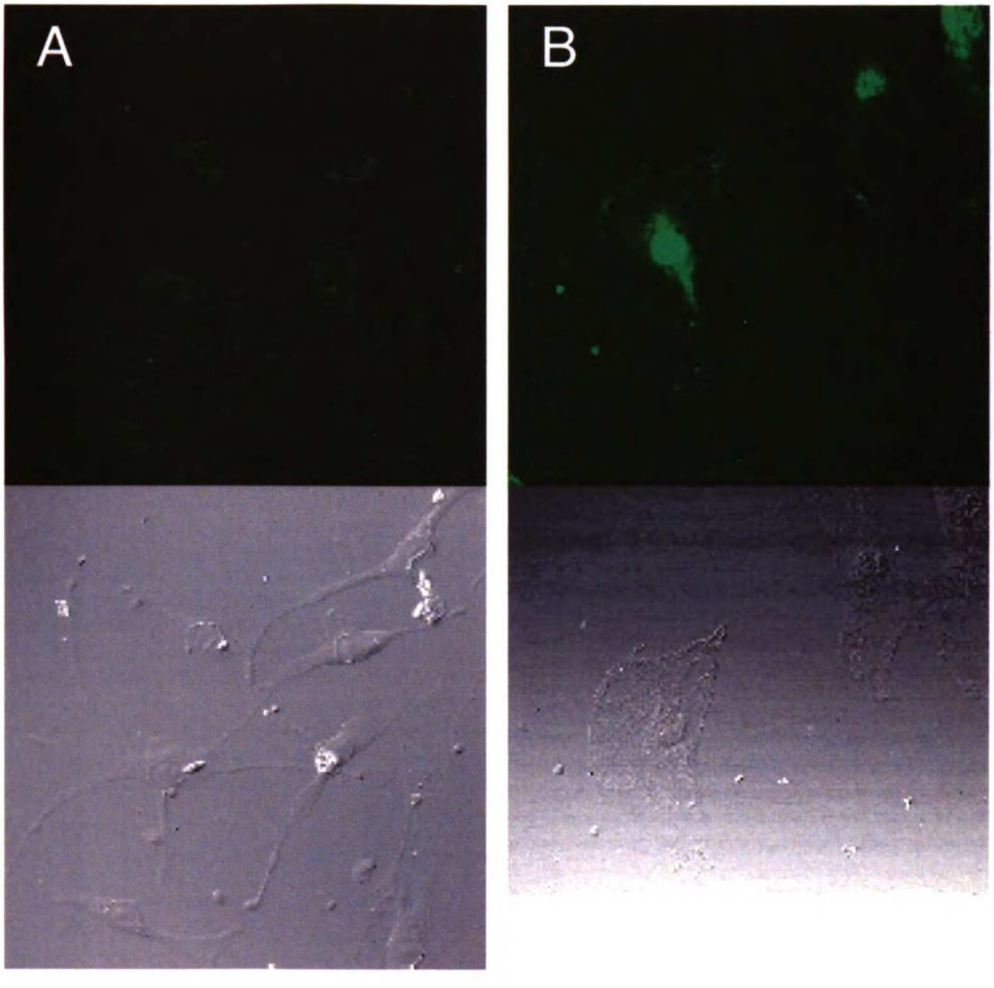

Figure 5-5. Protease Inhibitor Does Not Covalently Modify Monomeric KSHV Protease. Following incubation with a biotinylated phosphonate inhibitor and SDS-PAGE, only wild-type (wt) enzyme shows the presence of biotin as detected by streptavidin-HRP. The monomeric enzyme (M197D) shows no labeling even in dramatically overloaded samples.

Figure 5-5.

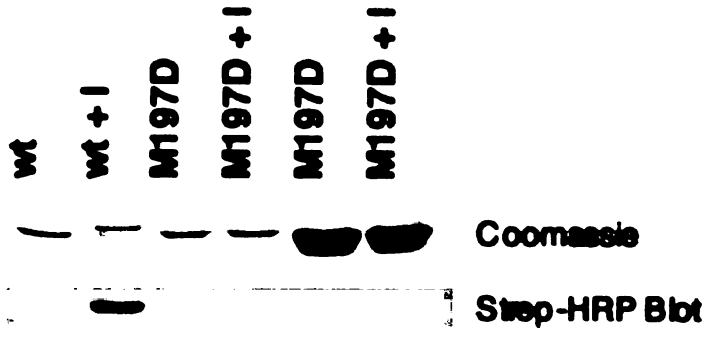

Figure 5-6. Protease Inhibitor Binds Reversibly to Monomeric KSHV Protease. Titrations of increasing concentrations of M197D in the presence of fluorescently labeled inhibitor result in a large increase in fluorescence polarization.

Figure 5-6.

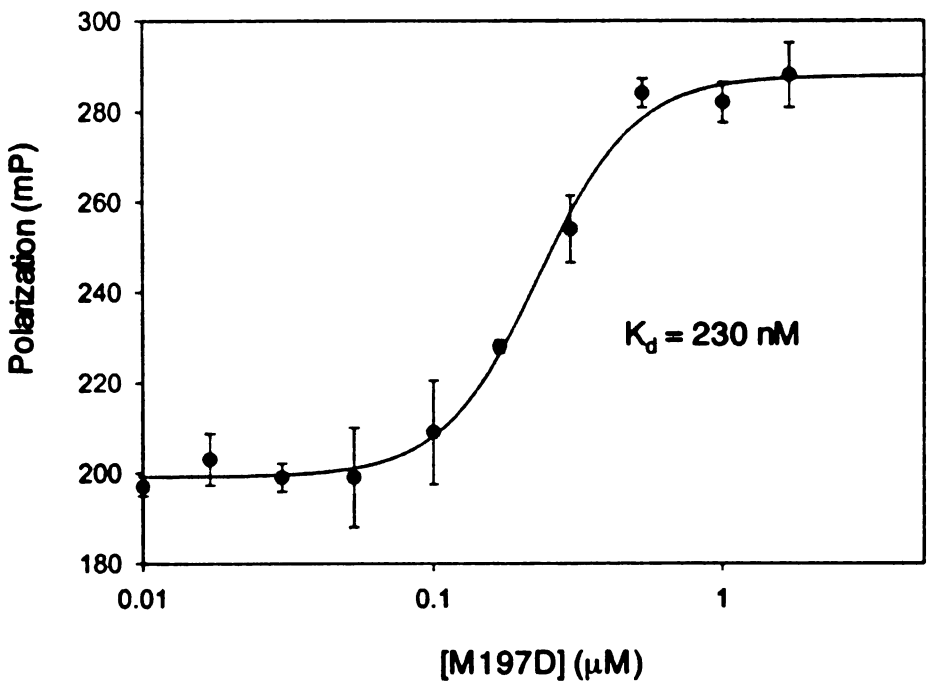
300
280
260
240
220
200
180
Polarization (mP)
0.01
0.1
1
[M197D] (μM)
K_d = 230 nM

Chapter 6 | **Conclusions and Future Directions**

Kaposi's Sarcoma-associated herpesvirus protease represents a novel class of dimerization-activated enzymes that play an essential role in viral replication. A combination of biochemical, biophysical and virological techniques has demonstrated the mechanistic details of activation of the protease and illustrated the legitimacy of the protein as a therapeutic target. Although it may seem that many of the major questions regarding herpesvirus proteases may have been addressed, a number of important experiments remain. In this chapter, we will not only review the findings presented in the current work, but also highlight directions and experiments for future consideration.

Proteases play an essential role in virtually all biological processes at some level. Therefore, proteolytic enzymes have emerged as important therapeutic targets for preventing disease progression and maintaining biological homeostasis. However, given that the human genome encodes for approximately 600 proteases, the physiological role for many of these enzymes remains unknown. Implication of an "orphan" protease in a biological process often occurs upon determination of substrates that are cleaved by the enzyme. As reviewed in Chapter 2, several exciting techniques have emerged for substrate identification and have been applied to proteases involved in apoptosis and cancer. The experimental advancements described in Chapter 1 may be applicable to the identification of additional substrates for KSHV Pr particularly early in viral infection, as discussed later in this section.

Previous work in the field based on genetics and virology implicated the protease as an essential enzyme for viral replication, yet the molecular mechanism of protease regulation and activation remained a mystery. Using a chemical biological approach described in Chapter 3, we synthesized inhibitors of the protease that provided important

insight into the mechanism of protease activation. Using positional scanning synthetic combinatorial libraries, we revealed KSHV Pr to be highly selective showing strong substrate specificity even at positions P3 and P4. Addition of a diphenyl phosphonate to the optimized substrate specificity determinants resulted in a potent transition-state analog inhibitor targeting the active site of the enzyme. Organophosphonate inhibition of the enzyme resulted in a dramatic stabilization of the protease, shifting the equilibrium almost completely to the dimeric form of the enzyme. Truncated versions of the inhibitor revealed that oxyanion formation alone was sufficient for the stabilization and argued that substrate binding determinants were not essential in dimer stabilization and activation. Titration experiments illustrated that while the active site and dimer interface directly communicate, the active sites themselves were independent from each other and capable of processing substrate simultaneously.

The findings reported in Chapter 3 provide the basis for a number of future experiments pertaining to the structure-function relationship of KSHV Pr. While peptide substrates undergo a single transition-state structure during hydrolysis, diphenylphosphonates may exist as two distinct compounds: the monophenyl phosphonate or the aged complex, depending on whether one or both or the phenoxy groups have been hydrolyzed, respectively. While the geometry at the phosphorous remains similar, the charge-state is dramatically different, with the aged complex carrying more negative charge. Comparison of the rate of dimer stabilization by NMR or size exclusion chromatography to the rate of formation of the aged complex upon inhibition by ^{31}PNMR may provide the molecular details of stabilization. Since the structural model of stabilization includes two hydrogen bonds to the phosphoryl oxygen,

it is possible that two stabilized dimer species actually exist based on the strength of the hydrogen bonds formed to the differentially charged monophenylphosphonate or aged complex. Although a recently solved co-crystal structure of the inhibited protease (A. Lazic, unpublished results) reveals the aged complex bound to the enzyme, it is not clear whether this complex is the required moiety for stabilization or rather is a result of complex hydrolysis in crystal conditions for two months.

While an inhibited KSHV Pr crystal structure may not resolve the stabilization question, it certainly would provide structural insight into the high degree of substrate specificity for aromatic residues seen at the P4 position. Because an obvious S4 pocket does not exist in the apo structure of KSHV Pr, it is possible that an induced fit mechanism occurs as substrate binds. Regardless of the binding site for the P4 residue, the strict substrate specificity at the distal site suggests residues further removed may also play a role in substrate specificity. Kinetic analysis of a hexapeptide substrate of KSHV Pr revealed a 10-fold improvement in K_m and a two-fold deterioration of k_{cat}, but specificity at these residues was not addressed. Elongation of the substrate to P10 or P15 would address the importance of extended binding determinants in the protease. It is possible that herpesvirus proteases use an "exosite" for substrate specificity as has been reported for other proteases.

Our results with both organophosphonate inhibitors and anisotropy experiments suggest the binding pockets on the protease are not essential for activation and stabilization; however, it has yet to be shown that the monomer and dimer bind substrate with equal affinity. To address this, analysis of the binding constant of the fluorescently labeled phosphonate inhibitor with the inactivated dimer (S114A) by anisotropy could be

performed. However, the binding experiment is complicated by the natural dimerization constant of the protease as the concentration of enzyme increases during the experiment, potentially affecting inhibitor binding as well as polarization values.

Although *in vitro* analysis of the relationship between protease structure and function is a simpler system, ultimately, the correlation of protease structure and viral replication is an important focus. Specifically, our finding that substoichiometric inhibition of the protease *in vitro* activated the other active site in the dimer suggests that substoichiometric addition of inhibitor in the virus would actually aid viral replication at some level. Given the difficulty in quantifying the concentration of protease in an infected cell, it is unclear what concentrations of inhibitor are necessary to completely abolish proteolytic activity. A series of viral replication experiments in the presence of serial dilutions of the protease inhibitor may provide insight into this issue. However, due to the poor sensitivity of the current assay the effect may be difficult to observe.

Building on the model of protease stabilization and activation generated from the inhibitor studies, the work described in Chapter 4 provided the molecular mechanism of protease activation upon dimerization. NMR data identified and localized a large conformational change to helices 5 and 6, revealing that both secondary structural elements were lost in the inactive monomer. To support the importance of the conformational change in protease activation, a disulfide bond was engineered into KSHV Pr, which prevented the structural transition from occurring. In fact, protease activation was converted from a concentration-dependent mechanism to a redox-controlled process. Following reduction of the bond and inactivation of the protease,

addition of oxidized glutathione reversed the process, catalyzing the formation of the disulfide bond and subsequent enzyme activation.

Incorporation of the disulfide bond into the monomer also recovered catalytic activity, representing the first example of a rationally designed active monomer. Though activity was recovered, kinetic analysis of the active monomer has proven difficult. The main challenge has been separating monomers containing the reduced versus oxidized disulfide bond. One potential method for removing the reduced disulfide species may be to pass the protein sample over a thiol sepharose or N-ethylmaleimide-bound resin. However, even in this case, incorrectly oxidized thiols (to sulphenic acid as opposed to disulfide bond) would not be removed from the sample and would make exact determination of the disulfide-linked protein concentration impossible. Determination of kinetic constants for an active monomer would allow comparisons to wild-type enzyme to reveal the contribution that dimerization makes toward overall activity.

The concept of induced fit in enzymology is well-established, yet the idea of induced structure is less well documented. A classic example of structural changes that regulate protein function is seen in hemoglobin, where conformational changes upon oligomerization and substrate binding result in an increased binding affinity for subsequent oxygen molecules. While the conformational change in hemoglobin is very subtle, the mechanism of regulation of herpesvirus proteases represents one of the most dramatic structural rearrangements upon oligomerization reported to date. The phenomenon of induced structure is a powerful mechanism by which protein function may be controlled and will undoubtedly emerge as an important regulatory mechanism in years to come.

Despite the overwhelming chemical, biophysical and virological evidence we have presented that our work is relevant to an *in vivo* function of the protease, we must acknowledge a major caveat to our work and the field in general. During lytic replication, the protease is expressed as a fusion protein to viral assembly protein. As we, and many in the field, have experienced, working with the full length native construct has proven difficult and as a result, our work has been performed using only the catalytic domain of the fusion. However, it is clear that studying the intact Pr-AP fusion would resolve many unanswered questions. In fact, the structural basis for many of the processes we know occur, such as dimerization, activation and substrate cleavage, is unknown in the context of assembly protein. It is possible that AP affects the dimerization constant of the protease; however, according to our estimates of protease concentration in the cell, it appears that large changes in the dimerization constant of the protease in either direction would be detrimental to viral replication.

To ensure protease activity is not prematurely activated, it is possible that AP occludes the active site of the enzyme until a conformational change occurs in the nucleus upon capsid formation. Examination of the amino acid sequence of AP revealed a region of homology (P-I-Y-V-Q-A^{435}-P^{436}) to the natural cleavage sequence of the protease (P-V-Y-L-K-A^{230}-S^{231}), but lacking the critical Ala-Ser bond required for substrate cleavage. It is possible that these amino acids bind in the active site, further preventing premature substrate hydrolysis and representing yet another level of protease regulation. Should the hurdle of protein expression be overcome, fluorescence polarization using BODIPY-labeled inhibitors would allow for direct comparison between active site accessibility in the catalytic versus full-length protein. Furthermore,

analysis of standard dimerization and activity curves would be informative in understanding the full physiological role of AP. The function of assembly protein remains one of the most tantalizing and elusive aspects for the field of herpesvirus proteases in general.

In the absence of successful full-length Pr-AP expression, systematic elongation of native protease-AP may provide soluble variants that may be studied biochemically or crystallographically given the recently identified crystal conditions for KSHV Pr (A. Lazic). Extension of AP past the R-site would be extremely useful in understanding the structural relationship between protease and AP when in the native conformation. As an alternative to bacterial expression, large scale *in vitro* transcription and translation remains an alternative methodology for producing protein for the structural studies described.

Despite the difficulties in expression of full length protease, we utilized active site inhibitors described in Chapter 3 to probe the function of the protease in the context of viral replication. Using a cell culture model of replication, we demonstrated that the peptidyl-diphenylphosphonates were cell permeable and showed an effect on viral replication. In fact, in the assay used, polymerase inhibitors currently used in the clinics showed a similar effect as the protease inhibitor illustrating the validity of the herpesviral protease as a potential therapeutic target. While the inhibitor was clearly shown to cross the outer cell membrane, confocal microscopy indicated that the inhibitor may not cross nuclear membranes. However, in the presence of replicating virus, this phenomenon was reversed, with essentially all intracellular protease inhibitor localized to the nucleus. Fluorescence anisotropy validated that the active site inhibitor bound to the inactive

monomer with mid nanomolar affinity, providing evidence for a model in which monomeric protease binds the inhibitor in the cytosol, translocates it to the nucleus and then reacts with it to form the covalently inhibited enzyme-inhibitor adduct.

Given the homology between herpesvirus proteases, it is anticipated that the findings and reagents derived from this study will be applicable to all members of the herpesvirus family. To test the widespread applicability of the inhibitor, future work may include assaying the inhibitor against other herpesviruses. Given active site protease inhibition reduces viral replication, it is also possible that dimer interface inhibition will also arrest the virus. A first step would be to demonstrate that KSHV M197D is incapable of replication when wild-type Pr is replaced with the monomer in the virus. This finding would pave the way for further experiments in which dimerization inhibitors, such as the APP scaffold (N. Shimba) would be transfected or transported into the infected cell. Optimization and minimization of the dimerization inhibitor may lead to a more stable compound for cell-based use.

Aside from the traditional role of the protease in capsid formation during lytic replication, recent results suggest the protease may play an additional role at a much earlier point in viral infection. Surprisingly, analysis of a mature virion for mRNA content revealed the second highest viral transcript present encoding for the protease. The level of protease transcript was far above that expected for random incorporation in the nucleus of an infected cell during virion production. Using a bioinformatics search program, Prediction of Protease Substrates (PoPS, S. Boyd), potential protease cleavage sequences were identified in several human and viral proteins. In fact, a number of KSHV proteins are packaged in the virion and released into cells upon infection. All of

these proteins show possible KSHV Pr cleavage sites. Based on this preliminary bioinformatics analysis, it is possible that protease activity within the first several hours of infection is required for establishment of a long-term latent infection. This concept has been shown for a subset of lytic genes that are either brought in with the virion or expressed immediate after infection. However, the putative additional role of the viral protease need not be restricted to early infection processes, as many other potential KSHV and human proteins exist later in the life cycle during viral replication.

Although full length Pr-AP mRNA has been detected, protease promoters have not been mapped so it is unknown whether full-length protein is actually translated. While *in vitro* transcription and translation of a Pr-AP fusion construct would address whether active protease could be generated from a fusion protein, the subcellular localization would remain unclear. A GFP-Pr-AP construct transfected into TIME cells would provide an opportunity to monitor Pr localization by fluorescence. Should the protease be localized specifically to the cytosol or nucleus, the search for substrates could be reduced based on co-localization. Additionally, the fluorescently labeled active site inhibitor may allow for detection of active enzyme shortly after viral infection.

It is clear that while many questions regarding protease stabilization and activation have been answered, there remain a number of interesting directions to pursue. Enticing preliminary data regarding alternate roles of the protease during infection and replication represents an exciting new direction for further investigations.

Appendix A | **Permission to Include Published Material**

We commemorate the founding of the House of Elsevir in 1580 and celebrate the establishment of the Elsevier company in 1880.

7 September 2005

Our ref: HG/ND/Sept05/j039

Alan Marnett
UCSF
600 16th Street
San Francisco 94143-2280
USA

Dear Mr Marnett

TRENDS IN BIOTECHNOLOGY, Vol 23, Issue 2, 2005, pp59-64, Marnett et al, "Papa's Got a Brand....."

As per your letter dated 6 September 2005, we hereby grant you permission to reprint the aforementioned material at no charge **in your thesis** subject to the following conditions:

1. If any part of the material to be used (for example, figures) has appeared in our publication with credit or acknowledgement to another source, permission must also be sought from that source. If such permission is not obtained then that material may not be included in your publication/copies.

2. Suitable acknowledgment to the source must be made, either as a footnote or in a reference list at the end of your publication, as follows:

   "Reprinted from Publication title, Vol number, Author(s), Title of article, Pages No., Copyright (Year), with permission from Elsevier".

3. Reproduction of this material is confined to the purpose for which permission is hereby given.

4. This permission is granted for non-exclusive world **English** rights only. For other languages please reapply separately for each one required. Permission excludes use in an electronic form. Should you have a specific electronic project in mind please reapply for permission.

5. This includes permission for UMI to supply single copies, on demand, of the complete thesis. Should your thesis be published commercially, please reapply for permission.

Yours sincerely

Helen Gainford
Rights Manager